Investigation of the genetic basis for virus tropism and virulence of classical swine fever virus

Johnston, Camille Melissa

Publication date:
2018

Document Version
Publisher's PDF, also known as Version of record

Investigation of the genetic basis for virus tropism and virulence of classical swine fever virus

Ph. D. Thesis August 2018 Camille Melissa Johnston

DTU Vet
National Veterinary Institute

Investigation of the genetic basis for virus tropism and virulence of classical swine fever virus

Ph.D. thesis by Camille Melissa Johnston, 2018

Technical University of Denmark

National Veterinary Institute, Lindholm

Supervisor:

Thomas Bruun Rasmussen, Senior Researcher

DTU National Veterinary Institute, Technical University of Denmark, Lindholm, Denmark

Co-supervisors:

Graham J. Belsham, Professor

DTU National Veterinary Institute, Technical University of Denmark, Lindholm, Denmark

Anders Gorm Pedersen, Professor

DTU Department of Bio and Health Informatics, Technical University of Denmark, Denmark

Table of Contents

Preface

This thesis is the result of 3 years' Ph.D. study and work at the National Veterinary Institute, Technical University of Denmark (DTU), Lindholm, and has been internally funded by DTU Vet. My research stay at Hokkaido University, under the guidance of Professor Yoshihiro Sakoda, was partially funded by Augustinus Fond, Norma & Frode Jacobsens Fond, Otto Mønsteds Fond, Sasakawa Fonden, and Torben & Alice Frimodts Fond.

This thesis would not have been conceivable without the support and help from colleagues and loved ones during the past three years. It is only my name which is on the cover, but trust me, a thesis is not something you can create entirely by yourself. Firstly, I would like to thank my main supervisor Thomas Bruun Rasmussen for selecting me to do this Ph.D. I was truly despairing in my capabilities as a scientist, until I got the job interview and subsequent position. I am so grateful that I got to work with what has been my passion since I was 12 years old: virology. Secondly, I wish to express my gratitude to co-supervisor Graham J. Belsham for his help and late night email responses.

I would like to acknowledge all the supporting people at Lindholm. Working on that island, has indeed been a unique experience. I have many mornings looked forward to playing cards on the ferry. I would also like to thank the 'coffee-table people'. It is nice to start the mornings off with a little get-together; fresh baked bread on Thursdays has brought much joy (and a few extra pounds). I would especially like to thank Marianne and Angelo for cheering me up on my moody days. Lab-technician student Marie also deserves a little shout out. It has been fun working with you (for the short while I did), and I appreciate your hard work. I also wish to thank the Ph.D. students at Lindholm, as your inputs have been much appreciated. I really enjoyed sharing an office with my fellow Ph.D. student Christina and I will miss our chats. Last, but not least, a very special thanks goes to my very good friend Vibeke. It was incredibly entertaining working with you in the laboratory when you were a lab-technician student, and you teaching me to crochet has been a great stress-relief.

Another round of thanks goes to Professor Yoshihiro Sakoda for hosting me during my 5 months' research stay at the Laboratory of Microbiology, Graduate School of Veterinary Medicine, Hokkaido University, Japan, and also Noriko Fukushi, for showing the way around the lab, as well as acting as an interpreter when I had to navigate daily life in Japan.

Last but not least, I am eternally thankful for the support from family and friends. You might not all understand my research, but you have always been there when I have needed you.

Camille Johnston, August 2018

Summary

Classical swine fever virus (CSFV) is the causative agent of classical swine fever, an economically important and highly contagious disease of pigs. CSFV is a positive-stranded RNA virus and CSFV strains vary considerably in their virulence, with high, moderate and low virulence strains. The E2 glycoprotein is the major surface component of the virion and modifications introduced into this glycoprotein appear to have an important effect on CSFV virulence. E2 shows a high variability among different CSFV strains, and a specific amino acid motif within the E2 varies between strains of different virulence. In the highly virulent CSFV strains, Koslov and ALD, this motif comprises residues E761/S763/L764 in the polyprotein, and has been termed the 'SL'-motif. However, CSFV strains encoding R761/S763/L764 represent the predominant alleles across all published CSFV genomes.

Positive-strand RNA viruses evolve rapidly, due to error-prone RNA replication and the lack of proof-reading activity of the RNA-dependent RNA polymerase. With error rates ranging from 10^{-6} to 10^{-4} mutations per nucleotide incorporated, this results in a virus population that exists as a quasispecies of different, but closely related variants. Certain variants, or haplotypes, emerge or change continuously and the variation within the virus population enables the virus to change and adapt during infection. The diversity and quasispecies composition of CSFV and their role as determinants of virulence have not been studied in depth.

In this thesis, the focus has been on elucidating which haplotypes constitute the virus population through establishing a high-throughput method for cloning of full-length CSFV cDNA. Deep sequencing cannot easily resolve the different haplotypes that constitute the virus populations, therefore obtaining full-length cDNA clones represents an alternative approach to identify the individual haplotypes present. Numerous clones were obtained, sequenced by NGS, and phylogenetic analysis revealed that they were all unique. A majority of the unique mutations were also observed in the serum samples of CSFV infected pigs, or in published sequences. Animal experiments were performed with infectious cDNA clones, containing substitutions in the 'SL'-motif. One pig infected with a specific substitution variant, exhibited earlier signs of disease compared to pigs infected with other variants. The virus populations in different tissues and serum were investigated by deep sequencing to identify adaptations and diversity of the populations. Several non-synonymous mutations were identified in some variants. This laid the basis for further *in vitro* study of the role of the 'SL'-motif in the highly and moderately virulent strains Koslov and ALD/A76, respectively. The results of this analysis, based on growth kinetics and serial passaging in several different cell types, revealed no discernible difference in growth of these variants in these cells *in vitro*.

This thesis is comprised of three parts: **Part I**, is an introduction to CSFV, virus genome and protein functions, virus lifecycle, virus quasispecies, role of the E2 glycoprotein in virulence with the focus on the 'SL'-motif, and molecular virology, with the application of cloning of full-length viral cDNA and NGS. **Part II**, comprises the manuscripts published or in preparation. **Manuscript I** describes the establishment of a high-throughput cloning method for generation of full-length cDNA clones from a virus population, to gain insight into which haplotypes constitute the virus population. Several clones were obtained, and NGS employed for whole genome sequencing and phylogenetic analysis. **Manuscript II** describes the role of residues 763 and 764 in the virulence of CSFV strain Koslov through two infection experiments of pigs. Unexpectedly, one variant, vKos_LP exhibited earlier signs of disease in infected pigs, compared to the other variants. The evolution of the viral population during *in vivo* infection was investigated by NGS and several interesting adaptations were observed for some of the variants, such as vKos_SP, which contained several linked non-synonymous mutations at the consensus level of the sequenced CSFV genome. **Manuscript III** builds upon the results observed in **manuscript II**, with an *in vitro* study of residues 761, 763 and 764 in CSFV strains Koslov and ALD/A76 to elucidate their potential role in cell specificity. This was investigated by growth kinetics and serial passaging in different cell types, which revealed no discernible difference in the variants. One adaptation in the 'SL'-motif was observed: a K761R substitution in the 9^{th} passage of vKos_KSL in primary plexus choroideus cells. NGS revealed that a selective sweep had taken place in this passage, and that the R761 variant contained several non-synonymous mutations in the NS5A/B. **Part III** sums up the findings of this thesis and provides a general discussion and overall conclusions, as well as future perspectives.

Resumé (Danish)

Undersøgelse af den genetiske basis for virus tropisme og virulens af klassisk svinepestvirus.

Klassisk svinepest er en alvorlig smitsom sygdom hos svin forårsaget af klassisk svinepest virus (CSFV). CSFV er en positiv-strenget RNA-virus, og forskellige virusstammer varierer betydeligt i deres virulens med høj-, moderat-, og lav-virulente stammer. E2 glykoproteinet er en vigtig overfladekomponent i viruspartiklen, og modifikationer i dette glykoprotein synes at have en vigtig virkning på CSFV virulens. E2 udviser høj variabilitet blandt forskellige CSFV-stammer, og et specifikt motiv, 'SL'-motivet, i E2 varierer mellem stammer med forskellig virulens. I de høj-virulente CSFV-stammer Koslov og ALD, omfatter dette motiv aminosyrerne E761/S763/L764 i polyproteinet, mens den mest forekommende variant er R761/L763/P764 hvis man sammenligner på tværs af alle offentliggjorte CSFV-genomer.

Positivt-strenget RNA-virus udvikler sig hurtigt grundet virus RNA-polymerasens fejlagtige RNA-replikation og mangel på korrekturlæsning. Med fejlfrekvenser på 10^{-6} til 10^{-4} mutationer per inkorporeret nukleotid resulterer dette i viruspopulationer, der eksister som quasispecies af forskellige men nærtbeslægtede varianter. Visse varianter, eller haplotyper, opstår eller ændrer sig løbende og variationen inden for viruspopulationen gør det muligt for virus at ændre sig under infektionen. Diversitet og quasispecies sammensætningen i CSFV og deres rolle som markør for virulens er ikke blevet undersøgt dybdegående.

I denne afhandling er der fokuseret på at belyse hvilke haplotyper der udgør viruspopulationen, ved at etablere en high-throughput metode til kloning af fuldlængde CSFV cDNA. Dybdesekventering er svær at bruge til at detektere de forskellige haplotyper som udgør viruspopulationerne. En alternativ tilgang til identificering af haplotyperne er generering af cDNA-kloner i fuld virusgenom længde. Talrige kloner blev genereret, sekventeret med NGS og fylogenetisk analyse afslørede, at de alle var unikke. Hovedparten af de unikke mutationer blev også observeret i serumprøverne fra de CSFV-inficerede svin eller i publicerede sekvenser. Infektionsforsøg i grise blev udført med virus med substitutioner i 'SL'motivet. En gris inficeret med én bestemt variant udviste tidligere tegn på sygdom sammenlignet med grisene inficeret med de andre varianter. Viruspopulationerne i forskellige prøver fra blod samt forskellige organer blev undersøgt ved dybdesekventering for at identificere ændringer og diversiteten under infektion. Adskillige aminosyreændringer blev identificeret i flere varianter. Dette udgjorde grundlaget for yderligere *in vitro* undersøgelser af 'SL'-motivet i henholdsvis de høj- og moderat-virulente stammer Koslov og ALD/A76. Resultaterne af disse undersøgelser, baseret på vækstkinetik og seriel passage i forskellige celletyper, afslørede ingen signifikant forskel i virus med ændringer i dette motiv.

Denne afhandling består af tre dele: **Del I** er en introduktion til CSFV, virusgenomet og proteinfunktioner, viruslivscyklus, quasispecies, E2-glykoproteinets rolle i virulens med fokus på 'SL'-motivet og kloning af fuldlængde viralt cDNA og NGS. **Del II** omfatter de manuskripter, der er udgivet eller under forberedelse. **Manuskript I** beskriver etableringen af en effektiv kloningsmetode til generering af fuldlængde cDNA-kloner fra en viruspopulation for at få indsigt i hvilke haplotyper der udgør viruspopulationen. Adskillige kloner blev genereret og NGS blev anvendt til fuldgenom-sekventering samt til fylogenetisk analyse. **Manuskript II** beskriver infektionsforsøg i svin for at belyse rollen af aminosyrepositionerne 763 og 764 i virulensen af CSFV-stammen Koslov. Her viste en variant, vKos_LP, tidligere tegn på sygdom hos inficerede svin sammenlignet med de andre varianter. Evolutionen af viruspopulationerne under *in vivo* infektion blev undersøgt ved brug af NGS, og adskillige interessante ændringer i viruspopulationerne blev observeret, såsom vKos_SP som indeholdt adskillige sammenhængende mutationer i CSFV genomet på konsensusniveau. **Manuskript III** bygger på resultaterne fra **manuskript II**, med *in vitro* undersøgelse af aminosyrepositionerne 761, 763 og 764 i CSFV-stammerne Koslov og ALD/A76 for at belyse deres potentielle rolle i cellespecificitet. Dette blev undersøgt ved brug af vækstkinetik og seriel passage i forskellige celletyper, hvilket afslørede, at der ingen signifikante forskelle var imellem varianterne. Dog blev én ændring i 'SL'-motivet observeret med en substitution af K761R i 9. passage i vKos_KSL i primære plexus choroideus celler. NGS afslørede, at et selektivt 'sweep' havde fundet sted i denne passage og at R761-varianten indeholdt flere aminosyreændringer i NS5A/B. **Del III** opsummerer resultaterne i denne afhandling og indeholder en generel diskussion og konklusioner samt fremtidige perspektiver.

Part I - Introduction

Classical Swine Fever Virus

Classical swine fever virus (CSFV) is the causative agent of classical swine fever (CSF), an economically important and highly contagious disease of pigs, formerly known as hog cholera, and is classified as a notifiable disease by the Office International des Epizooties (OIE). The only natural hosts are wild boars (*Sus scrofa scrofa*) and domestic pigs (*Sus scrofa domesticus*) (Depner et al., 1995; Blacksell et al., 2006; Postel et al., 2012), although recently the susceptibility of common warthogs *(Phacochoerus africanus*) and bushpigs (*Potamochoerus larvatus*) was demonstrated (Everett et al., 2011). CSF was first recognized in USA in the 19th century then subsequently reported across the globe (Edwards et al., 2000). CSF has successfully been eradicated from domestic pigs and wild boars in North America, Western Europe, Australia and New Zealand by vaccination and/or stamping-out (Paton & Greiser-Wilke, 2003; Ji et al., 2015), but still has a severe impact in Asia, South America and parts of the former Soviet Union (Lindenbach et al., 2013). CSFV, together with bovine viral diarrhea virus (BVDV) and border disease virus (BDV), belong to the genus *Pestivirus* within the *Flaviviridae* family (**Figure 1**) (Lindenbach et al., 2013; Simmonds et al., 2017; Smith et al., 2017). Recent publications have described additional pestiviruses, which are genetically distinct. These

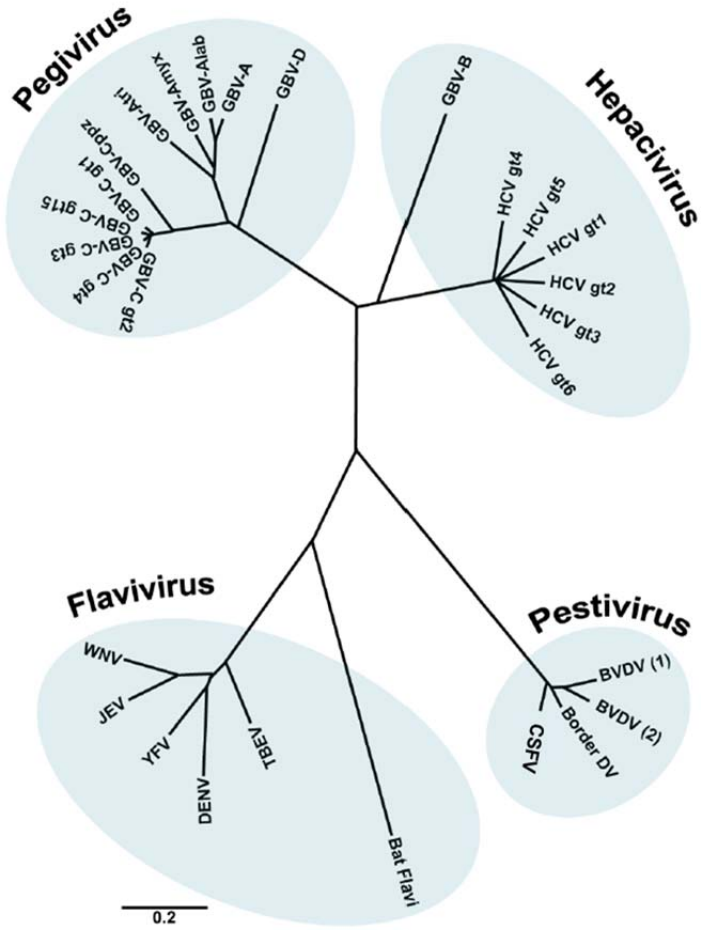

Figure 1

Phylogenetic tree of the *Flaviviridae* family based on neighbor joining analysis of aligned conserved motifs in the RNA dependent RNA polymerase. Selected members are shown. A distance scale corresponding to amino acids substitutions per position is shown. Modified from Romero-Brey & Bartenschlager, 2014.

viruses include Hobi-like pestivirus (Schirrmeier et al., 2004), Bungowannah virus (Kirkland et al., 2007), Aydin-like pestivirus (Becher et al., 2012), and atypical porcine pestivirus (Hause et al., 2015; Postel et al., 2016a) isolated from domestic animals. In addition, giraffe pestivirus (Becher et al., 1997; Avalos-Ramirez et al., 2001) and pronghorn antelope pestivirus (Vilcek et al., 2005; Neill et al., 2014) have been isolated from wildlife species. Pestivirus sequences have also been observed in rats (Firth et al., 2014) and bats (Wu et al., 2012), however, virus isolates have not been obtained yet (Smith et al., 2017).

A revision was recently made to the taxonomy of the genus *Pestivirus* (see **Table 1**) to include seven additional species, to name all *Pestivirus* species according to a standard format, and to modify the criteria by which pestivirus species were demarcated (Smith et al., 2017; King et al., 2018). Previously, the *Pestivirus* names were derived from virus isolate names, and these in turn were based on virus host range, disease attributes, or geographical location of the first isolate (Smith et al., 2017).

The various strains of CSFV reflect a narrow range of evolutionary divergence as they consist of one serotype (Vanderhallen et al., 1999; Deng et al., 2005), and CSFV is the least variable member within the highly variable pestiviruses (Lowings et al., 1996). CSFV has been classified into three genotypes (gt 1, 2, and 3), with several subgroups (gt 1.1-1.4, 2.1-2.3, 3.1-3.4) (Lowings et al., 1996; Paton et al., 2000; Deng et al., 2005; Postel et al., 2013). Most genotypes show a distinct geographical distribution pattern (Paton et al., 2000), but there is no clear correlation between genotype and virulence. Phylogenetic analyses indicate that a virus genotype shift from gt 1 or gt 3 to gt 2 has occurred in many European and Asian countries

Table 1

Characteristics of proposed pestivirus species, from Smith et al., 2017.

Existing species name	Proposed species name	Virus names	Abbreviation	Isolate type	GenBank Accession	Host	Complete coding region sequences	Disease
Bovine viral diarrhea virus 1	*Pestivirus A*	Bovine viral diarrhea virus 1	BVDV-1	NADL	M31182	Cattle, sheep, other ruminants, pig	79	Bovine viral diarrhea/ mucosal disease (BVD/MD)
Bovine viral diarrhea virus 2	*Pestivirus B*	Bovine viral diarrhea virus 2	BVDV-2	890	U18059	Cattle, sheep, other ruminants pig	99	BVD/MD
Classical swine fever virus	*Pestivirus C*	Classical swine fever virus, hog cholera virus	CSFV	A187	X87939	Pig	96	Classical swine fever
Border disease virus	*Pestivirus D*	Border disease virus, reindeer pestivirus	BDV	X818	AF037405	Sheep, reindeer, chamois, other ruminants, pig	13	Border disease Hairy shaker syndrome Fuzzy lamb syndrome
	Pestivirus E	Pronghorn antelope pestivirus	Pronghorn		AY781152	Antelope	1	Unknown
	Pestivirus F	Bungowannah virus	Bungo	Bungowannah	EF100713	Pig	1	Porcine myocarditis syndrome
	Pestivirus G	Giraffe pestivirus	Giraffe	H138	AF144617	Giraffe, cattle	2	MD-like (giraffe)/unknown (cattle)
	Pestivirus H	Hobi-like pestivirus, atypical ruminant pestivirus, bovine viral diarrhea virus 3	Hobi-like, BVDV-3	Th/04_KhonKaen	FJ040215	Cattle, buffalo	12	BVD/MD
	Pestivirus I	Aydin-like pestivirus,		Aydin/04-TR	JX428945	Sheep, goat	2	Abortions, congenital malformations
	Pestivirus J	Rat pestivirus		NrPV/NYC-D23	KJ950914	Rat	1	Unknown
	Pestivirus K	Atypical porcine pestivirus	APPV	000515	KR011347	Pig	6	Congenital tremor

(Beer et al., 2015). Recent disease outbreaks by gt 1 have been limited to Central and South America (Postel et al., 2013; Silva et al., 2017), while outbreaks in China mainly consist of gt 2.1 (Luo et al., 2011, Luo et al., 2016; Jiang et al., 2013; Beer et al., 2015; Zhang et al., 2015; Hu et al., 2016). The classification into genotypes is based mostly on partial sequences, namely 150 nucleotides (nt) of the 5' untranslated region (UTR), 190 nt of the glycoprotein E2 coding region and 409 nt of the NS5B (Greiser-Wilke et al., 1998; Paton et al., 2000). The full E2 coding sequence (1119 nt) has also been demonstrated to be reliable for detailed phylogenetic analyses (Postel et al., 2012; Beer et al., 2015).

CSF infection is typically transmitted oronasally, by direct or indirect contact between infected pigs, by contaminated food or swill feeding. Transmission via contact to humans, or agricultural and veterinary equipment is also possible (van Oirschot, 1999; Postel et al., 2012; Lindenbach et al., 2013). CSF epidemics result in immense economic losses in areas with intensive pig farming (Dong & Chen, 2007). The outbreak in the Netherlands in 1997-98 had a total financial cost of USD 2.3 billion (Meuwissen et al., 1999). Some 700,000 infected pigs were slaughtered, and an additional 11 million pigs were preemptively culled (Stegeman et al., 2000). The EU has been free of CSF in recent years, due to a strict stamping out policy, except for minor outbreaks in Lithuania and Latvia (Moennig & Becher, 2015). Wild boar populations have been shown to be an important reservoir for CSFV and act as a source for reintroduction of the virus into domestic pig populations (Fritzemeier et al., 2000; Rossi et al., 2015). Prophylactic vaccination is banned in the EU but emergency vaccination can be implemented in cases of severe outbreaks in domestic pigs (Moennig & Becher, 2015). Safe and highly efficient live attenuated CSF vaccines have existed for many years (van Oirschot, 2003a). The vaccine strains, such as the C-strain, Lapinized Phillippines Coronel, the Thiverval or the GPE^- strain (derived from the virulent strain ALD (Sasahara, 1970; Shimizu et al., 1970)), were attenuated through serial passages in animals or cell culture (Greiser-Wilke & Moennig, 2004) and all belong to gt 1 (Yoo et al., 2018). Vaccination has also been practiced to control the disease in wild boar (Kaden et al., 2002; von Rüden et al., 2008; Rossi et al., 2010; Blome et al., 2011), where the vaccines have been adapted to a bait format for oral immunization (Kaden et al., 2000, Kaden et al., 2002, Kaden et al., 2010). The issue with current modified live vaccines (MLVs) is that they elicit the full spectrum of antibodies, and therefore vaccinated animals cannot be distinguished from infected pigs by serological methods (so called DIVA concept) (van Oirschot, 2003a). Due to trade restriction imposed on pigs vaccinated with MLVs (Moennig & Becher, 2015), only DIVA vaccines are considered a feasible option for immunization of domestic pigs (Blome et al., 2013). Two E2 subunit vaccines are commercially available and have been tested extensively for their efficacy (Greiser-Wilke & Moennig, 2004). These vaccines have been shown to be safe, provide clinical protection and limit the spread of CSF (Blome et al., 2017a), although they exhibit drawbacks with regard to their inability to provide early protection and protection against vertical

transmission (Depner et al., 2001; van Oirschot, 2003a, van Oirschot, 2003b). However, the European Medicines Agency (EMA) licensed the chimeric vaccine candidate 'CP7_E2alf' in 2014, after extensive testing in the framework of an EU-funded research project (Blome et al., 2017a). 'CP7_E2alf' was constructed based on the infectious cDNA clone of the BVDV-1 strain 'CP7'. The E2 coding region in the BVDV backbone was replaced with that of CSFV strain Alfort/187 (Reimann et al., 2004). So far this first live marker vaccine against CSF has proven to be safe and efficient (Blome et al., 2017b), and is still under investigation. It could be a potent tool for emergency vaccination of domestic pigs and wild boar (Blome et al., 2017a). Genetic variability of the E2 glycoprotein among the CSFV sub-genotypes has resulted in differential antigenicity and neutralizing efficiency of anti-C-strain (common vaccine strain) polyclonal antibodies (Chen et al., 2010). There are concerns that vaccine-escape mutants have emerged, due to outbreaks of CSFV in vaccinated pig farms in China, where CSFV is endemic (Luo et al., 2014, Luo et al., 2016; Zhang et al., 2015; Hu et al., 2016). However, this might be due to failed vaccination, caused by the variable types and quality of the vaccines used, due to insufficient regulation, as well as incomplete vaccination coverage of the susceptible population , especially in remote villages and backyard farms (Luo et al., 2014, Luo et al., 2017).

The virulence of CSFV isolates varies, including low or avirulent strains, which mainly are vaccine strains (e.g. C-strain and GPE^-), and highly virulent strains that cause up to 100% mortality (Kaden et al., 2000; Mittelholzer et al., 2000; Li et al., 2006; Floegel-Niesmann et al., 2009; Tao et al., 2009), such as the gt 1 strains Koslov, Brescia, Eystrup and ALD (Leifer et al., 2011). CSF can manifest as acute hemorrhagic fever and ataxia with respiratory, gastrointestinal and central nervous system (CNS) disorders resulting in high mortality rates, or as a chronic disease with atypical symptoms (Kaden et al., 2000; Moennig et al., 2003; Luo et al., 2011). Infection with highly virulent strains, such as Koslov, show a less age-dependent clinical course than moderate and low virulent strains, and usually results in 100% mortality with severe CNS disorders, such as pronounced convulsions and seizures, within 7-10 days (Mittelholzer et al., 2000; Fahnøe et al., 2014; Tarradas et al., 2014), due to infection of cells localized in and around the blood vessels in the cerebrum and cerebellum. The infected cells in the study by Hansen et al. were mostly endothelial cells in the plexus choroideus and lymphocytes, however, dendritic-like cells were also observed to be infected in white and grey matter (Hansen et al., 2011).

Several studies have been undertaken to investigate the genetic basis for the observed differences in CSFV virulence. Several determinants have been identified, such as the N^{pro} (Mayer et al., 2004), the E2 (Risatti et al., 2005), the ribonuclease activity and the dimerization of the E^{rns} (Meyers et al., 1999; Tews et al., 2009), and NS4B (Tamura et al., 2012). Glycosylation of the structural proteins was shown to affect virulence (Risatti et al., 2007a, Risatti et al., 2007b; Sainz et al., 2008; Tang et al., 2008; Wu et al., 2010). Full-length

sequences are being employed for the investigation of virulence determinants, high resolution molecular epidemiology, as well as for quasispecies analyses (Leifer et al., 2010, Leifer et al., 2011; Töpfer et al., 2013; Fahnøe et al., 2014, Fahnøe et al., 2015; Goller et al., 2016). Further investigations of virulence determinants are needed to understand their role in the properties of different CSFV strains.

Virus Genome and Protein Functions

CSFV is enveloped and contains a single-stranded, positive sense RNA genome, approximately 12.3 kb in length. This RNA contains a single, long, open reading frame (ORF), encoding a large polyprotein, flanked by 5'- and 3'-UTRs (Lindenbach et al., 2013) that are critical for the autonomous replication of the genome (Collett et al., 1988; Meyers et al., 1989). The genome lacks a 5' cap and 3' poly(A) tail. Cap-independent translation initiation is mediated by the internal ribosome entry site (IRES). The polyprotein is co- and post-translationally processed by cellular and viral proteases to yield 12 mature cleavage products: 4 structural (C, E^{rns}, E1 and E2) and 8 non-structural (N^{pro}, p7, NS2, NS3, NS4A, NS4B, NS5A, and NS5B) (**Figure 2**) (Lindenbach et al., 2013).

5'- and 3'-UTR

The 5'- and 3'-UTRs are approximately 373 and 228 nt in length, respectively, and form stem-loop structures at the ends of the genome (Lindenbach et al., 2013). The 5'-UTR lacks the cap-structure found in cellular mRNAs, and instead harbors an IRES to initiate cap-independent translation (Rijnbrand et al., 1997; Li et al., 2017). The UTRs in pestiviruses have been shown to form extensive secondary structures (Brown et al., 1992; Deng & Brock, 1993), with 70% of the nt in the 5'-UTR being involved in base pairing. Key elements for translation of the CSFV genome have been identified in the 5'-UTR (Fletcher & Jackson, 2002; Friis et al., 2012). The 3'-UTR of pestiviruses consists of four stem-loops with a variable and conserved region. The secondary and tertiary structural motifs in the 3'-UTR are considered to be important functional elements for the negative-strand RNA (Vilcek et al., 1999).

N^{pro}

The N^{pro} (19 kDa) is an autoprotease with approximately 168 amino acids (aa) (Ruggli et al., 2005). It is a cysteine protease and the *cis*-acting protease activity results in the release of N^{pro} from the polyprotein (Rümenapf, 1998). N^{pro} is required for virulence in animals, but is dispensable for pestivirus replication in cell culture (Behrens et al., 1998; Tratschin et al., 1998; Moser et al., 1999; Tautz et al., 1999; Mayer et al., 2004). N^{pro} inhibits interferon (IFN) production (Ruggli et al., 2003, Ruggli et al., 2005; La Rocca et al., 2005; Gil et al., 2006; Chen et al., 2007) by targeting the cellular transcription factor IFN regulatory factor (IRF) 3 and IRF7 for degradation, thereby decreasing the antiviral reaction in the cells (Ji et al., 2015). However, CSFV mutants that lack this inhibitory activity still remain virulent in animals (Ruggli et al., 2009).

a

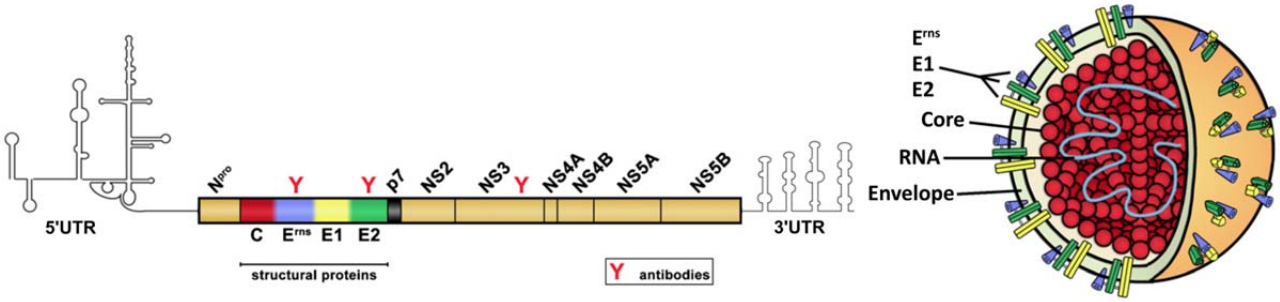

b

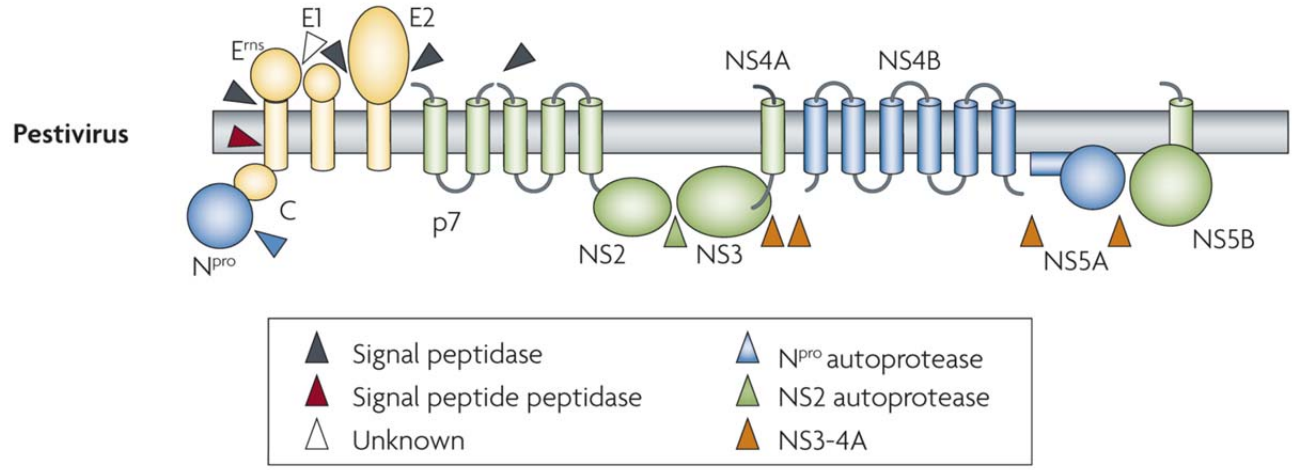

Figure 2

Schematic representation of the genome organization, topology and virion of CSFV. a) The single stranded positive-sense RNA genome of CSFV (12.3 kb) contains 5'- and 3'- untranslated regions (UTRs) and a large open reading frame (ORF) that encodes a large polyprotein. The polyprotein is processed into four structural and eight nonstructural proteins by cellular and viral proteases. Antibodies are mainly generated against E^{rns}, E2 and NS3. Modified from Beer et al., 2007 and Li et al., 2017.

b) Processing and putative topologies of pestivirus polyproteins. Structural proteins are shown in yellow, and non-structural proteins are shown in green or blue (depending on their requirement for infectious virus production or not, respectively). Modified from Murray et al., 2008a.

C

The core (C) protein (14 kDa) is an RNA binding protein that influences the host gene expression and is approximately 99 aa, highly basic, rich in lysine and arginine residues (Liu et al., 1998; Heimann et al., 2006; Murray et al., 2008b). The C protein has been shown to be dispensable for virus propagation in cell cultures, but important for virulence of the virus (Riedel et al., 2012). The N-terminus is generated by the

autocleavage of N^{pro} (Wiskerchen et al., 1991), and the C-terminus is generated by cleavage by a host signal peptidase (Heimann et al., 2006). The C protein includes a C-terminal signal peptide that leads to translocation of E^{rns} into the endoplasmic reticulum (ER) (Heimann et al., 2006). The C protein may be involved in the small ubiquitin-like modifier (SUMO)ylation pathway by interacting with SUMO-1 and SUMO conjugating enzyme UBC9, which ultimately mediates virus proliferation by unknown functions of the C protein (Gladue et al., 2010) and immune evasion of CSFV (Ji et al., 2015).

E^{rns}

The E^{rns} (short for envelope protein RNase secreted) is a glycoprotein (44 kDa) of 227 aa (van Gennip et al., 2000), which is heavily glycosylated with carbohydrate moieties at seven arginine glycosylation sites (Langedijk et al., 2002; Branza-Nichita et al., 2004). Neutralizing antibodies against E^{rns} are induced in the host during infection (Weiland et al., 1992). E^{rns} is, in general, present as a homodimer (Thiel et al., 1991) and a heterodimer with E2 in the virion (Lazar et al., 2003). E^{rns} associates with membranes and virus particles via its C-terminal amphipathic helix (Fetzer et al., 2005; Tews & Meyers, 2007). It has no transmembrane domain and can be secreted in soluble form from infected cells after maturation (Weiland et al., 1992, Weiland et al., 1999; Rümenapf et al., 1993). E^{rns} possesses ribonuclease (RNase) activity, can regulate the synthesis of RNA in host cells, inhibits protein synthesis, induces lymphocyte apoptosis and inhibits the induction of type I IFN signaling, and thereby inhibits early-stage immunization of the host (Lindenbach et al., 2013; Ji et al., 2015; Li et al., 2017). Mutations in E^{rns} that destroy the enzymatic activity give rise to attenuated viruses *in vivo* (Meyer et al., 2002; von Freyburg et al., 2004; Meyers et al., 2007). E^{rns} mediates virus attachment through interactions with host membrane associated heparan sulfate (HS) (Hulst et al., 2000) or laminin receptor (LamR) (Chen et al., 2015), and can attach to the cell surface of various species (Hulst & Moormann, 1997). Cleavage of E^{rns} and E1 is processed by the host signal peptidase in the ER lumen (Bintintan & Meyers, 2010).

E1

The E1 glycoprotein (33 kDa) consists of 195 aa and contains three *N*-linked putative glycosylation sites (Weiland et al., 1990) and six cysteine residues. E1 is a type I transmembrane protein with an N-terminal ectodomain and a C-terminal hydrophobic anchor that attaches E1 to the envelope of the virus (Weiland et al., 1990; Thiel et al., 1991). E1 and E2 form heterodimers via disulfide bridges between cysteine residues. These heterodimers are located on the lipid envelope and mediate virus attachment and entry (Wang et al., 2004; El Omari et al., 2013).

E2

The E2 glycoprotein (55 kDa) consists of 373 aa and is the major neutralizing antigen and induces protection against lethal virus challenge (König et al., 1995; Yu et al., 2001; Li et al., 2007; Sun et al., 2011). E2 contains six *N*-linked and one *O*-linked putative glycosylation sites (Risatti et al., 2007b). E2 is like E1, a type I transmembrane protein with a transmembrane domain in its C-terminus that attaches E2 to the viral envelope (Risatti et al., 2007b; Y. Li et al., 2013). E2 has also been characterized as a truncated class II fusion protein harboring an internal fusion peptide (Garry & Dash, 2003; Holinka et al., 2016). The E2 glycoprotein forms disulfide-linked homodimers or E1-E2 heterodimers (Weiland et al., 1990; Wensvoort et al., 1990; Thiel et al., 1991; Rümenapf et al., 1993). Heterodimer formation is necessary for viral entry and involves the interaction of charged residues within the transmembrane domains of E1 and E2 (Hulst & Moormann, 1997). Cleavage between E1 and E2 is carried out by the host signal peptidase located in the ER lumen (Bintintan & Meyers, 2010).

p7

p7 is a two-transmembrane viroporin protein (7 kDa) consisting of 70 aa (Elbers et al., 1996). Pestivirus p7 can form ion channels *in vitro* and *in vivo* (Griffin et al., 2004; Luscombe et al., 2010). p7 is required for the formation of infectious virions (Harada et al., 2000; Liang et al., 2009), and plays a role in virulence of CSFV *in vivo* (Gladue et al., 2012) but it is dispensable for CSFV RNA replication (Behrens et al., 1998). It is a short-lived protein degraded by the proteasome and induces secretion of the pro-inflammatory cytokine interleukin (IL)-1β, which is a fundamental reaction of the innate immune response against viral infection (Lin et al., 2014). Cleavage between E2 and p7 is carried out by host signal peptidases, as is the cleavage between p7 and NS2 (Bintintan & Meyers, 2010).

NS2-3

The nonstructural protein NS2-3 (120 kDa) consists of 1140 aa. Processing of NS2-3 is carried out by the *cis*-cleavage of the cysteine autoprotease activity of NS2 (Lackner et al., 2005, Lackner et al., 2006). NS2-3 cleavage is essential for pestivirus replication. The NS2-3 cleavage is incomplete, and the uncleaved NS2-3 is essential for the generation of infectious virions (Agapov et al., 2004; Moulin et al., 2007). NS2-3 recruits NS4A to form the NS2-3-4A complex needed to produce infectious virus particles (Moulin et al., 2007; Lamp et al., 2013). The NS2 autoprotease and NS3 consist of 457 aa and 683 aa, respectively (Lackner et al., 2006; Lamp et al., 2013). The NS3 protein is a multifunctional protein that acts as a serine protease, helicase and nucleoside triphosphatase (NTPase) and plays an important role in transcription and translation (Sheng et al., 2007). NS3 and its co-factor, NS4A, process all downstream cleavages of nonstructural proteins (Tautz et al., 2000), through *cis*-cleavage of NS3-4, and *trans*-cleavage of NS4A-4B-5A-5B (Ji et al., 2015).

NS4A

The nonstructural protein NS4A (10 kDa) consists of 64 aa and is a cofactor of the NS3 serine protease. It influences RNA replication and the formation of infectious virus particles (Xu et al., 1997; Tautz et al., 2000; Moulin et al., 2007).

NS4B

The nonstructural protein NS4B (38 kDa) consists of 347 aa and exhibits NTPase activity (Gladue et al., 2011). It is a multi-spanning membrane protein that associates with rearranged cellular membranes involved in RNA replication (Weiskircher et al., 2009).

NS5A

The nonstructural protein NS5A (58 kDa) consists of 497 aa and is essential for RNA replication, but its exact functions have not been fully elucidated (Grassmann et al., 2001; Tellinghuisen et al., 2006). It can stimulate the assembly of polyproteins and inhibit transcription and translation (Xiao et al., 2009; Sheng et al., 2010). It has been reported that NS5A can induce autophagy of host cells, thereby enhancing viral replication and maturity of CSFV in host cells, and it may be related to immune evasion (Pei et al., 2014).

NS5B

The nonstructural protein NS5B (75 kDa) is the RNA-dependent RNA polymerase (RdRp) consisting of 718 aa that binds to 3'-CCCGG in the positive strand and 3'-CAUAUGCUC of the negative strand to initiate transcription (Xiao et al., 2002, Xiao et al., 2004, Xiao et al., 2006). The pestiviral NS5B proteins exhibit the typical general fold of RdRp, resembling a right hand with fingers, thumb and palm domains (Choi et al., 2006). NS5B preferentially binds to negative-strand RNA to produce more positive-strand RNA during RNA replication (Xiao et al., 2004).

Virus Life-cycle

The life cycle of CSFV involves the following essential steps (**Figure 3**):

- Attachment and entry
- Translation and assembly of the replication complex
- RNA replication (transcription)
- Assembly and egress

Attachment and entry

It is assumed that the initial phase of pestivirus infection is at least a two-step process (Hulst & Moormann, 1997), where E^{rns} first mediates contact with the host cell, and then E2 binds to a specific cellular receptor, and internalization is achieved after E1-mediated fusion (Dräger et al., 2015a). Recent studies have

indicated that E1 contains the fusion motif and E2 acts as a structural scaffold for E1, based on the crystal structure analysis of the BVDV E2 protein (Y. Li et al., 2013; El Omari et al., 2013). The route of infection of CSFV is likely similar to that of BVDV, as inhibition experiments have shown that both CSFV and BVDV displayed decreased infectivity in the presence of CSFV E2 (Hulst & Moormann, 1997). It has been shown that the main cellular receptor for BVDV is the bovine complement regulatory protein CD46 (Schelp et al., 2000; Maurer et al., 2004; Krey et al., 2006). Porcine CD46 seems to play an important role as a cellular receptor for CSFV. However, it is not the only component involved (Dräger et al., 2015a). HS and LamR are also indicated as attachment receptors for CSFV (Hulst et al., 2000; Chen et al., 2015; Dräger et al., 2015a). HS is a common receptor, ubiquitously present on the surface of many cell types and used by various viruses for attachment (Sawitzky et al., 1990; Jackson et al., 1996; Germi et al., 2002; Misinzo et al., 2006; Madu et al., 2007). LamR is also a known receptor for dengue virus (Tio et al., 2005), which also belongs to the *Flaviviridae* family.

The cell entry process of CSFV through a dynamin-dependent, cholesterol-dependent, clathrin-mediated endocytosis is consistent with that used by BVDV (Lecot et al., 2005; Zürcher et al., 2014; Shi et al., 2016). Membrane cholesterol also seems to play an important role in CSFV internalization (Shi et al., 2016), and has also been reported to be involved in other stages of the virus life cycle, such as egress (Brogden et al., 2015). Clathrin-mediated endocytosis is used by many enveloped viruses (Sieczkarski & Whittaker, 2002; van der Schaar et al., 2008). A recent study by Shi *et al.* (2016) indicated that pestiviruses require Rab proteins and fusion with an acidic endosomal compartment for clathrin-mediated endocytosis. It appears that CSFV particles are first transported to the early endosomes and then guided to the late endosomes through a Rab5- and Rab7-dependent manner, respectively (Shi et al., 2016). The fusion between cellular membranes and the virus envelope is pH dependent and is triggered by the acidification of the endosome (Lecot et al., 2005; Shi et al., 2016). It has also been demonstrated that the E2 mediates fusion between the viral envelope and the cellular membrane (Fernández-Sainz et al., 2014; Holinka et al., 2016). CSFV uncoating likely depends on endosomal maturation and the late endosomal environment may provide an important signal for RNA release (Shi et al., 2016). After uncoating, the viral genome is released into the cytosol (Lindenbach et al., 2013).

Translation and assembly of the replication complex

After entry of the virus and release of the viral RNA into the cytosol, the positive-stranded RNA can serve directly as mRNA. The ribosomes binds directly to the IRES and cap-independent translation (Fletcher & Jackson, 2002) gives rise to a polyprotein that is co- and post-translationally processed by viral and cellular proteases (Lindenbach et al., 2013). Once the NS3 protein has been released by NS2, NS3 interacts with NS4A and the downstream nonstructural proteins to form the replication complex on the ER membranes,

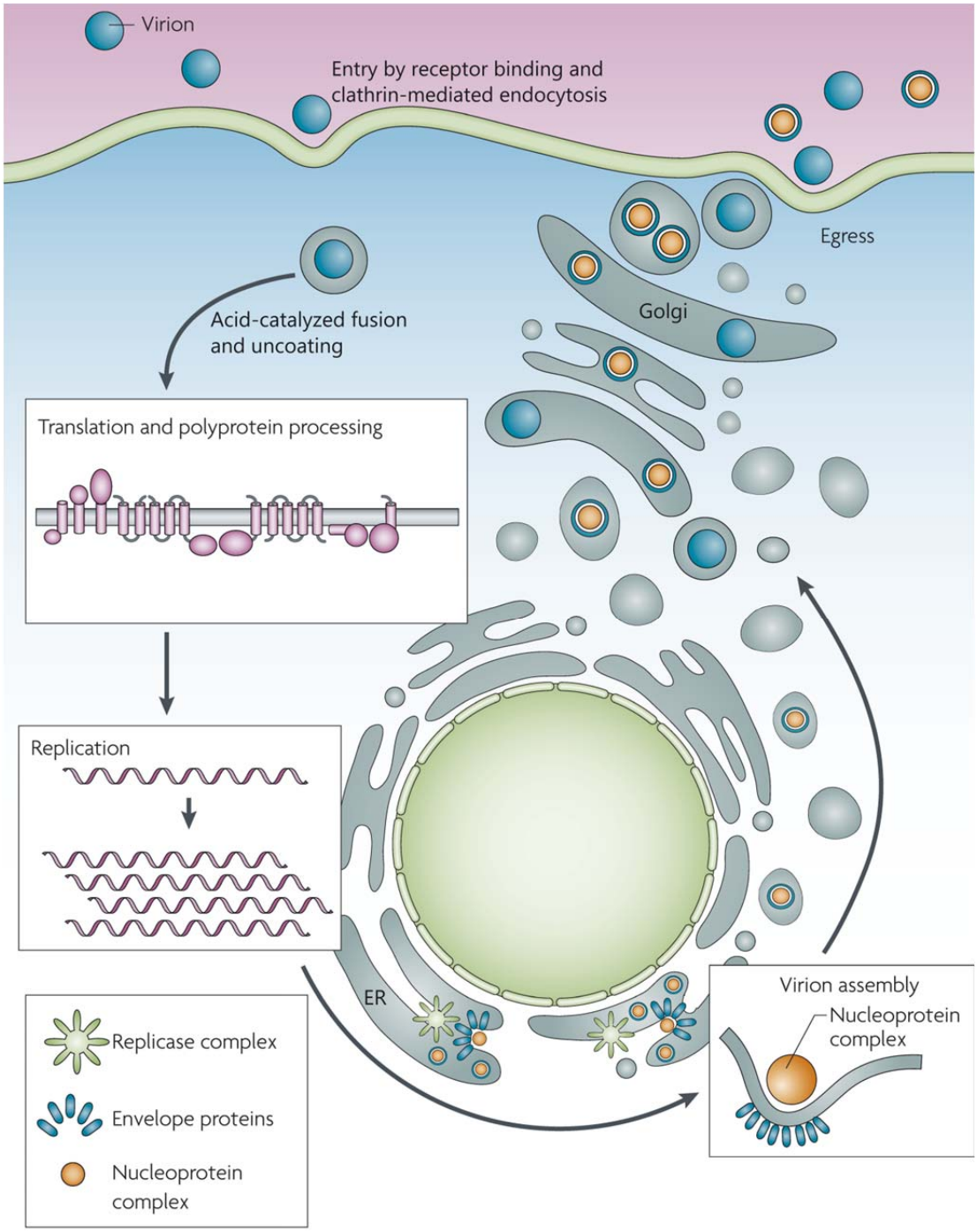

Figure 3

Schematic representation of the life cycle of CSFV. Interactions between E^{rns} and host cellular receptors, heparan sulfate and/or laminin receptor, mediate virus attachment. Virus then binds to unknown entry receptor(s) and triggers clathrin-dependent endocytosis. Low pH in the endosomes facilitates viral envelope and membrane fusion. Translation and processing of viral proteins and viral genome replication takes place at the ER lumen. Virion morphogenesis occurs by unknown mechanism. Mature virions are released from the cell via an unknown secretory pathway. Modified from Murray et al., 2008a.

where negative-strand RNA templates and viral progeny genomes are produced (Xu et al., 1997; Tautz et al., 2000; Lackner et al., 2004; Moulin et al., 2007). NS3 can bind to IRES and promote IRES-mediated translation (Xiao et al., 2008). NS5A on the other hand, inhibits IRES-mediated translation, whereas NS5B can suppress the effect of NS5A on the IRES (Sheng et al., 2012) and also stimulates NS3 to increase the efficiency of viral genome translation (Xiao et al., 2008). NS2-3 binds to NS4A and together they recruit NS4B, NS5A, and NS5B to form the replication complex (Moulin et al., 2007), which is associated with altered intracellular membranes on the surface of the ER (Salonen et al., 2004).

RNA replication

The CSFV genome is transcribed into negative-strand RNA that can then function as the template to produce the positive-strand RNA. The RNA synthesis is carried out by the NS5B, which binds to the 3'-UTR of the positive-strand RNA (Gong et al., 1996). NS5A regulates viral RNA synthesis through interacting with NS5B and the 3'-UTR (Chen et al., 2012). NS5A preferentially interacts with NS5B at lower expression levels in the cells, however, when the level of NS5A exceeds a certain threshold it will interact with the 3'-UTR and thus inhibit viral RNA replication (Xiao et al., 2009; Chen et al., 2012). The NS2-mediated cleavage of NS2-3 and its temporal modulation by the cellular cofactor DNAJC14 (originally identified as Jiv) is an essential process in the pestivirus life cycle (Lackner et al., 2004, Lackner et al., 2005, Lackner et al., 2006), acting as a switch between RNA replication and infectious particle formation (Moulin et al., 2007). Reduced cleavage between NS2 and NS3 during the later stage of infection provides uncleaved NS2-3 that associates co-translationally with NS4A and enters the particle assembly process. Another consequence of this reduction in cleavage is decreased viral RNA replication, as NS2-3 cannot functionally replace NS3 in the replication complex (Lackner et al., 2004).

Assembly and egress

Virion morphogenesis is mediated by NS2-3 and NS4A (Moulin et al., 2007). Not much is known about the assembly and release of pestiviruses. Electron microscopic examinations of infected cells have suggested that pestiviruses mature in intracellular vesicles and are released by exocytosis (Bielefeldt Ohmann & Bloch, 1982; Gray & Nettleton, 1987). Pestivirus envelope proteins are retained within the secretory pathway, which is consistent with intracellular budding (Greiser-Wilke et al., 1991; Weiland et al., 1999). Assembly is assumed to take place in the ER lumen (Grummer et al., 2001). Virus particles have been shown in intracellular vesicles and the Golgi complex, as well as during exocytosis (Schmeiser et al., 2014). Considerable amounts of infectious virus remain cell-associated (Danner & Bachmann, 2010).

Quasispecies

Positive-stranded RNA viruses evolve rapidly due to error-prone RNA replication and the lack of proof-reading activity of the RdRp, thus making them unable to correct mistakes made during replication (Drake et al., 1998). The mutation rate determines the average number of mutations each progeny molecule will have compared to the parental genome (Peck & Lauring, 2018). RNA viruses have mutation rates ranging between 10^{-6} and 10^{-4} mutations per nt copied (Lauring & Andino, 2010; Peck & Lauring, 2018), which is orders of magnitude greater than those of nearly all DNA-based viruses and organisms (Batschelet et al., 1976; Holland et al., 1982; Steinhauer & Holland, 1987). The high evolutionary rates of many viruses have been attributed to the large population sizes, short generation times, and high mutation rates, as well as additional factors such as within-host dynamics (e.g. virus growth rate, virus clearance rate, cell infection rate, cell death rate, etc.) or cell tropism. When it comes to viruses, the mutation rate is the rate at which errors are made during replication of the viral genome, whereas the substitution rate is the rate at which mutations become fixed in a population (Peck & Lauring, 2018). Evolutionary theory predicts that high mutation rates are favored in dynamic environments, as the short-term cost of mutation is in equilibrium with the long-term benefit of adaptability, and viral error rates may have been optimized by natural selection (Holmes, 2003; Elena & Sanjuán, 2005). Studies of viral mutational fitness effects show that most mutations are lethal or deleterious, a minority are neutral, and only a few are actually beneficial (Sanjuán et al., 2004; Carrasco et al., 2007; Domingo-Calap et al., 2009; Sanjuán, 2010; Cuevas et al., 2012; Fahnøe et al., 2015; Visher et al., 2016).

The high evolutionary rate causes the RNA virus population to exist as a quasispecies of different, but closely related variants (Domingo, 1978; Peck & Lauring, 2018). Quasispecies are often depicted using the concept of sequence space, a geometric representation of all possible variants (**Figure 4**), where the physical distance reflects genetic similarity. After each round of viral genome replication, the viral progeny will differ at roughly one nt position due to the error rate of the RdRp. Subsequent rounds for replication will introduce more errors into the genome, thereby creating a more and more complex distribution of variants, lying farther away from each other in sequence space. This ensemble of mutants forms a 'cloud' of variants, or viral quasispecies, that are genetically linked through mutation, interact cooperatively on a functional level, and collectively contribute to the characteristics of the population (Lauring & Andino, 2010). The low fidelity of RNA viruses allows them to create a large population size to continuously 'sample' the so-called sequence space around the parental genome sequence (Whitfield & Andino, 2016). These variants form a flat fitness landscape in sequence space of a selectively neutral network of variants, making the population more robust to withstand mutations and evade host responses, as a flat quasispecies can explore vast regions of sequence space without consequence. This effect has been termed the survival of

the flattest (Wilke, 2005; Lauring & Andino, 2010). Within the sequence space, certain variants, or haplotypes, may exist either with single nt changes or, alternatively, predominantly in combination with other changes within the same genome. A low fitness variant can be maintained at higher than expected frequency if it is linked to a well-represented haplotype (Lauring & Andino, 2010). Fitness of a particular virus sequence may not rely on its own replicative capacity, but more on its freedom to mutate into related variants. Individual clones isolated from a virus population typically displays lower than average fitness values than the entire population from which they were isolated, indicating that complementation occurs among variants of the quasispecies population (Domingo, 1978; Duarte et al., 1994).

Quasispecies are not independently acting variants, as the internal interactions of the variants determine the overall behavior of the viral population (Domingo et al., 2012). The functional interactions among genetically distinct variants is therefore of critical importance to pathogenesis in infected hosts (Lauring & Andino, 2010). However, viruses with little quasispecies diversity can also have highly virulent phenotypes (Ojosnegros et al., 2010). Consensus sequences are commonly determined as they serve as the basis for virus identification, determining phylogenetic relationships among viral isolates, or elucidate the drive behind virus evolution, such as selection and random drift (Domingo et al., 2012). Invariant consensus sequences do not reflect an absence of mutations, rather a continuous replenishment of the mutant pool to yield the same average. The consensus sequence may change as a result of modifications of the equilibrium of the variants or a random bottleneck event. At any given time the quasispecies can be considered a cloud in sequence space, which shifts its position (ergo variant composition) in response to

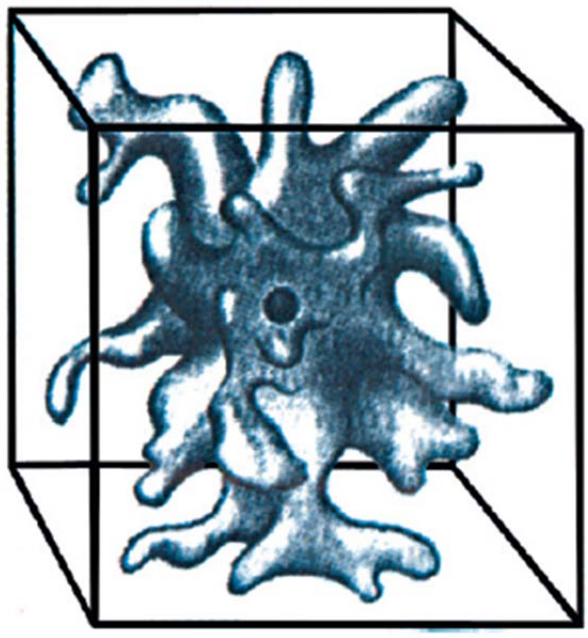

Figure 4

Depiction of the quasispecies concept in sequence space. The box represents the sequence space, i.e. the confines of all possible variant that might occur through viral replication. The central spot represent the parental (or ancestral) sequence. The 'cloud' represents the viral population diversity. From MacLachlan & Dubovi, 2010.

selective forces (immune response, antiviral agents, etc.), or if a new cloud is started as result of a bottleneck or founder event. Bottleneck events seem to be frequent in the course of the life cycles of viruses, not only in the most obvious case of host-to-host transmission, but also during intra-host spread of virus (Domingo et al., 2012). Many viruses operate near a threshold of 'error catastrophe', which is the maximum error rate compatible with the maintenance of the genetic information for any given complexity (amount of non-redundant genetic information conveyed by a replicative system) (Eigen & Schuster, 1977; Domingo et al., 2012). According to the original formulations of quasispecies theory, a quasispecies can remain at equilibrium despite a high mutation rate (Eigen, 2002; Biebricher & Eigen, 2005). However, a small increase in mutation rate will upset this equilibrium as the master sequence itself will disappear, and meaningful information is lost in an avalanche of errors (Lauring & Andino, 2010; Domingo et al., 2012).

The diversity and quasispecies composition of CSFV and other pestiviruses have not been studied in great detail. Limited analyses of the evolutionary forces that drive sequence change and the role of the quasispecies composition as a determinant of virulence have been reported (Töpfer et al., 2013; Rios et al., 2017). Quasispecies diversity *per se* does not seem to be responsible for virulence of CSFV, as viruses rescued from CSFV cDNA clones of highly virulent isolates 'Eystrup' and 'Brescia' triggered severe clinical signs *in vivo* (Mayer et al., 2003; Risatti et al., 2005). Furthermore, highly virulent CSFV cDNA clones have been shown to be generated on the basis of the consensus sequence alone (Fahnøe et al., 2014). It is expected that the quasispecies derived from cDNA clones are a lot less diverse than those of field strains, due to having less time to evolve. Recent studies have shown that a majority of field virus variants are non-functional (Fahnøe et al., 2015). CSFV appears to be stable at the quasispecies level under chronic conditions (Jenckel et al., 2017), which contrasts with what is seen during persistent infection (PI) with BVDV and Hobi-like pestiviruses , where the viral populations differ widely in size and diversity in infected animals (Dow et al., 2015; Ridpath et al., 2015; Weber et al., 2016). An increase in genetic variability of the viral quasispecies was observed over time in Hobi-like PI animals (Weber et al., 2017), and in BVDV PI animals, the viral populations were genetically distinct between different body compartments, likely due to local selection pressures (Dow et al., 2015).

Role of CSFV Glycoprotein E2

The glycoprotein E2 is the major surface component of the virion; it is essential for virus replication and is the main immunogen (Hulst & Moormann, 1997). It has been implicated, together with E^{rns} and E1, in virus adsorption to host cells (Hulst & Moormann, 1997; van Gennip et al., 2000; Liang et al., 2003; Wang et al., 2004), and for determining tropism in cell culture (van Gennip et al., 2000; Liang et al., 2003). Chimeric pestiviruses exhibit infectivity and cell tropism phenotypes consistent with those of the E2 donor (van

Gennip et al., 2000; Liang et al., 2003). The E2 glycoprotein shows a high variability among different CSFV strains (Leifer et al., 2012). Modifications introduced into this glycoprotein can have an important effect on CSFV virulence (van Gennip et al., 2004; Risatti et al., 2005, Risatti et al., 2006, Risatti et al., 2007a, Risatti et al., 2007b).

Homology modeling of CSFV E2, based on the BVDV-1 E2 structure, shows that the E2 monomer is an elongated molecule consisting of four structural domains, DA, DB, DC, and DD (**Figure 5**) (Rios et al., 2017). The DA domain (residues 689-776) contains a chain formed by six β-sheets with Ig-like folding. The DB domain (residues 777-852) showed similar structural composition and folding to the DA-domain. The DC domain (residues 853-959) consists of a series of small β-sheet modules. The DC-folding and topology share significant similarity with the BVDV-1 E2 template structure. The DD domain (residues 960-1021) is the most conserved domain among pestiviruses and is predicted to have an almost identical shape to the template structure (Rios et al., 2017). Four antigenic domains have been identified, A-D, in the N-terminal half of the E2. They constitute two independent antigenic units, antigenic domains B/C (residues 689-779) and A/D (780-859) (Wensvoort, 1989; Wensvoort et al., 1990; van Rijn et al., 1994), located in the structural DA and DB domains (Rios et al., 2017). According to the model by Rios *et al.*, disulfide bridges link C693-C737 in the DA domain and C818-C856 connect DB to DC, and there are three additional links in DC between residues C869-C877, C893-C914, and C896-C930 (Rios et al., 2017). However, it was previously thought that the antigenic domains A/D were linked by two disulfide bonds between C792-C856 and C818-C828 (van Rijn et al., 1994). The antigenic domain B/C are responsible for the antigenic specificity of various CSFVs, while the antigenic domains A/D of various CSFVs are relatively conserved (Chang et al., 2010a, Chang et al., 2010b). Both conformation-dependent and linear epitopes are present in the antigenic domains (van Rijn et al., 1993, van Rijn et al., 1994; Yu et al., 1996; Lin et al., 2000; Zhang et al., 2006; van Rijn, 2007; Peng et al., 2008; Chang et al., 2010a; Kortekaas et al., 2010). A linear epitope, ^{772}LFDGTNP^{778}, has been identified at the border between antigenic domains B/C and A/D (Peng et al., 2008). A highly conserved linear epitope, ^{829}TAVSPTTLR^{837}, located in domain A/D (Lin et al., 2000), has been used to develop epitope-based vaccines (Reimann et al., 2010; Tarradas et al., 2011). Recently, the linear epitope ^{753}RYLASLHKKALPTSV^{767} in domain B/C was identified using a set of synthetic cyclized peptides and monoclonal antibodies (mAbs), and specific residues K761, L763 and P764 were identified as being critical for the reactivity of the epitope with mAbs (Chang et al., 2012). We have termed the residues 761-764 the 'SL'-motif.

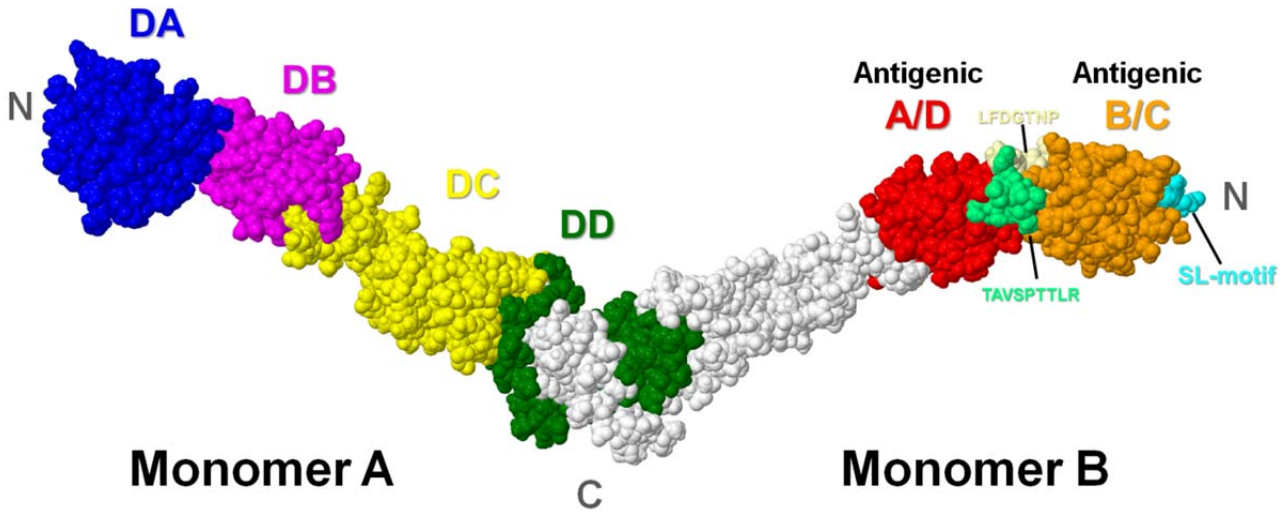

Figure 5

Cartoon and surface predicted model of E2 homodimer of CSFV. Structural domains are represented on monomer A from the N-terminus DA (dark blue), DB, (magenta), DC (yellow), and DD (dark green). Positions of the antigenic regions B/C (orange) and A/D (red) were located on monomer B. The linear epitopes LFDGTNP (residues 772-778, light yellow) and TAVSPTTLR (residues 829-837, light green) are also represented, as well as the SL-motif (residues 761-764; cyan). Modified from Rios et al., 2017 in Geneious (Biomatters, Auckland, New Zealand).

Virulence

Several studies have indicated that modification introduced into E2 have an important effect on the virulence of CSFV. However, the virulence determinants are still far from being understood, and do not seem to be transferrable among strains (Blome et al., 2017a). Substitution of E2 in the highly virulent strain Brescia with that of a vaccine strain leads to attenuation (Risatti et al., 2005). It was later determined that it was the 12 residues (T886M, P889L, Q892R, S927L, T928A, H955R, D958G, A975E, R979S, A988T, R994K, and I1032V) in the carboxyl-terminus of E2, between residues 882 and 1032, which were responsible for the attenuation (Risatti et al., 2007a). Replacing the conserved linear epitope ^{829}TAVSPTTLR^{837} with the corresponding sequence of BVDV-1 NADL strains also produced a significant attenuation of the highly virulent parental strain (Risatti et al., 2006). Specifically residue 830 seems to play an important role for virulence and viral spread in swine cells. T830A was identified, together with two substitutions in NS4B (V2475A and A2563V) as being responsible for the restoration of virulence to the GPE$^-$ vaccine strain into its natural host after multiple passages in pigs (Tamura et al., 2012). Recently, aa changes S763L and P968H were shown to cause the attenuation of highly virulent CSFV strain Koslov in swine (Fahnøe et al., 2014).

Residue 710, in combination with point mutations in E^{rns}, has also been implicated in reduced virulence of CSFV strain Brescia (van Gennip et al., 2004). M979K has been found to be responsible for enhancement of viral replication and pathogenicity in the attenuated chimeric vSM/CE2 backbone (highly virulent strain Shimen containing the E2 of the C-strain vaccine), but R979S in CSFV strain Brescia did not influence replication or virulence (Risatti et al., 2007a; Wu et al., 2016). The glycosylation sites at residue 805 and in the regions between residues 805 and 837 have been found to be important determinants of virulence of the CSFV strain Brescia (Risatti et al., 2007b). Introducing synonymous mutations in the E2 by de-optimizing the codon pair bias also causes attenuation (Velazquez-Salinas et al., 2016). However, no remarkable difference in codon usage has been related to virulence in CSFV (Tao et al., 2009; Leifer et al., 2011).

Numerous sites under positive selection have been described, such as residues 702, 706, 707, 709, 711, 716, 723, 725, 730, 738, 747, 750, 761, 764, 767, 776, 777, 889, 929, and 972 (Tang et al., 2008; Shen et al., 2011; Pérez et al., 2012; Ji et al., 2014; Hu et al., 2016; Rios et al., 2017). An additional three residues which are under selection have been described for gt 1 (residues 854, 857, and 884) and five for gt 2 (residues 692, 779, 780, 868, and 881) (Yoo et al., 2018). Residues 713, 725, 761, and 854 contribute to the antigenic incompatibility between gt 1 and 2, as these residues affect the recognition by anti-C-strain pig polyclonal serum (Chen et al., 2010; Chang et al., 2012). Interestingly, comparison of low virulent strain CSFV/Spain-01 and virulent strain Margarita revealed aa replacements in sites under positive selection pressure (D723S, N725G, T738V, G761R and S777N), suggesting that these changes could be involved in the viral escape from neutralizing antibodies (Pérez et al., 2012).

Alignment of the E2 proteins from cell culture-adapted vaccine strains with different CSFV strains revealed residues I745, S763, L764, G864, V917, and D940 to be unique to the virulent strain and absent from the vaccine strains (Kumar et al., 2015). Site-directed mutagenesis has demonstrated that residues at positions 705, 713, 729 and 761 are responsible for the differences in antigenicity between vaccine and field strains (Chang et al., 2010b). Only 7 aa substitutions (G761R, L763S, I780V, H852Y D899V, L957S, and T1028A) were found to differ in the E2 between the virulent strain Margarita and the low virulent strain Pinar del Rio isolated in Cuba (Coronado et al., 2017).

‘SL’-Motif

The ‘SL’- motif in E2 comprises residues 761-764, where residue A762 is highly conserved among CSFV strains of all genotypes and virulence (**Figure 6**). As mentioned above, residues K761, L763 and P764 were identified as being critical for the reactivity of E2 with mAbs (Chang et al., 2012). Several studies have also indicated that residue 761, especially, is under positive selection (Tang et al., 2008; Wu et al., 2010; Pérez

et al., 2012; Hu et al., 2016; Rios et al., 2017) and that residue 761 influences the virulence of field strains, and promotes virus escape from the host immune response (Pérez et al., 2012; Hu et al., 2016).

Residues R761, L763 and P764 are the most common variants in CSFV strains (**Figure 6 A**). especially in gt 2 (**Figure 6 C**), which contains mostly moderately virulent strains (Leifer et al., 2011). The gt 1, consisting of high virulence, low virulence and avirulent strains (Leifer et al., 2011), is more varied at residue 761 (G, E, R, K, and D), with highly virulent strains containing E, G, and D at residue 761, while K761 and R761 are only observed in vaccine strains (**Figure 6 E**). The gt 1 shows variation at residues 763 (L and S), and 764 (L and P) (**Figure 6 B**). No residue other than L763 is observed in the vaccine strains, whereas residues P, L, and S are observed for position 764. Residues E761, S763, and L764 are observed in the highly virulent CSFV strains

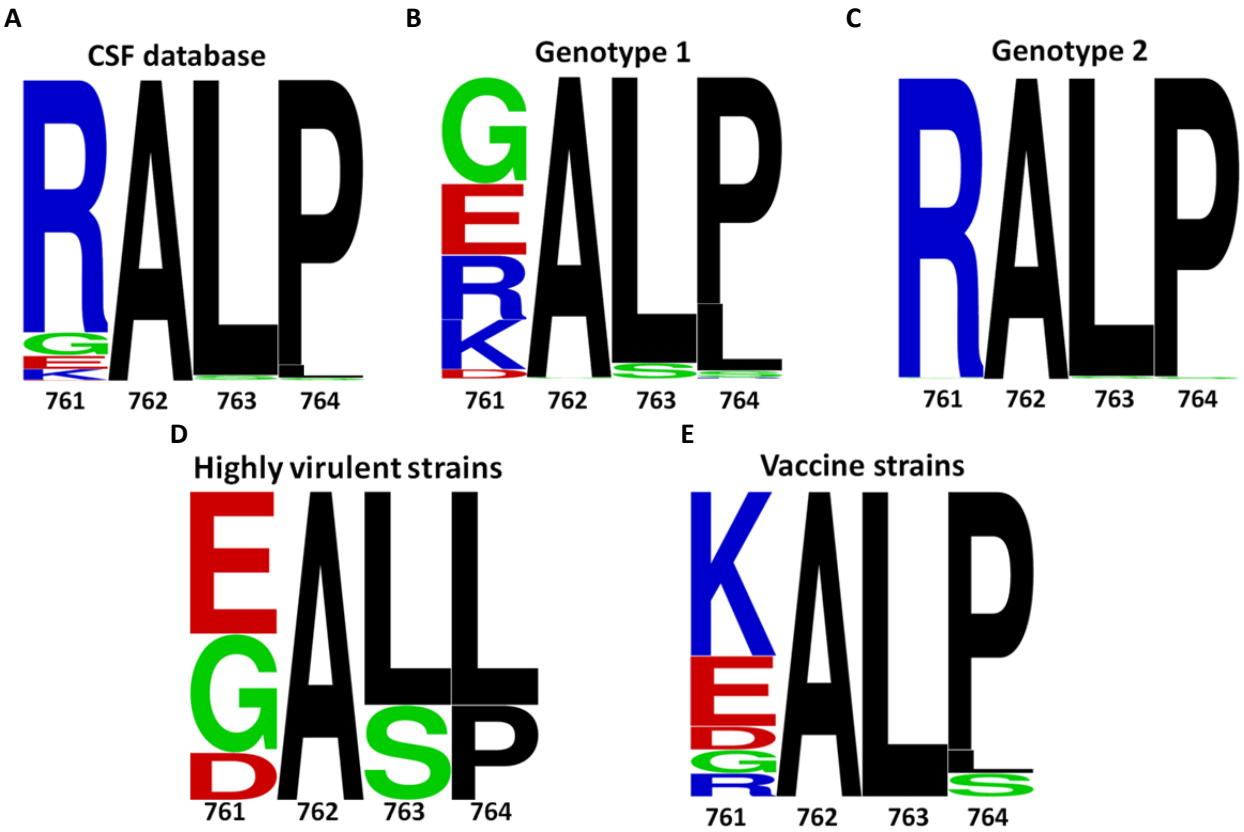

Figure 6

Sequence logos of the 'SL'-motif residues. A) E2 fragments from the CSF database. B) E2 fragments of the CSF database filtered for genotype 1. C) E2 fragments of the CSF database filtered for genotype 2. D) Complete coding sequence (CDS) of CSFV high virulent strains of genotype 1. E) CDS of vaccine strains of genotype 1. Sequence logos were made using WebLogo (Crooks et al., 2004), based on multiple alignments of translated nucleotide sequences in MAFFT using Geneious (Biomatters, Auckland, New Zealand). E2 fragment sequences (190 nt) were obtained from the CSF database (Postel et al., 2016b). CDS were identified according to virulence status (Leifer et al., 2011) and obtained from GenBank (Clark et al.).

Koslov, Brescia, Eystrup and ALD, however, E2 sequences of Koslov in the CSF database of the European Reference Laboratory (Postel et al., 2016b) also contains the S763L variant for Koslov. This indicates that the S763L is a common variant of wildtype Koslov, as it has also been seen in the viral subpopulation of infected pigs, in previous studies (Fahnøe U, Pedersen AG, Höper D, Beer M, Rasmussen TB., unpublished data). Interestingly, L764P was observed as a minority variant (2%) in pigs inoculated with vKos rescued from the BAC consensus clone Kos, and L764P appeared subsequently at high frequency (100%) in the virus population of an infected contact pig (Fahnøe et al., 2014). The vALD/A76 strain was derived from the highly virulent ALD strain (Leifer et al., 2011) by serial passages in swine testicle cells (Komaniwa et al., 1981), and vALD/A76 exhibits moderate virulence in pigs (Tamura et al., 2012). It contains the L763/L764 motif in combination with K761, in contrast to ALD, and also has a total of 26 non-synonymous substitutions in the coding sequence. Vaccine strains C-strain and GPE^- both contain the K761/L763/P764 motif.

Molecular Virology

The ability to manipulate viral genomes and then determine the phenotype has been very important for understanding the underlying mechanisms responsible for virulence, tropism, replication, etc. Using reverse genetics, sequence specific alterations are made to the genome and then the phenotypic characteristics of rescued viruses are analyzed *in vitro* or *in vivo*. A crucial tool for such studies for RNA viruses is the generation of functional full-length cDNA clones, a process which can be both lengthy and arduous, often requiring many sequential cloning and subcloning steps.

Molecular Cloning of Full-length Pestivirus cDNA

Some of the first pestivirus cDNA clones were of CSFV vaccine strain C-strain (Moormann et al., 1996), CSFV strain Alfort/Tübingen (Meyers et al., 1996), and CSFV strain Alfort/187 (Ruggli et al., 1996). This was followed by other infectious cDNA clones, such as BVDV-1 strain NADL (Mendez et al., 1998), CSFV strain Eystrup and Brescia (Mayer et al., 2003; van Gennip et al., 2004; Risatti et al., 2005). However, many of these cDNA clones were not stable when propagated as multicopy plasmids in bacteria, as mutations were introduced after only a few generations (Ruggli & Rice, 1999; Fan & Bird, 2008). Bacterial artificial chromosomes (BACs) were found to be perfectly suited for the stable maintenance of large sequences derived from viral genomes (Messerle et al., 1997). This system was used to create cDNA clones of the Japanese encephalitis virus (JEV) and dengue virus, two other members of the *Flaviviridae* family (Yun et al., 2003; Pierro, 2006), and subsequently BAC clones have been obtained for BVDV-1 strain SD-1 and CSFV Shimen (Fan & Bird, 2008; C. Li et al., 2013). Using long RT-PCR for full-genome amplification (Rasmussen et

al., 2008) BAC cDNA clones were generated for BDV strain Gifhorn, and CSFV strains Paderborn (gt 2.1), C-strain Riems (gt 1.1), Koslov (gt 1.1) and Roesrath (gt 2.3) (Rasmussen et al., 2010, Rasmussen et al., 2013; Fahnøe et al., 2014, Fahnøe et al., 2015). With the long RT-PCR approach, the individual cDNA clones corresponds to single sequences within the parental viral RNA population that may contain extensive genetic heterogeneity, due to the quasispecies nature of the population. This will be reflected as synonymous and non-synonymous mutations (compared to the consensus sequence of the population), with a range of fitness effects: from lethal (or strongly deleterious) to slightly deleterious, to neutral, slightly advantageous and strongly advantageous (Keightley & Eyre-Walker, 2010). Synonymous mutations may not be selectively neutral due to the existence of secondary RNA structures in RNA virus species (Simmonds et al., 2004; Weaver et al., 2016). Although defective genomes in viral populations seem to be a common occurrence, judged by the identification of stop codons within ORFs, their biological roles are largely unknown (Domingo et al., 2012). Complementation, the process by which a genome expressing a functional protein can promote replication of another closely related genome whose corresponding protein is defective, has been extensively described between viral variants, and it governs the maintenance of defective genomes in viral populations (Domingo et al., 2012). Therefore, the obtained cDNA clones may not correspond to the consensus sequence of the viral RNA population and may not be functional. For example, analysis of multiple cDNA clones from a cell culture passage of the moderately virulent CSFV strain Roesrath showed that all cDNA clones were unique and only a minor proportion (12%) produced infectious RNA transcripts (Fahnøe et al., 2015).

However, using site-directed mutagenesis, a consensus sequence clone can be reconstructed (Fahnøe et al. 2014; Fahnøe et al. 2015). Infection experiments in pigs demonstrated that the virus vKos, rescued from the BAC clone Kos encoding the aa consensus sequence of CSFV Koslov was as virulent as the parental Koslov strain (Fahnøe et al., 2014).

Once full-length cDNA clones have been established, full-length viral RNA can be transcribed *in vitro* using T7 RNA polymerase from a T7 promoter within the BAC clone as a template. Introduction of the RNA into susceptible cells, using electroporation, allows for virus rescue of replication competent viruses, and a subsequent passage is needed to prove infectiousness. The rescued viruses can then be used for animal infection experiments or passaged in cell culture for *in vivo* and *in vitro* study, respectively. Obtaining full-length cDNA clones also represents an approach to identify the individual haplotypes present within a virus population, as even deep sequencing cannot easily resolve the different haplotypes that constitute the whole population (e.g. if single nt polymorphisms (SNPs) are spaced further apart on the genome than the length of the sequencing reads). The individual cDNA clones can also be used for phenotypic characterization.

Cloning Systems

In addition to the standard BAC cloning with restriction enzymes and ligation (e.g. Rasmussen et al., 2010; Fahnøe et al., 2014), we have now established two different improved cloning systems, as described in Johnston et al., 2018 (Manuscript I): (i) In-Fusion cloning into a BAC by *in vitro* recombination, and (ii) cloning into the pCR-XL-2-TOPO vector, a high-copy plasmid, using its built-in topoisomerase activity. They both rely on the production of full-length amplicons from long RT-PCRs of viral RNA using high fidelity DNA polymerases.

Standard BAC cloning

After full-length amplification of cDNA by RT-PCR with a cDNA primer and PCR primers flanked by *Not*I sites, a *Not*I digestion is performed and the cDNA amplicon is purified by gel electrophoresis. The purified cDNA amplicon is then inserted into *Not*I-digested pBeloBAC11 (New England Biolabs) and ligated. After electroporation into *E. coli*, transformants are isolated on selective LB plates. After miniprep plasmid purification of selected colonies, the correct inserts are identified by restriction analysis using *Not*I, and confirmed by long PCR.

In-Fusion cloning

In-Fusion cloning (Clontech, USA) uses *in vitro* recombination to fuse blunt-end PCR-generated sequences and linearized vectors by recognizing a 15 base pair (bp) overlap at their ends. This 15 bp overlap is engineered by designing the long PCR primers with 15 nt 'overhangs' that are homologous to the linearized pBeloBAC11. After the In-Fusion enzyme has fused the insert and vector, chemically competent *E. coli* are transformed, selected, and correct inserts identified as above.

TOPO XL-2 cloning using the pCR-XL-2-TOPO vector

TOPO XL-2 cloning (Thermo Scientific) uses the high-copy number pCR-XL-2-TOPO vector in a linearized form with the *vaccinia* virus DNA topoisomerase I covalently bound to the 3' end of each DNA strand. The topoisomerase functions both as a restriction enzyme and as a ligase, as its biological role is to cleave and rejoin DNA ends during replication. The pCR-XL-2-TOPO vector allows for direct selection of recombinant DNA by disrupting the lethal *E. coli* gene, *ccd*B. The vector is mixed with blunt-ended PCR generated fragment and transformed into *E. coli*. Transformants are isolated on selective LB plates, and the presence of plasmids with the correct size identified by linearization with *Not*I, as it only contains one *Not*I restriction site. Correct insert size is then confirmed by long PCR.

Site-Directed Mutagenesis

Targeted modification of BAC clones is obtained through a site-directed mutagenesis method, known as megaprimer PCR (Risager et al., 2013). The BAC clone is used as template for the megaprimer PCR with a

forward primer containing the desired mutations and a reverse primer further downstream. The generated megaprimer PCR amplicon is purified by gel electrophoresis and used for the site-directed mutagenesis with the BAC clone as vector backbone, to amplify the whole vector. The products are then digested with *Dpn*I, which cleaves methylated and hemi-methylated DNA, to remove the original template. This method can be used to correct cDNA clones to their parental consensus sequence, or to introduce mutations into the virus genome backbone for phenotypic characterization.

Next Generation Sequencing

With next generation sequencing (NGS) techniques, virulence determinants, the role of quasispecies, and viral evolutionary dynamics can be studied at an unprecedented level of detail (Töpfer et al., 2013; Fahnøe et al., 2014; Orton et al., 2015). The relatively short genome of RNA viruses together with the high-throughput nature of the NGS, virus samples (which contain billions of virions) can be analyzed at a very high depth. The diversity of the viral population can be examined and evolutionary events, such as selection and bottlenecks, can be identified through the use of ultra-deep coverage sequencing of the genomes (Orton et al., 2015). The high depth also allows for the identification of important variants present in the viral populations at low frequencies, such as those that increase pathogenicity or virulence (Flaherty et al., 2012). However, as RNA viruses replicate to immense populations sizes, resulting in many genomic variants existing at very low frequencies within the viral population, the low frequency variants can be hard to distinguish from NGS errors (Whitfield & Andino, 2016). As the viral RNA samples also have to undergo processing, such as reverse transcription and PCR amplification, before sequencing, errors in the form of artefactual mutations can be introduced into the sequences (Orton et al., 2015). There are a number of tools designed to detect low frequency variants in NGS data, such as Segminator II (Archer et al., 2012), V-Phaser, which uses information on the co-location of variants on reads (Macalalad et al., 2012; Yang et al., 2013), and Lo-Freq which uses quality scores to model base miscalls (Wilm et al., 2012). New methods have been developed to overcome the limitations of NGS errors, such as circular sequencing (CirSeq). This method uses circularized genomic RNA fragments to generate tandem repeats that serve as substrates for NGS. All the repeats will share the mutations that were originally present in the viral RNA, and differences within the linked repeats must stem from enzymatic or sequencing errors, and can thereby be excluded computationally from the analysis (Acevedo et al., 2014). However, to utilize CirSeq efficiently, 1 µg of pure viral RNA must be obtained, which is a challenge. Also, due to the read length and currently available analysis, viral haplotypes are not taken into consideration (Whitfield & Andino, 2016). Viral haplotypes can be identified through sequencing techniques with long read lengths, such as those employed by Pacific Biosystems (PacBio) using single molecule real-time (SMRT) sequencing, resulting in reads averaging 10-20

kb. However, the error rate is very high at an estimated 11-14%, which can be mitigated in part by repeated forward and reverse sequencing passes by circular sequencing. The MinIon, from Oxford Nanopore Techniques (ONT), uses nanopore sequencing in real time and results in sequence read lengths from several hundred bases to ultra-long reads of >800 kb, and costs are for consumable reagents only. There appears to be no intrinsic read-length limit, other than the size of the DNA fragments. However, the error rate is comparable to that of PacBio, and a component of the error is systematic and context-specific (Bleidorn, 2016; Pollard et al., 2018; Tyson et al., 2018).

We currently identify low frequency SNPs from Ion PGM or Illumina MiSeq data using a combination of BWA (Li, 2013), Samtools (Li et al., 2009), Lo-Freq and SnpEff (Cingolani et al., 2012), as described previously (Fahnøe et al., 2014, Fahnøe et al., 2015). Viral haplotypes can be identified through full-length cloning of the viral population, as described in Manuscript I. The SNPs observed in cDNA clones could also be due to errors introduced by the reverse transcriptase, and in the case of viruses rescued from BAC clones, the T7 RNA polymerase. It is difficult to disentangle the error of the T7 RNA polymerase from that of the reverse transcriptase (Orton et al., 2015). However, as reverse transcriptases have a skewed error distribution (Orton et al., 2015), SNPs randomly distributed across the genome are most likely not due to introduced errors by the sampling process.

Part II – Manuscripts

Manuscript I

Strategy for efficient generation of numerous full-length cDNA clones of classical swine fever virus for haplotyping

Published in BMC Genomics

Johnston et al. BMC Genomics (2018) 19:600
https://doi.org/10.1186/s12864-018-4971-8

BMC Genomics

METHODOLOGY ARTICLE Open Access

Strategy for efficient generation of numerous full-length cDNA clones of classical swine fever virus for haplotyping

Camille Melissa Johnston[1], Ulrik Fahnøe[2,3], Graham J. Belsham[1] and Thomas Bruun Rasmussen[1*]

Abstract

Background: Direct molecular cloning of full-length cDNAs derived from viral RNA is an approach to identify the individual viral genomes within a virus population. This enables characterization of distinct viral haplotypes present during infection.

Results: In this study, we recover individual genomes of classical swine fever virus (CSFV), present in a pig infected with vKos that was rescued from a cDNA clone corresponding to the highly virulent CSFV Koslov strain. Full-length cDNA amplicons (ca. 12.3 kb) were made by long RT-PCR, using RNA extracted from serum, and inserted directly into a cloning vector prior to detailed characterization of the individual viral genome sequences. The amplicons used for cloning were deep sequenced, which revealed low level sequence variation (< 5%) scattered across the genome consistent with the clone-derived origin of vKos. Numerous full-length cDNA clones were generated using these amplicons and full-genome sequencing of individual cDNA clones revealed insights into the virus diversity and the haplotypes present during infection. Most cDNA clones were unique, containing several single-nucleotide polymorphisms, and phylogenetic reconstruction revealed a low degree of order.

Conclusions: This optimized methodology enables highly efficient construction of full-length cDNA clones corresponding to individual viral genomes present within RNA virus populations.

Keywords: RNA, Genome, Bacterial artificial chromosome, RNA virus, Pestivirus, Haplotyping

Background

Classical swine fever (CSF) is a highly contagious disease of pigs caused by infection with classical swine fever virus (CSFV) which belongs to the genus *Pestivirus*, within the *Flaviviridae* family. Pestiviruses are enveloped and the particles contain a linear, positive-sense RNA of approximately 12.3 kb. This genome includes a single, long, open reading frame (ORF) encoding a large polyprotein, flanked by 5′ and 3′ untranslated regions (UTRs) [1] that are critical for the autonomous replication of the genome [2, 3]. The viral polyprotein is co- and post-translationally processed by cellular and viral proteases to yield 12 mature products. There are 4 structural proteins (C, E^{rns}, E1 and E2) and 8 non-structural proteins (N^{pro}, p7, NS2, NS3, NS4A, NS4B, NS5A, and NS5B) [1]. Positive-strand RNA viruses evolve rapidly, due to error-prone RNA replication and the lack of proof-reading activity of the RNA-dependent RNA polymerase [4]. The high error rate results in a virus population that exists as a quasispecies (different, but closely related variants). These variants form a flat fitness landscape in sequence space of a selectively neutral network of variants, making the population more robust to withstand mutations and evade host responses [5]. Within this sequence space, certain variants, or haplotypes, may exist either with single nucleotide (nt) changes or, alternatively, predominantly in combination with other changes within the same genome. The diversity and quasispecies composition of CSFV and other pestiviruses have not been studied in great depth. Limited analyses of the evolutionary forces that drive sequence change, and the role of the quasispecies composition as a determinant of virulence have been reported [6, 7]. Consensus sequencing (and even deep sequencing) cannot

* Correspondence: tbrur@vet.dtu.dk
[1]DTU National Veterinary Institute, Technical University of Denmark, Lindholm, DK-4771 Kalvehave, Denmark
Full list of author information is available at the end of the article

easily resolve the different haplotypes that constitute the whole population. Obtaining full-length cDNA clones represents an approach to identify the individual haplotypes present within the virus population and also enables phenotyping. However, a prerequisite for this is generation of full-length cDNA suitable for cloning.

In the present study, the generation of full-length cDNA clones was achieved by the use of long RT-PCR for full-length genome amplification in combination with TOPO XL-2 and In-Fusion cloning. Numerous full-length cDNA clones representing the diversity within the CSFV population were obtained directly from RNA present within the serum of virus-infected pigs. This methodology provides the necessary tools for the robust characterization of virus subpopulations and haplotypes.

Methods

Primers

Oligonucleotide primers used are listed in Additional file 1.

Preparation of full-length cDNAs from viral RNA

Viral RNA was extracted, using a combined TRIzol/RNeasy protocol [8] from a serum sample collected at 7 days post-inoculation (dpi) from a euthanized (by intravascular injection of pentobarbital) crossbred pig obtained from the high health status swine herd at DTU. The pig had been infected with vKos (rescued from the BAC clone Kos (GenBank KF977607.1, [9]) and passaged once in PK15 cells) and exhibited severe clinical signs of CSFV infection. This extracted RNA was used to generate full-length cDNA amplicons, using a modified version of the long RT-PCR method described previously [9, 10]. Briefly, the total RNA was reverse transcribed using the Maxima H Minus Reverse Transcriptase (Thermo Scientific) and the specific cDNA primer, CSF-cDNA-1 (Additional file 1). The cDNA was then amplified by long PCR using the primers CSF-Kos_1–59 and CSF-Kos_12313aR (Additional file 1) and the Q5 high-fidelity DNA polymerase kit (New England BioLabs). The products were gel purified with a GeneJET Gel extraction kit (Thermo Scientific) and quantified using a Qubit Fluorometric quantitation system (Thermo Scientific).

Production of bacterial artificial chromosomes (BACs)

The cDNA amplicons were inserted into the BAC vector pBeloBAC11 (New England BioLabs) using the In-Fusion HD Eco-Dry Cloning Kit (Clontech). Briefly, pBeloBAC11 was converted to a linearized form using the long PCR as above, with primers Kos15_NotI_pBelF and Kos15_NotI_pBelR (Additional file 1), which contain 15-nt overhangs identical to regions of the primers used for the preparation of the cDNA amplicons. The linear product was gel purified and quantified as described above. The linearized pBeloBAC11 vector was mixed with amplicons (ca. 1:2 molar ratio) in a volume of 10 μl, which was transferred to the In-Fusion HD EcoDry tube. The mixture was incubated at 37 °C for 15 min and then at 50 °C for 15 min. A 2.5 μl aliquot was used to transform *E. coli* Stellar competent cells according to the manufacturer's protocol, and colonies grown on LB plates containing chloramphenicol (CAM) (15 μg/ml).

Cloning of amplicons in pCR XL-2-TOPO vector

The cDNA amplicons were also cloned using the TOPO XL-2 kit (Thermo Scientific). Briefly, the linearized pCR-XL-2-TOPO vector was mixed with amplicons (ca. 1:2 molar ratio) in a volume of 6 μl, according to the manufacturer's protocol. pCR-Xl-2-TOPO is a linearized vector covalently bound at the 3′ ends of each DNA strand to the vaccinia virus DNA topoisomerase I [11]. The mixtures of vector and amplicons were incubated at 25 °C for 30 min. A 2-μl aliquot was used to transform *E. coli* One Shot™ OmniMAX™ 2TI^R competent cells according to the manufacturer's protocol, and colonies were grown on LB plates containing kanamycin (KAN) (50 μg/ml) and 1 mM isopropyl β-D-1-thiogalactopyranoside (IPTG).

Characterization of cloned cDNAs

BACs containing cDNA inserts were identified by colony PCR targeting the vector-insert junction at the terminus of the CSFV 5' UTR, using primers CSF192-R and pBelo69R (Additional file 1) and visualized on 1% TAE agarose gels. Selected BACs and TOPO X-2 clones were purified from 4 ml overnight (ON) cultures (LB medium with 12.5 μg/ml CAM and 50 μg/ml KAN, respectively) using the GeneJET Plasmid Miniprep kit (Thermo Scientific), and the presence of full-length CSFV cDNA inserts was identified using *Not*I digestion and visualized on 0.5% TAE agarose gels. The presence of full-length CSFV cDNA was confirmed by long PCR and full-length sequencing, as described previously [9, 12].

Validation of fidelity of cloning systems

Cloned cDNA amplicons were used for assessing the fidelity of the PCR and cloning process. For this, full-length amplicons were obtained from a cloned BAC cDNA (termed BAC clone Kos_KSP) corresponding to a variant of the CSFV strain Koslov [7], which contains 2 non-synonymous mutations in the coding region for the E2 glycoprotein (resulting in the E72K and L75P substitutions). Briefly, the cloned BAC cDNA was used as the template in a long PCR with the primers CSF-Kos_1–59 and CSF-Kos_12313aR (Additional file 1) and the Q5 high-fidelity DNA polymerase kit (New England BioLabs). The products were digested with *Dpn*I (Fast Digest, Thermo Scientific), gel purified with a GeneJET Gel extraction kit (Thermo Scientific) and quantified

using a Qubit Fluorometric quantitation system (Thermo Scientific). In-Fusion and TOPO XL-2 cloning was performed as described above. The resultant In-Fusion clones were screened by colony PCR and differentiated from the original clone using *Sma*I digestion of the vector-insert PCR product. The original Kos_KSP clone contains a T7 promoter and a *Sma*I site before the CSFV genome whereas the expected product lacks this site. Confirmation of correct insert size was performed as described above, on selected In-Fusion and TOPO X-2 clones. Selected full-length clones were then sequenced and compared to the original clone Kos_KSP, to determine the fidelity of the system.

Next generation sequencing (NGS) and phylogenetic analysis

Full-length amplified cDNA amplicons and cDNA clones were sequenced by NGS at the DTU Multi-Assay Core (DMAC, Kgs. Lyngby, Denmark) using an Ion PGM system (Life Technologies, Carlsbad, USA). Consensus sequences were obtained by mapping the reads to the vKos reference sequence (KF977607.1) using CLC Genomics Workbench v.9.5.2 (CLC bio, Aarhus, Denmark). Consensus sequences were aligned using MAFFT in Geneious (Biomatters, Auckland, New Zealand). Low frequency single nucleotide polymorphisms (SNPs, > 0.5%) were identified for cDNA amplicons using a combination of BWA, Samtools, Lo-Freq-snp-caller, and SnpEff, as described previously [9, 12]. Phylogeny was constructed using MrBayes v3.2.1 [13, 14] on a full-length cDNA sequence alignment using the General Time Reversible (GTR) model with default parameters (nst = 6). The Markov chain Monte Carlo algorithm was run for 10,000,000 iterations, with a sampling frequency of 7000 using two independent runs with three chains each, in order to check for convergence. Burn in was set at 25% of samples. The consensus tree was visualized in FigTree v.1.4.3.

Results

Fidelity of PCR and cloning

The fidelity of the PCR and cloning system was determined using the BAC clone Kos_KSP as the template for PCR and In-Fusion cloning of the generated amplicons (Table 1). In-Fusion cloning generated over 100 clones from each product and up to 50% of the screened clones were of the correct size. Ten randomly selected clones were full-length sequenced and the sequences were aligned with that of the original Kos_KSP, and showed 100% identity (Fig. 1). This shows that the long PCR together with the In-Fusion cloning process generates clones with high fidelity. The use of gel extraction to purify the amplicons, generated up to twice as many clones and 100% of the screened clones were of the correct size (Table 1).

The fidelity of the cloning system using TOPO-XL-2 was also validated, as described for the BAC clones (see Table 1). TOPO XL-2 cloning generated over 1000 clones and up to 80% of the screened clones were of the correct size. Eleven of these clones were full-length sequenced and aligned as above, revealing a 100% identity (Fig. 1). This shows that the long PCR together with TOPO XL-2 cloning also produces clones with high fidelity.

Full-length amplicons from the Kos_KSP BAC or cDNA derived from RNA were cloned into the BAC or pCRXL-2-TOPO vector using In-Fusion or TOPO-XL-2, respectively. In-Fusion clones were screened using colony PCR, and subsequently positive colonies were further screened following *Not*I digestion to confirm the correct

Table 1 Efficiency of cloning full-length amplicons from Kos_KSP and cDNAs

Amplicon	Cloning method	# of clones	Positive/no. screened	#Correct insert size/#Screened with *Not*I	% correct of screened total	No. of clones sent for NGS
Kos_KSP	In-Fusion[d]	232	12/24	12/12	50%	5
Kos_KSP	In-Fusion[d]	111	8/24	8/8	33.3%	5
Kos_KSP	In-Fusion[b]	472	24/24	6/6	100%	–
Kos_KSP	In-Fusion liq.[b]	> 1000	10/10	10/10	100%	–
cDNA[a]	In-Fusion[b]	24	6/24	3/6	12.5%	3
Kos_KSP	TOPO XL-2[b]	> 1000	n.d.	8/10	80%	7
Kos_KSP	TOPO XL-2[b]	> 1000	n.d.	6/10	60%	4
cDNA[ac]	TOPO XL-2[b]	31	n.d.	4/10	40%	4
cDNA[ac]	TOPO XL-2[b]	43	n.d.	7/10	70%	7
cDNA[a]	TOPO XL-2[b]	33	n.d.	4/10	40%	4

n.d. Not done
[a]RNA derived cDNA
[b]Gel purified amplicons
[c]Same RT-PCR used
[d]amplicons purified by PCR clean-up kit

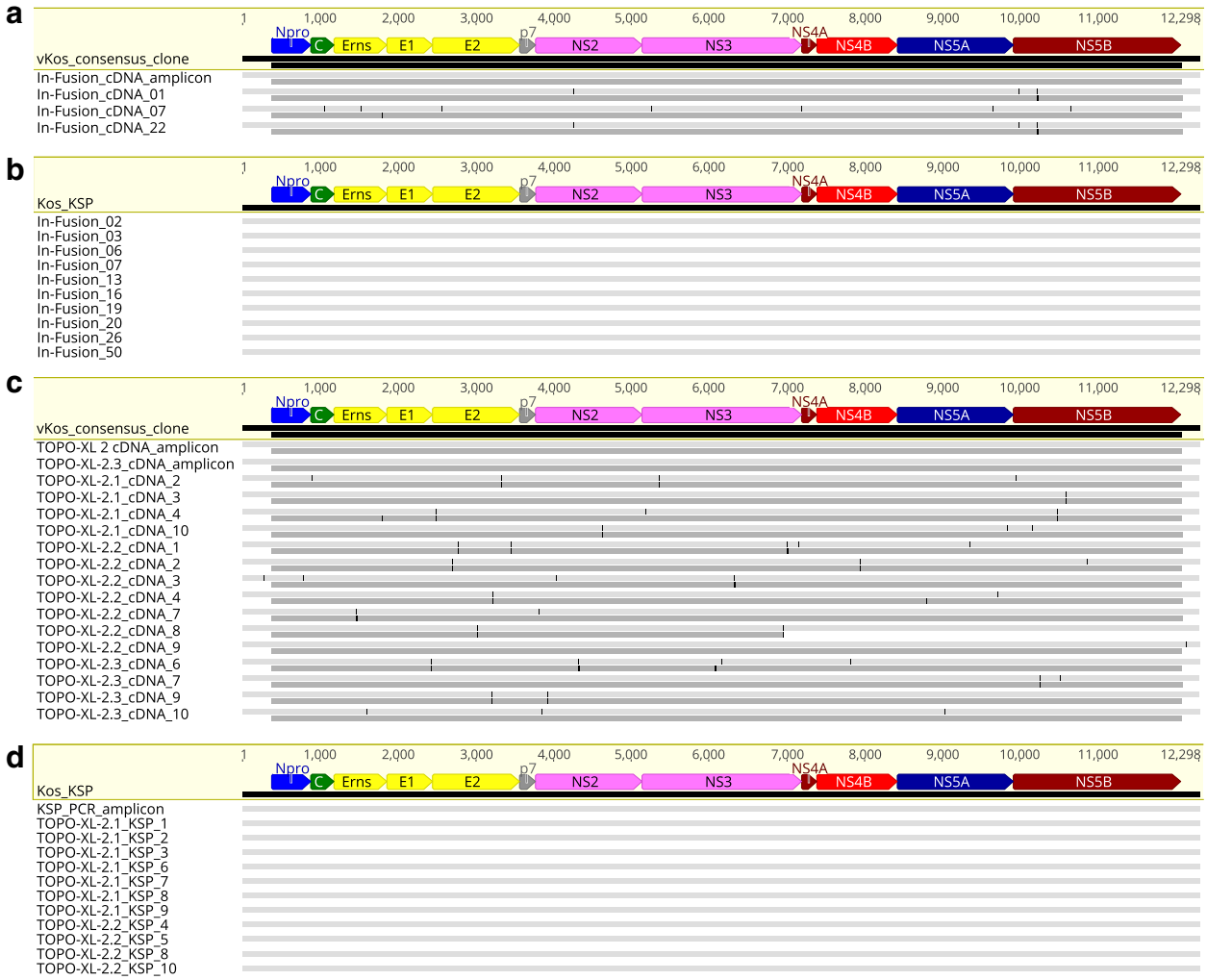

Fig. 1 Multiple-sequence alignment of amplicons and cDNA clones. Multiple-sequence alignment of cDNA amplicons and cDNA clones (**a** and **c**) and Kos_KSP amplicons and clones (**b** and **d**). **a** In-Fusion cloning of cDNA amplicons generated from the serum of an infected pig. The cDNA amplicons used for the cloning is shown as the first sequence. **b** In-Fusion cloning of Kos_KSP derived amplicons. **c** TOPO-XL-2 cloning of cDNA generated from the serum of an infected pig. The sequences of two independent cDNA amplicons used for the cloning are shown **d** TOPO-XL-2 cloning of Kos_KSP derived amplicons. In **a** and **c** the top bars (light gray) depict differences from the consensus sequence at the nucleotide level, while the lower bars (dark gray) depict differences from the consensus sequence at the amino acid level

size of insert. TOPO-XL-2 colonies were also screened by *Not*I digestion to confirm the correct insert size.

Cloning of cDNAs

Full-length cDNAs were amplified from CSFV RNA, isolated from serum of infected pigs (at 7 dpi), by long RT-PCR. Optimal results were obtained by substituting the SuperScript III reverse transcriptase with Maxima H minus Reverse Transcriptase, and the Accuprime High Fidelity with the Q5 high-fidelity DNA polymerase, the latter produces blunt-ended PCR products. Using these conditions, high yields of full-length amplicons of approximately 12.3 kb from the viral RNA were obtained (Additional file 2).

The amplified cDNAs were inserted directly into the linearized pBeloBAC11 vector by in vitro recombination using the In-Fusion system. Inserts of the correct size were identified by colony PCR, followed by restriction enzyme digestion with *Not*I (data not shown) and long PCR (Additional file 3a). A 10-fold lower number of bacterial colonies was observed compared to the cloning of the Kos_KSP-derived amplicons, and only 3 (12.5%) of these colonies contained an insert of the correct size (Table 1). These cDNA clones were full-length sequenced and aligned to the parental sequence. Two clones were 100% identical to each other representing one haplotype, but contained 6 SNPs compared to the reference vKos sequence, whereas the third clone was unique and had 9 SNPs (Fig. 1a).

Due to the low percentage of full-length cDNA clones obtained using the In-Fusion procedure, we then used the TOPO XL-2 cloning method, which relies upon the activity of DNA topoisomerase I. The amplified genomes were inserted directly into the linearized pCR-Xl-2-TOPO vector using DNA topoisomerase I. Transformation of *E. coli* with the products from three independent insertions into the vector yielded 31, 43, and 33 colonies (an average of 36). Correct inserts were identified by digestion with *Not*I (data not shown) and full-length PCR amplification (Additional file 3b). Up to 70% of the colonies contained an insert of the correct size (Table 1). Fifteen of these cDNA clones were full-length sequenced and these sequences were aligned with the parental consensus sequence. Each of the cDNA clones was unique with 2–8 SNPs compared to the reference sequence (Fig. 1c). A total of 68 SNPs were observed. Some 51.5% of all observed SNPs in the coding sequence were synonymous mutations while 48.5% were non-synonymous, out of which one resulted in the introduction of a premature stop codon; 3% of all the SNPs were located in the 5' UTR and 3' UTR, which together constitute approximately 5% of the total genome.

SNP analysis of cDNAs used for cloning

The cDNA amplicons derived from a serum sample, obtained from a CSFV Koslov-infected pig, were deep sequenced by NGS (coverage of approx. 11,000 reads per nt). The consensus sequence of these amplicons showed 100% identity to the vKos BAC clone. The cDNA amplicons used for the In-Fusion cloning displayed low-level sequence variation (below 5% frequency) scattered across the genome as synonymous and non-synonymous mutations (Fig. 2), which was also seen for the cDNA amplicons used for TOPO XL-2 cloning, although fewer SNPs were detected with a coverage of approx. 1800 and 2500 reads per nt, respectively. The SNPs (41) seen in the In-Fusion cDNA amplicons comprised both synonymous mutations (54%) and non-synonymous at 46%. Some 22% of the SNPs seen herein could also be detected in the cloned cDNAs, from both In-Fusion and TOPO-XL-2 cloning. A separate pool of amplicons, generated from a separate RNA extraction and RT-PCR of the same serum sample, was also deep sequenced by NGS (this produced a coverage of approximately 20,000 reads per nt). As above, the SNPs (693 in total) comprised both synonymous mutations (60.1%) and non-synonymous (39.9%) in the coding sequence with low-level sequence variation (below 5%) scattered across the genome, with 126 SNPs present at above 1% frequency. Some 50% of the SNPs observed in the cloned cDNAs could be detected in the amplicons sequenced at greater depth. An additional 20% of the SNPs detected in the cloned cDNAs could be detected

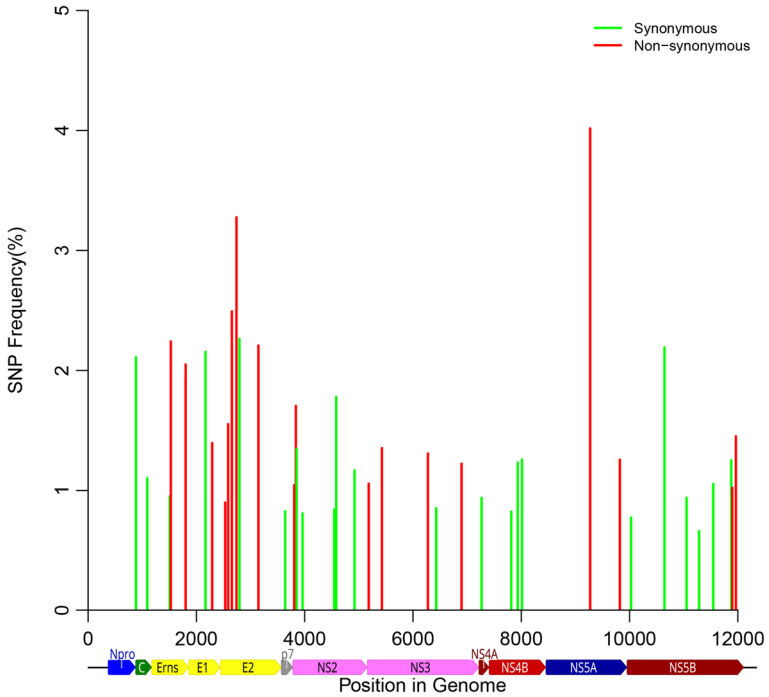

Fig. 2 SNP analysis of RT-PCR amplicon. Deep sequencing of the amplicons derived by RT-PCR from the vKos infected serum at 7 days post infection. The histograms depict SNP frequency on the y-axis and genome position on the x-axis. The green and red colors indicate SNPs grouped as synonymous and non-synonymous, respectively

in deep sequenced cDNA amplicons of serum from pigs infected with either vKos or vKos BAC clone variants (data not shown). Furthermore, another 9% SNPs have been observed in full-length CSFV genomes and full-length E2 glycoprotein sequences reported previously (complete coding sequence (CDS) and full-length E2 glycoprotein sequences were retrieved from GenBank [15] and the CSF database of the European Community Reference Laboratory [16] as described [17]). The unique mutations seen in the cDNA clones, most of which are located in the E2 and NS3 coding regions, are therefore most likely low frequency SNPs present in the populations (< 0.3%), and not errors introduced by the procedures (see Discussion).

Phylogenetic reconstruction

A phylogenetic tree for the cDNA clones was inferred using Bayesian methods (Fig. 3) in order to elucidate the population structure. The unrooted tree was star-like, with the cDNA sequences branching out from a single node that corresponds to the Koslov reference sequence. The majority of the cDNA clones were unique, forming no apparent clades, and with a low degree of order; just 2 In-Fusion clones were 100% identical and 2 TOPO XL-2 clones shared one mutation.

Discussion

The aim of this study was to establish methodology for efficient, direct cloning of cDNAs corresponding to the full-length genomes of CSFV from infected pigs. Generation of full-length cDNA clones has often been a lengthy and arduous process. However, the technology is improving. BACs are ideally suited for the stable maintenance of large DNA/cDNA sequences derived from viral genomes [18]. Several BACs, containing full-length cDNAs of different CSFV strains, have been established [9, 12, 19]. Similarly, BACs containing cDNAs corresponding to the genomes of other members of the *Flaviviridae* family have also been described [10, 20–22]. In this study, In-Fusion cloning of amplicons derived from an established cDNA clone in a BAC vector was efficient, with an apparent fidelity of 100%. However, In-Fusion cloning of cDNA amplicons generated directly from viral RNA yielded only a few clones with the correct insert size. In contrast, using the TOPO XL-2 cloning method, we generated many more cDNA clones with a high proportion having the

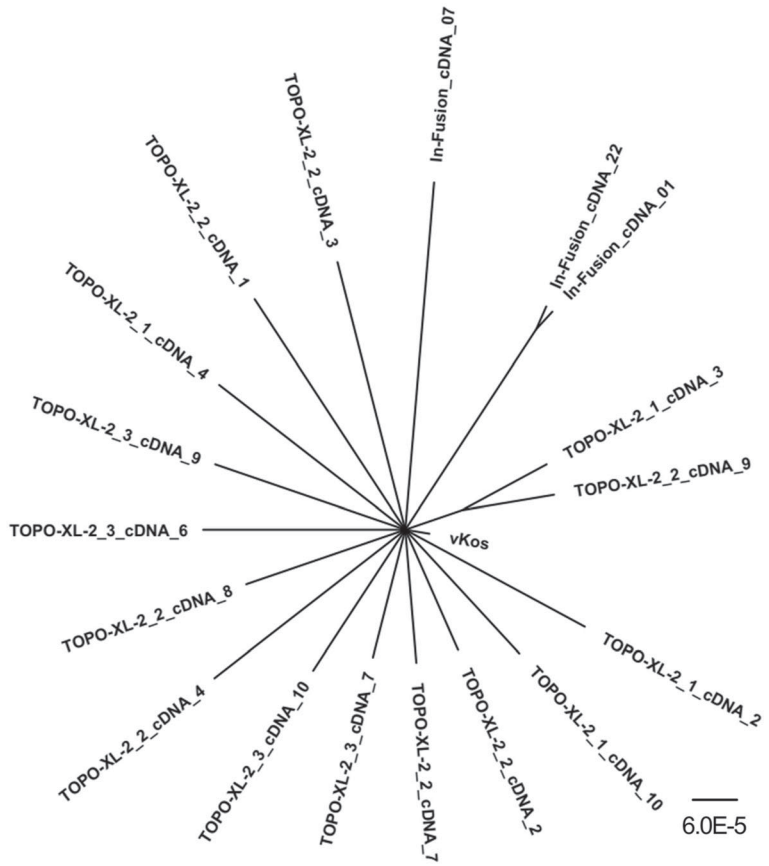

Fig. 3 Phylogenetic reconstruction inferred from cDNA clones. Phylogenetic structure of the virus population present in the vKos infected pig serum inferred from the cDNA clones by tree reconstruction using MrBayes [14]

correct insert size. The advantages of this optimized methodology are: (i) circumvention of multiple cloning steps (since full-length amplicons can be directly inserted into plasmid vectors by in vitro recombination or using DNA topoisomerase), (ii) provision of a system for identifying sequence diversity within virus populations and the haplotypes within the entire genome, (iii) enabling the construction of genetically distinct viral cDNA clones and (iv) enabling phenotypic characterization of haplotypes.

The In-Fusion cloning system is not dependent upon the use of restriction enzymes or ligases and allows for the insertion of fragments at any suitable location within the vector [23]. In-Fusion cloning has previously been used for replacing cDNA corresponding to one CSFV strain with that of another in already established CSFV cDNA BAC clones [24, 25], and for CSFV field isolates using amplicons generated by in vitro overlap extension PCR [26]. CSFV BAC clones have previously been found to be stably maintained through multiple generations in *E. coli* [26], as seen for other full-length cDNA clones corresponding to other members of the *Flaviviridae* [19, 20, 22]. The stability of the TOPO XL-2 clones was not assessed here, as the constructs were used directly for NGS analysis, in order to map virus subpopulations and to perform haplotyping. However, if necessary, it should be possible to obtain a stable BAC clone, using the insert from a TOPO XL-2 clone, following PCR amplification which can then be cloned using the In-Fusion system since this cloned cDNA to amplicon cloning process works with high fidelity and success rate.

All cDNA clones generated from viral RNA contained SNPs, as expected, for individual virus genomes obtained from an RNA virus population, owing to its quasispecies nature. Interestingly, 3 of the SNPs detected in the TOPO XL-2 cDNA clones (G270A, T784C, and L764P) and one from the In-Fusion cDNA amplicon (A9821G) were also found at the consensus level in a contact pig infected with vKos at 6 dpi in the study by Fahnøe et al. [9]. In the present study, the SNP analysis of the cDNA amplicon used for In-Fusion cloning revealed the presence of 41 SNPs in total, all with a frequency below 5%, whereas the cDNA amplicon sequenced with 2-fold higher coverage, revealed 693 SNPs in total (< 5% frequency), with 126 SNPs detected above a frequency of 1%. In another study (Fahnøe U, Pedersen AG, Höper D, Beer M, Rasmussen TB., unpublished), we observed 159 SNPs scattered across the genome (> 1% frequency) in the inoculum used to challenge pigs; this inoculum was derived from the blood of pigs infected with the Koslov strain of CSFV [27]. Ten of these SNPs were observed at about 40% frequency. The larger number of SNPs found in the latter study at higher frequencies, is most likely due to the Koslov strain being a wild-type virus, which has had a lot of time to evolve in its natural host, whereas vKos, as used in the present study, is a virus preparation derived from a unique cloned cDNA. Therefore, the rescued virus may be expected to consist of a less diverse quasispecies with respect to high frequency haplotypes than a highly virulent "field" isolate, as reported previously [28]. Over 79% of the SNPs observed in the clones, were detected in either the RNA-derived amplicons used in our study, in the serum of pigs infected with either vKos or vKos BAC clone variants, or in published CSFV sequences. The remaining 21% of SNPs which were not observed elsewhere are most likely very low frequency SNPs in the viral population, and were located mostly in the E2 and NS3 coding regions. The N-terminal half of the E2 glycoprotein is one of the most variable regions in the CSFV genome [29], presumably due to E2 being under immune pressure. In addition, E^{rns} and NS3 also induce detectable antibodies [30–32]. E2 is under purifying selection pressure [33], likely due to the immune response, this is most probably also the case for NS3, although perhaps to a lesser degree, as it is a nonstructural protein and does not elicit neutralizing antibodies [34], however it is a strong activator of cytotoxic T lymphocytes [35–37]. In principle, these apparent SNPs could be due to errors by the reverse transcriptase; however, this is unlikely as most of the SNPs were detected in multiple independent cDNAs and also in previously published sequences. Furthermore, the SNPs which were not detected were randomly distributed, which one would not expect if these SNPs were caused by reverse transcriptase errors, due to the skewed nature of its error distribution [38]. However, as the virus population originally stems from a BAC clone, which was in vitro transcribed using a T7 RNA polymerase, errors could have been introduced into the virus inoculum by this process. This is not a concern when using field isolates, as no T7 RNA polymerase is utilized.

The phylogenetic reconstruction of the cDNA clones from both In-Fusion and TOPO XL-2 cloning formed no apparent clades, with a low degree of order. This is most likely due to the clone-derived virus inoculum used for the infection experiment, which is consistent with the less diverse quasispecies seen in the SNP analysis. This is also in agreement with our earlier study, in which a higher degree of order was seen in the phylogenetic reconstruction of cDNA clones from a field isolate of the moderately virulent CSFV strain Roesrath [12]. That SNP analysis also revealed several SNPs at a frequency above 5%; this is a typical quasispecies distribution, in which most haplotypes are present at a very low frequency while a few are dominant [7].

This optimized high-throughput strategy for obtaining full-length cDNA clones, described here, avoids the time-consuming and costly processes inherent in traditional

methods. This methodology allows the identification of the individual components of the quasispecies that comprise the virus population and reveals how mutations are linked on individual viral genomes. This approach will help improve understanding of the molecular mechanisms involved in the virulence of CSFV, enabling new approaches for disease control including development of novel vaccine strategies.

Conclusions

In summary, we report the high efficiency construction and sequence analysis of numerous full-length CSFV cDNA clones using RNA prepared directly from the serum of virus-infected pigs by applying long RT-PCR and TOPO XL-2 topoisomerase cloning. This methodology allows the identification of the individual haplotypes that constitute the viral quasispecies. In addition, it can be applied to any RNA virus for which the viral genome can be amplified by a long RT-PCR approach.

Additional files

Additional file 1: List of oligonucleotide primers used in this study. (DOCX 17 kb)

Additional file 2: Gel electrophoresis of long RT-PCR amplicons used for In-Fusion and Topo XL-2 cloning. (DOCX 71 kb)

Additional file 3: Gel electrophoresis of full-length PCR products from generated cDNA clones. (DOCX 160 kb)

Abbreviations

BAC: Bacterial artificial chromosome; CAM: Chloramphenicol; CDS: Coding sequence; CSF: Classical swine fever; CSFV: Classical swine fever virus; dpi: Days post-inoculation; GTR: General time reversible; IPTG: Isopropyl β-D-1-thiogalactopyranoside; KAN: Kanamycin; NGS: Next generation sequencing; nst: Number of substitution types; nt: Nucleotide; ON: Overnight; ORF: Open reading frame; SNP: Single nucleotide polymorphism; UTR: Untranslated region

Acknowledgements

We are grateful for excellent assistance from Marlene D. Dalgaard (DMAC, DTU).

Funding

The studies were funded from internal resources of DTU National Veterinary Institute.

Availability of data and materials

All relevant data are included in this published article and its additional files. The datasets used and/or analyzed during the current study are available from the corresponding author on reasonable request.

Authors' contributions

TBR, UF, GJB and CMJ conceived the study and developed the approach. CMJ carried out and optimized the experiments. TBR, UF, and CMJ carried out sequence analyses. All authors contributed to result interpretation. All authors contributed to the drafting and revision of the manuscript. All authors read and approved the final manuscript.

Ethics approval

Experimental procedures and animal management protocols were carried out in accordance with the requirements of the Danish Animal Experimentation Inspectorate, under reference 2012–15–2934-00182.

Consent for publication

Not applicable.

Competing interests

The authors declare that they have no competing interests.

Publisher's Note

Author details

[1]DTU National Veterinary Institute, Technical University of Denmark, Lindholm, DK-4771 Kalvehave, Denmark. [2]Copenhagen Hepatitis C Program (CO-HEP), Department of Infectious Diseases, Hvidovre Hospital, Hvidovre, Denmark. [3]Department of Immunology and Microbiology, Faculty of Health and Medical Sciences, University of Copenhagen, Copenhagen, Denmark.

Received: 6 April 2018 Accepted: 31 July 2018
Published online: 09 August 2018

References

1. Lindenbach BD, Murray CL, Thiel HJ, Rice CM. Flaviviridae: the viruses and their replication. In: Fields virology. 6th ed. New York: Lippincott Williams & Wilkins; 2013. p. 712–46.
2. Collett MS, Anderson DK, Retzel E. Comparisons of the pestivirus bovine viral diarrhoea virus with members of the Flaviviridae. J Gen Virol. 1988;69:2637–43.
3. Meyers G, Rümenapf T, Thiel HJ. Molecular cloning and nucleotide sequence of the genome of hog cholera virus. Virology. 1989;171:555–67.
4. Drake JW, Charlesworth B, Charlesworth D, Crow JF. Rates of spontaneous mutation. Genetics. 1998;148:1667–86.
5. Lauring AS, Andino R. Quasispecies theory and the behavior of RNA viruses. PLoS Pathog. 2010;6:e1001005.
6. Rios L, Coronado L, Naranjo-Feliciano D, Martínez-Pérez O, Perera CL, Hernandez-Alvarez L, et al. Deciphering the emergence, genetic diversity and evolution of classical swine fever virus. Sci Rep. 2017;7:17887.
7. Töpfer A, Höper D, Blome S, Beer M, Beerenwinkel N, Ruggli N, et al. Sequencing approach to analyze the role of quasispecies for classical swine fever. Virology. 2013;438:14–9.
8. Rasmussen TB, Reimann I, Hoffmann B, Depner K, Uttenthal Å, Beer M. Direct recovery of infectious Pestivirus from a full-length RT-PCR amplicon. J Virol Methods. 2008;149:330–3.
9. Fahnøe U, Pedersen AG, Risager PC, Nielsen J, Belsham GJ, Höper D, et al. Rescue of the highly virulent classical swine fever virus strain "Koslov" from cloned cDNA and first insights into genome variations relevant for virulence. Virology. 2014;468–470:379–87.
10. Rasmussen TB, Reimann I, Uttenthal Å, Leifer I, Depner K, Schirrmeier H, et al. Generation of recombinant pestiviruses using a full-genome amplification strategy. Vet Microbiol. 2010;142:13–7.
11. Shuman S. Novel approach to molecular cloning and polynucleotide synthesis using vaccinia DNA topoisomerase. J Biol Chem. 1994;269:32678–84.
12. Fahnøe U, Pedersen AG, Dräger C, Orton RJ, Blome S, Höper D, et al. Creation of functional viruses from non-functional cDNA clones obtained from an RNA virus population by the use of ancestral reconstruction. PLoS One. 2015;10:e0140912.
13. Ronquist F, Huelsenbeck JP. MrBayes 3: Bayesian phylogenetic inference under mixed models. Bioinformatics. 2003;19:1572–4.
14. Huelsenbeck JP, Ronquist F. MRBAYES: Bayesian inference of phylogenetic trees. Bioinformatics. 2001;17:754–5.
15. Clark K, Karsch-Mizrachi I, Lipman DJ, Ostell J, Sayers EW. GenBank. http://www.ncbi.nlm.nih.gov/genbank/. Accessed 27 Oct 2017.
16. Greiser-Wilke I, Zimmermann B. The CSF database of the European community reference laboratory. http://viro60.tiho-hannover.de/eg/csf/. Accessed 27 Oct 2017.
17. Postel A, Schmeiser S, Zimmermann B, Becher P. The European classical swine fever virus database: blueprint for a pathogen-specific sequence database with integrated sequence analysis tools. Viruses. 2016;8:302.
18. Messerle M, Crnkovic I, Hammerschmidt W, Ziegler H, Koszinowski UH. Cloning and mutagenesis of a herpesvirus genome as an infectious bacterial artificial chromosome. Proc Natl Acad Sci U S A. 1997;94:14759–63.

19. Rasmussen TB, Risager PC, Fahnøe U, Friis MB, Belsham GJ, Höper D, et al. Efficient generation of recombinant RNA viruses using targeted recombination-mediated mutagenesis of bacterial artificial chromosomes containing full-length cDNA. BMC Genomics. 2013;14:819.
20. Yun S, Kim S, Rice CM, Lee Y. Development and application of a reverse genetics system for Japanese encephalitis virus. J Virol. 2003;77:6450–65.
21. Pierro DJ. Infectious clone construction of dengue virus type 2, strain Jamaican 1409, and characterization of a conditional E6 mutation. J Gen Virol. 2006;87:2263–8.
22. Fan Z-C, Bird RC. An improved reverse genetics system for generation of bovine viral diarrhea virus as a BAC cDNA. J Virol Methods. 2008;149:309–15.
23. Irwin CR, Farmer A, Willer DO, Evans DH. Vaccinia virus and poxvirology. Totowa: Humana Press; 2012.
24. Tamura T, Sakoda Y, Yoshino F, Nomura T, Yamamoto N, Sato Y, et al. Selection of classical swine fever virus with enhanced pathogenicity reveals synergistic virulence determinants in E2 and NS4B. J Virol. 2012;86:8602–13.
25. Tamura T, Ruggli N, Nagashima N, Okamatsu M, Igarashi M, Mine J, et al. Intracellular membrane association of the N-terminal domain of classical swine fever virus NS4B determines viral genome replication and virulence. J Gen Virol. 2015;96:2623–35.
26. Kamboj A, Saini M, Rajan LS, Lal C, Chaturvedi VK, Gupta PK. Construction of infectious cDNA clone derived from a classical swine fever virus field isolate in BAC vector using in vitro overlap extension PCR and recombination. J Virol Methods. 2015;226:60–6.
27. Blome S, Gabriel C, Schmeiser S, Meyer D, Meindl-Böhmer A, Koenen F, et al. Efficacy of marker vaccine candidate CP7-E2alf against challenge with classical swine fever virus isolates of different genotypes. Vet Microbiol. 2014;169:8–17.
28. Jenckel M, Blome S, Beer M, Höper D. Quasispecies composition and diversity do not reveal any predictors for chronic classical swine fever virus infection. Arch Virol. 2017;162:775–86.
29. Lowings P, Ibata G, Needham J, Paton D. Classical swine fever virus diversity and evolution. J Gen Virol. 1996;77:1311–21.
30. Paton DJ, Ibata G, Edwards S, Wensvoort G. An ELISA detecting antibody to conserved pestivirus epitopes. J Virol Methods. 1991;31:315–24.
31. Moser C, Ruggli N, Tratschin JD, Hofmann MA. Detection of antibodies against classical swine fever virus in swine sera by indirect ELISA using recombinant envelope glycoprotein E2. Vet Microbiol. 1996;51:41–53.
32. Langedijk JPM, Middel WGJ, Meloen RH, Kramps JA, de Smit JA. Enzyme-linked immunosorbent assay using a virus type-specific peptide based on a subdomain of envelope protein erns for serologic diagnosis of pestivirus infections in swine. J Clin Microbiol. 2001;39:906–12.
33. Tang F, Pan Z, Zhang C. The selection pressure analysis of classical swine fever virus envelope protein genes erns and E2. Virus Res. 2008;131:132–5.
34. Greiser-Wilke I, Dittmar KE, Liess B, Moennig V. Heterogeneous expression of the non-structural protein p80/p125 in cells infected with different pestiviruses. J Gen Virol. 1992;73:47–52.
35. Pauly T, Elbers K, Konig M, Lengsfeld T, Saalmuller A, Thiel HJ. Classical swine fever virus-specific cytotoxic T lymphocytes and identification of a T cell epitope. J Gen Virol. 1995;76:3039–49.
36. Armengol E, Wiesmüller K-H, Wienhold D, Büttner M, Pfaff E, Jung G, et al. Identification of T-cell epitopes in the structural and non-structural proteins of classical swine fever virus. J Gen Virol. 2002;83:551–60.
37. Rau H, Revets H, Balmelli C, McCullough KC, Summerfield A. Immunological properties of recombinant classical swine fever virus NS3 protein in vitro and in vivo. Vet Res. 2006;37:155–68.
38. Orton RJ, Wright CF, Morelli MJ, King DJ, Paton DJ, King DP, et al. Distinguishing low frequency mutations from RT-PCR and sequence errors in viral deep sequencing data. BMC Genomics. 2015;16:1–15.

Manuscript II

Identification of major virus haplotypes present within pigs infected with virulent, clone-derived, variants of the Koslov strain of classical swine fever virus

In preparation

Identification of major virus haplotypes present within pigs infected with virulent, clone-derived, variants of the Koslov strain of classical swine fever virus

Camille Melissa Johnston[1], Ulrik Fahnøe[2], Louise Lohse[1], Graham J. Belsham[1], Thomas Bruun Rasmussen[1*]

[1]DTU National Veterinary Institute, Technical University of Denmark, Lindholm, DK-4771 Kalvehave, Denmark.

[2]Copenhagen Hepatitis C Program (CO-HEP), Department of Infectious Diseases, Hvidovre Hospital and Department of Immunology and Microbiology, Faculty of Health and Medical Sciences, University of Copenhagen, Denmark

[*]Corresponding author

Camille Melissa Johnston: camejo@vet.dtu.dk

Ulrik Fahnøe: ulrik@sund.ku.dk

Louise Lohse: loloh@vet.dtu.dk

Graham J. Belsham: grbe@vet.dtu.dk

Thomas Bruun Rasmussen: tbrur@vet.dtu.dk

Abstract

Classical swine fever virus (CSFV) contains a specific motif within the E2 glycoprotein that varies between CSFV strains of different virulence. In the highly virulent CSFV strain Koslov, this motif comprises residues S74 and L75 in the N-terminal domain of E2 (S763 and L764 in the polyprotein). However, CSFV strains encoding L763 and P764 represent the predominant alleles across all published full-length CSFV genomes. In this study, mutations were introduced into the consensus cDNA clone of the CSFV strain Koslov, vKos (which is vKos_SL), to generate a set of E2 mutants with substitutions at residues 763 and 764; these mutants are termed: vKos_LL, vKos_SP and vKos_LP, respectively. Experiments were performed to compare the virulence of these E2 mutants in comparison to vKos in experimentally challenged pigs. Each of the strains was virulent, but vKos_LP induced earlier signs of CSFV infection compared to vKos and the two other E2 mutants. NGS was performed on viral RNA extracted from infected pigs, to investigate the diversity present in the virus populations during infection. The SNP profiles for vKos and vKos_LL displayed low-level sequence variation across the genome whereas vKos_SP and vKos_LP were more diverse with several consensus changes in the sequences. Samples from infected serum were cloned to determine the major haplotypes present in the viral populations. The obtained full-length cDNA clones reflected the major haplotypes observed in the SNP profiles.

Introduction

Classical swine fever virus (CSFV) is the causative agent of classical swine fever (CSF), an economically important and highly contagious disease of pigs. CSFV belongs to the genus *Pestivirus*, within the *Flaviviridae* family [1]. Pestiviruses are enveloped and contain a single-stranded, positive sense RNA genome, approximately 12.3 kb in length. This RNA contains a single, long, open reading frame (ORF), encoding a large polyprotein, flanked by 5' and 3' untranslated regions (UTRs) [1] that are critical for the autonomous replication of the genome [2, 3]. The polyprotein is co- and post-translationally processed by cellular and viral proteases to yield 12 mature cleavage products: 4 structural (C, E^{rns}, E1 and E2) and 8 non-structural (N^{pro}, p7, NS2, NS3, NS4A, NS4B, NS5A, and NS5B) [1]. Positive-strand RNA virus populations exist as a quasispecies of different, but closely related variants, due to their high evolutionary rates [4, 5] . Such virus populations contribute to the tropism phenotypes within the infected host [6, 7]. The high rate of change can partly be explained by the high error rate of the RNA-dependent RNA polymerase, which lacks proof-reading activity, although additional factors such as within-host dynamics or cell tropism also affect the evolutionary rate [8]. A large number of CSFV strains exist which vary considerably in their virulence, including high, moderate and low virulence variants [9]. Low virulence strains result in no or mild disease whereas highly virulent strains cause acute disease including high fever, hemorrhages, central nervous system (CNS) disorders and high mortality. The highly virulent CSFV strain Koslov induces pronounced convulsions and seizures due to infection of the CNS, thus showing a distinct phenotype (or tropism) compared to strains with lower virulence that do not affect the CNS [10, 11].

The glycoprotein E2 is the major surface component of the virion; it is essential for virus replication and is the main immunogen [12]. It has been implicated, together with E^{rns} and E1, in virus adsorption to host cells [12–15], and for determining tropism in cell culture [13, 14]. The E2 glycoprotein shows a high variability among different CSFV strains [16]. Modifications introduced into this glycoprotein appear to have an important effect on CSFV virulence [17–22].

In the present study, two separate infection studies in pigs were performed using vKos and rescued mutants containing non-synonymous mutations encoding residues 763 and 764 within the E2 glycoprotein, in order to elucidate their role in the virulence and possibly tropism of the highly virulent strain Koslov.

Results

Virus rescue and characterization. The BACs Kos_LL, Kos_LP and Kos_SP were generated by site-directed mutagenesis. Full-length amplicons of purified BAC DNAs were obtained by long PCR, and *in vitro* transcribed using T7 RNA polymerase. Virus was rescued from these RNA transcripts by electroporation of PK15 cells, passaged once and the titers were determined. The parental vKos and each of the mutant

rescued viruses grew to a similar level during serial passaging in PK15 cells (Figure S1 A). Furthermore, in low MOI growth curves in PK15 cells, the vKos and vKos_LL showed similar growth kinetics as wildtype (wt) 'field isolate' Koslov (Figure S1 B and C).

Animal experiment I. To elucidate the role of residue 763, virus challenge was performed in 3 pigs intranasally inoculated with 10^6 $TCID_{50}$ of vKos (with the SL motif) or vKos_LL, respectively; within each group were 2 contact pigs that were not inoculated. The vKos and vKos_LL both produced severe disease in pigs, and due to pronounced clinical signs including high fever, anorexia, dyspnea, ataxia and convulsions, all compatible with symptoms of CSF, all inoculated pigs were euthanized by post infection day (PID) 7 (Figure 1 A). High fever (above 41°C) was observed as early as PID3 in pigs inoculated with vKos_LL and at PID4 in pigs inoculated with vKos (Figure 1 B and C), coinciding with high viral RNA loads in both blood and nasal swabs (Figure 1 D-G). During PID5, the vKos_LL contact pig 4 developed high fever with high viremia on PID7 and so was euthanized on PID8. The vKos_LL contact pig 5 developed high fever by PID8, high viremia by PID9, and was euthanized later that day. The vKos contact pigs 9 and 10 both developed high fever by PID9 and PID8, respectively, with high viremia at PID10 (no blood samples were collected between PID7 and PID10), and were both euthanized later that day. The necropsies revealed gross-morphological changes in the form of discoloration and/or necrosis within the tonsils of all pigs. Furthermore, several pigs (in both groups) had excessive peritoneal fluid, petechial bleedings in the kidney and hemorrhage visible as blebs on the border of the spleen.

Animal experiment II. To elucidate the role of residue 764 alone or in conjunction with residue 763, virus challenge was performed in 4 pigs intranasally inoculated with 10^6 $TCID_{50}$ of vKos (SL motif), vKos_LP or vKos_SP, respectively. The vKos, vKos_LP and vKos_SP each produced severe disease in pigs, and due to pronounced clinical signs including high fever, anorexia, dyspnea, diarrhea, ataxia and convulsions, all inoculated pigs were euthanized, at the latest, by PID7 (Figure 2 A). Pigs inoculated with vKos_LP were euthanized 1-2 days earlier than pigs inoculated with vKos and vKos_SP, and exhibited earlier symptoms of CSF as shown by the clinical scores (Figure 2 B-D). High fever (above 41°C) was observed as early as PID3 in pigs inoculated with vKos_LP, while vKos and vKos_SP had high fever from PID4 and PID5, respectively (Figure 2 E-G). This coincided with high viral RNA loads in both blood and nasal swabs (Figure 2 H-M). The necropsies revealed various gross-pathological changes, which often involved discoloration and/or necrotic lesions within the tonsils, excessive peritoneal fluid and petechial bleedings in the kidney. RT-qPCR assays were performed on RNA extracted from tonsil, lymph nodes, spleen, bone-marrow, cerebellum and cerebrum from all pigs (Figure 2 N-P). Virus was detected in nearly all tissues of all pigs, with high amounts of viral RNA present in the tonsils, lymph nodes, spleen and bone-marrow. A much lower amount of viral RNA was detected in the cerebrum of pigs 5, 6 and 7, inoculated with vKos_LP, compared to the other

tissues, and viral RNA was undetectable in the cerebellum of these pigs. Pig 8 (euthanized PID6) had significantly more viral RNA present in both the cerebellum and cerebrum. The early euthanasia of pigs 5 and 7 (PID5 and PID4, respectively) may affect the low amount of viral RNA detected in the cerebrum and cerebellum, however, pig 6 was euthanized same day as pig 8, and also had very low amount of viral RNA present in these tissues. Viral RNA was detected in the cerebellum and cerebrum at lower levels compared to other tissues in the pigs inoculated with vKos and vKos_SP; no viral RNA was detected in the cerebellum of pig 2 infected with vKos_SP

SNP Analyses (Animal experiment I). Deep sequencing was performed on the inoculums vKos and vKos_LL used for infection of pigs, as well as on cDNA amplicons derived from serum (collected on the day of euthanasia) of the inoculated and contact pigs from each group. The vKos_LL products displayed low-level sequence variation (below 6% frequency) scattered across the genome as synonymous and non-synonymous mutations in the inoculated pigs (Figure 3). The vKos_LL motif was maintained at around 99% frequency in the serum (Figure 3 B-D). The two contact pigs in this group both contained a non-synonymous amino acid (aa) substitution T3004A (99% frequency) located in the NS5A coding region (Figure 3 E-F). The T3004A substitution occurred at approximately 1%, 0.5% and 4% in pigs 1, 2, and 3, respectively, and was also observed in the inoculum (<0.4%); it does not occur in any published CSFV coding sequences (CDS) (retrieved from GenBank [23]). An apparent transmission bottleneck was observed between the inoculated pigs and the contact pigs, as the single nucleotide polymorphisms (SNPs) scattered across the genome occurred at rather lower frequencies (<2.5%) compared to the inoculated pigs, except for the SNP A2460G (aa D696G) which was unique for contact pig 5 and occurred at around 4% and a unique SNP G3884A (aa V1171I) in contact pig 4 was present at a frequency of 2.7%. The vKos_LL, as used for inoculation of the pigs, contained a total of 1219 SNPs (>0.1% frequency), with 1177 in the coding genome (Figure 3 A). Only seven SNPs occurred at a frequency >5% in the coding part of the genome (A1053G (aa K227R), A2553G (aa Q727R), A3839G (aa I1156V), A7829G (aa T2486A), C7910T (aa L2513F), T10275C (aa V3301A), and T11948C (aa L3859)) but these SNPs were detected at a frequency <1% or not at all in the 3 inoculated pigs, as well as in the 2 contact pigs. However, 27-44% of the SNPs detected in pig 1, 2, and 3 inoculated with vKos_LL were also present in the inoculum. To identify the path of transmission to the contact pigs, 100 SNPs from each dataset were randomly selected and compared. Contact pigs 4 and 5 had 46 SNPs of the 100 in common with each other, as well as 31 and 37 SNPs in common with pig 2, respectively. As pig 4 developed fever before pig 5, it is likely that pig 2 infected pig 4, and that pig 4 in turn infected pig 5. Pig 1, 2 and 3 had 33, 48, and 29 SNPs in common with the inoculum, respectively, which well reflects the above mentioned frequencies of 27-44%.

vKos, as used as the inoculum for animal experiment I, had SNPs (frequencies up to 40%) scattered across the entire genome; these were all present at below 4% frequency in the inoculated pigs (Figure 3 H-J). The virus in the contact pig 9 contained one synonymous mutation (C11509T (aa S3712); 56% frequency) at the consensus level (Figure 3 K). Deep sequencing revealed 4 SNPs at a frequency between 8-9% (T90C, A1671G (aa A366), T7186A (aa G2271), and C7516G (aa D2381)), 1 SNP at 17% (A400G (aa L9)), and another 4 SNPs with frequencies between 27-34% (A372G, A7216G (aa V2281), A7222G (aa L2283), G10217A (aa G3282S)). A total of 10 SNPs occurred at a level <1% or were absent in all the other pigs. CSFV RNA from contact pig 10 contained 6 SNPs occurring at a frequency of 7-13% (Figure 3 L), of which 4 are in the coding region (A6220G (aa T1949), A7558G (aa E2395), C8002T (aa S2543), and C9757T (aa A3128)). They occurred at <1% or undetectably in the other pigs. The inoculum contained a total of 1142 SNPs (>0.1% frequency), with 1108 SNPs in the coding region (Figure 3 G). Nine of these SNPs occurred at a frequency between 23-36% but the 9 SNPs occurred at <3% frequency in the inoculated pigs, and at <0.7% in the contact pigs. Some 23-52% of the SNPs detected in pigs 6, 7, and 8 that were inoculated with vKos were also present in the inoculum. Interestingly, L764P was detected at >1% in the serum of all pigs except for pig 9, and it was also present in the inoculum. As above, 100 SNPs were randomly selected to identify the possible path of transmission to the contact pigs. Contact pigs 9 and 10 had 28 SNPs out of this 100 in common, as well as 28 and 40 SNPs in common with pig 8, respectively. It seems likely that pig 8 infected contact pig 10, but it is not discernable whether pig 8 or contact pig 10 infected contact pig 9, as contact pig 10 exhibited signs of fever before contact pig 9. Pigs 6, 7 and 8 had 26, 46, and 50 SNPs in common with the inoculum, respectively, which very well reflects the above mentioned frequencies of 23-52%.

SNP analysis (Animal experiment II). Deep sequencing was performed on cDNA amplicons derived from the virus inoculums: vKos_SP, vKos_LP, and vKos. The cDNA amplicons derived from serum of three pigs from each group (vKos_SP pigs 1, 2, 3; vKos_LP pigs 5, 7, 8; vKos pigs 9, 11, 12) were also deep sequenced. These pigs all reached the humane endpoints. One pig from each group (vKos_SP pig 1; vKos_LP pig 8; vKos pig 12) was selected for in-depth characterization of SNPs in tonsils, lymph node, spleen, bone-marrow, cerebellum, and cerebrum.

vKos_SP had SNPs scattered across the genome in the inoculated pigs, with 5 SNPs being present at a frequency above 70% (A2961G (aa N863S), T3735C (aa V1121A), T5756C (aa L1795), T6832C (aa S2153), and A8732G (aa N2787D)), which seemed to be associated with the L764P substitution (Figure S2 A-F and Figure 4 B-D). These SNPs were also present in the inoculum at above 50% frequency (Figure 4 A). The substitutions A2961G (aa N863S), T3735C (aa V1121A), and T5756C (aa L1795) are not present in any published CSFV sequences, while the encoded N2787D variant has only been observed in 1 other strain, YI9908, belonging to the genotype 3.2 (GenBank acc. no. KT716271.1). The SP variant was only seen, in

conjunction with R761, in 0.9% of E2 fragment (190 nt) sequences in the CSF database of the European Community Reference Laboratory [24], as described [25]. The population distribution of vKos_SP in pig 1 was very similar to the distribution seen for pigs 2 and 3 (Figure 4 B-D), and therefore appeared representative for the group. vKos_SP in pig 1 has 36 SNPs with a frequency above 5% across all tissues, and therefore seems much less stable compared to vKos and vKos_LP, even though the vKos_SP motif is kept at >98% in all tissues. Surprisingly, the virus population in the tonsil tissue of pig 1 contained stop-codons at the codons normally encoding residues K179 and K180 (Figure S2 A), at a frequency of approximately 11 and 13%, respectively. K179* was also detected in the cerebellum and cerebrum at a frequency of approximately 1% and 0.9%, respectively. K180* was also detected in the cerebrum at a frequency of approximately 0.8%. The K179* and K180* variants were not detected in the vKos_SP inoculum. The SNPs T3285C (aa I971T), T3837C (aa V1155A), A4082G (aa I1237V), T6078C (aa V1902A), T7135C (aa P2254), and A7850G (aa N2493D) occurred at a level of approximately 20-25% in the inoculum, but were only present at approximately 1% or below in all the pig tissues tested. I971T and V1155A were not detected in the cerebrum, and I971T was not detected in the cerebellum either. The inoculum contains 681 SNPs (>0.1% frequency), with 653 located in the coding region (Figure 4 A). Some 77-87% of the SNPs detected in the inoculum and in the different tissues of vKos_SP pig 1 were also observed in the serum (Figure 4 B) and 29% of the SNPs detected in the inoculum were also detected in the tonsils where the primary virus replication takes place [26]. Some 57-58% of the SNPs detected in the tonsils and spleen were also present in the bone-marrow. In total, 67-77% of the SNPs detected in the inoculum and serum of pigs 2 and 3 were also observed in pig 1.

vKos_LP had SNPs scattered across the entire genome in the inoculated pigs (Figure 4 F-H), with 4 SNPs present at above 80% frequency (G2078A (aa A569T), A2380G (aa V669), G3499A (aa G1042) and A5833G (aa G1820)). These changes seemed to be associated with the S763L;L764P motif, as G2078A (aa A569T) and A2380G (aa V669) were linked in the sequencing reads. These SNPs were also present in the inoculum at above 69% frequency and are observed in published CSFV complete CDS. The A569T substitution is located in E1. The population distribution in pig 8 was similar to that seen for pigs 5 and 7 (Figure 4 F-H), indicating that pig 8 was representative of the group. vKos_LP in pig 8 had 17 SNPs present at above a 5% level across all tissues (Figure S2 G-L), but seemed to be very stable whereas vKos only had 3 SNPs at this level (see below). The SNP A7896T (aa Y2508F) in vKos_LP occurred at approximately 11% in the inoculum but was not detectable in most tissues, and was only found at a frequency of 3% in the tonsils and lymph nodes. The inoculum contained a total of 519 detectable SNPs (>0.1% frequency) with 495 in the coding region (Figure 4 E). Some 47-68% of the SNPs detected in the inoculum and in the different tissues of pig 8 infected with vKos_LP were also observed in the serum and 63% of the SNPs detected in the inoculum,

were also observed in the tonsils. Furthermore, 57% of the SNPs detected in the tonsils and 79% of the SNPs detected in the spleen were also observed in the bone-marrow. In total, 50-65% of the SNPs detected in the inoculum and serum of pigs 5 and 7 were also observed in pig 8.

In samples from animal experiment II, vKos had SNPs scattered across the entire genome all at below 7% in the inoculated pigs (Figure S2 M-R and Figure 4 J-L), with only 3 SNPs at a frequency above 5% (A9396G (aa K3000R), C12003A (aa P3877Q) and C12078A). The frequency of these variants in the inoculum was approximately 3%, 3.5% and undetectable, respectively. The virus population distribution within pig 12 was similar to pigs 9 and 11 (Figure 4 J-L), indicating that pig 12 was representative for the group. The low level of high frequency SNPs detected in serum (Figure 4 J-L) and tissues of pig 12 (Figure S2 M-R) indicates that vKos was more stable than the other variants. The inoculum contained a total of 1147 SNPs (>0.1% frequency), with 1090 of these being found in the coding region (Figure 4 I). These SNPs occurred at <3% frequency. Some 67-86% of the SNPs detected in the inoculum in the different tissues of pig 12 infected with vKos were also observed in the serum (Figure 4 J-L), and 52% of the SNPs detected in the inoculum were also observed in the tonsils. In total, 68% of the SNPs detected in the tonsils and 81% of those observed in the spleen were also present in the bone-marrow. Furthermore, 67-74% of the SNPs detected in the inoculum and serum of pigs 9 and 11 were also present in pig 12. The SNP resulting in the substitution S763L occurred at a level of 1% in the serum of pig 11, and that for L764P was present in the tonsils, bone-marrow, and lymph node of pig 12 and in the inoculum (>0.4% frequency).

Haplotyping. Full-length cDNAs were amplified from CSFV RNA obtained from serum of pigs 1 and 7 infected with vKos_SP and vKos_LP (animal experiment II), respectively, by long RT-PCR and cloned using the TOPO XL-2 cloning method, as described previously [27]. Full-length cDNA clones were obtained for vKos_SP (10 clones) and vKos_LP (5 clones). These full-length cDNA clones were sequenced and the sequences were aligned with the parental consensus sequence. The vKos_SP cDNA clones reflected the haplotypes present in the virus population, as 6 out of the 10 cDNA clones contained the SNPs A2961G (aa N863S), T3735C (aa V1121A), T5756C (aa L1795), T6832C (aa S2153), and A8732G (aa N2787D), together in the same clone (Table 1 A). One more clone (ESP1.2) contained the same SNPs with the exception of A8732G (Table 1 A). This strongly indicates that these SNPs are linked, as the majority of these SNPs were not observed alone in the cDNA clones. Variants with these SNPs most likely represent the major haplotypes of the viral population. This correlates with the SNP analysis, where these SNPs were present at >75% in the serum of pig 1 infected with vKos_SP (Table 1 A). Each of the vKos_SP cDNA clone sequences was unique with 3-12 SNPs (at 100% frequency, as they are clones of individual genomes from the viral population) besides those seen in the major haplotypes of the vKos_SP viral population (data not shown). A total of 51 unique SNPs were observed in the CDS. Some 53% of all observed SNPs were synonymous

mutations, while 43% were non-synonymous, and 3% were located in the 3'-UTR. Some 49% of the unique SNPs were observed in the serum of pig 1 infected with vKos_SP. An additional 26% of the unique SNPs were observed in full-length CSFV CDS or in full-length E2 glycoprotein sequences report previously (full-length E2 glycoprotein sequences were retrieved from the CSF database of the European Community Reference Laboratory [24] as described [25]). The remaining SNPs (25%) not detected in either the serum samples or full-length CSFV CDS were randomly distributed across the genome.

The cDNA clones obtained for vKos_LP reflected the major haplotype observed in the virus population, as they all contained the SNPs G2078A (aa A569T), A2380G (aa V669), G3499A (aa G1042) and A5833G (aa G1820) (Table 1 B). This, together with the linked reads, strongly indicates that these SNPs are linked. This correlates with the SNP analysis where variants with these SNPs were present at >89% frequency in the serum of pig 7 infected with vKos_LP. Four out of the five the vKos_LP cDNA clones were unique with 2-6 SNPs (100% frequency) besides those seen in the major haplotypes of the vKos_LP viral population (data not shown). A total of 17 unique SNPs were observed, with 32% being synonymous mutations, 55% nonsynonymous, and 9% located in the 5'- and 3'-UTR. Some 47% of the unique SNPs were observed in the serum of pigs infected with vKos_LP or in full-length CSFV CDS and full-length E2 glycoprotein sequences.

Discussion

To monitor the molecular evolution of the viral populations *in vitro* and *in vivo* during infection of pigs, viral RNA from the inoculated viruses, as well as from the serum of each pig was amplified to make full-length amplicons (>12kb) that were deep sequenced. The deep sequencing revealed that both the vKos and vKos_LL samples used to inoculate the pigs and the viruses rescued from infected pigs, in animal experiment I, were 100% identical to their respective cDNA sequence at the consensus level, indicating that no adaptive mutations were needed for the rescued viruses to be functional. However, the vKos contact pig 9 contained a synonymous mutation (in the codon for S3712; 56% frequency) at the consensus level. The two vKos_LL contact pigs contained a non-synonymous mutation (resulting in T3004A; 99% frequency) at the consensus level. This non-synonymous mutation was also observed in the inoculated pigs, and in the inoculum (<4% frequency), but is not present in any published CDS of CSFV. This SNP may have risen to fixation in the virus population due to it being the most fit haplotype, though it is more likely due to the bottleneck effect, as it was present at low frequency in the inoculated pigs. Over 60% and 38-51% of the SNPs detected in the serum of pigs infected with vKos_LL and vKos, respectively, were present in the virus inoculums. There was a difference in the population distribution within the virus for the inoculated pigs and the contact pigs for both vKos and vKos_LL. This is likely due to the transmission to the contact pigs being a bottleneck, resulting in a founder effect with reduced amount of variation and genetic heterogeneity in the

viral population. This information can be used to infer possible routes of transmission. For example, it is likely that contact pig 4 infected contact pig 5, as they shared 40 of 100 random SNPs, and contact pig 4 exhibited signs of CSFV infection before contact pig 5. Contact pigs 4 and 10 were likely infected by pig 2 (inoculated with vKos_LP) and pig 8 (inoculated with vKos), as they shared 31 and 40 of 100 random SNPs, respectively. Contact pig 9 was likely infected by either pig 8 or contact pig 10, as it exhibited signs of CSFV infection later than contact pig 10, and shared 28 of 100 random SNPs with both pig 8 and contact pig 10.

vKos_SP contained 5 secondary mutations at the consensus level, three of which were non-synonymous (resulting in N863S, V1121A, and N2787D) located in the coding regions for E2, P7, and NS5A, respectively. The substitutions N863S and V1121A have not been observed in any published strains of CSFV, and the N2787D change has only been observed in one other published strain, YI9908, which belonged to genotype 3.2. The residues V1121 and N2787 are highly conserved in the genomes of CSFV (100% and 98%, respectively), while N863 is observed at 35% frequency, with K863 being most common at a frequency of 62%. These amino acid substitutions strongly indicate that adaptive mutations were needed for vKos_SP to function optimally, as these SNPs existed at a frequency of 52-54% in the inoculum, but a much higher frequency of above 70% was observed in the viruses collected from infected pigs. vKos_SP, in conjunction with residue E761, is not observed in the CSF database, and seems to be a somewhat artificial combination, as only R761 is observed together with S763;P764, and this might explain the compensatory network of mutations. Low or neutral fitness variants can be maintained at a higher than expected frequency due to being linked to a high-fitness variant, that is well represented in the virus population [4]. The synonymous mutations likely have no effect on the fitness of the virus, and may just be passively selected changes carried along with the non-synonymous mutations.

vKos_LP contained 4 secondary mutations at the consensus level, one of which was a non-synonymous mutation G2078A (aa A569T), which seemed to be linked to A2380G (aa V669). The T569 variant is observed in the majority of published CSFV strains (62%), with A569 occurring at 35.5% frequency. A569T is located in E1, within a putative fusion peptide-like motif (residues 551-579) consisting of hydrophobic aa residues [28]. A similar stretch of hydrophobic aa residues is found in the E1 of hepatitis C virus, another member for the *Flaviviridae*, and this is believed to play a role in fusion [29, 30]. A shift from a small hydrophobic aa residue to an uncharged polar aa residue with a hydroxyl group, could have an impact on this motif and its potential role in fusion. The 4 secondary mutations occurred at >69% frequency in the inoculum, and at >88% frequency in virus collected from infected pigs. This increase in frequency indicates that these SNPs are either advantageous for the virus or are coupled to an advantageous variant, with the synonymous mutations likely being passively selected haplotypes.

Low level SNPs (<7% SNP frequency) were scattered across the genome of vKos from animal experiment II. Together with vKos from animal experiment I, this data strongly indicates that vKos is highly stable at the quasispecies level, as is vKos_LL, which also seems to be a common variant of wt Koslov, as seen in our previous studies (Fahnøe U, Pedersen AG, Höper D, Beer M, Rasmussen TB., unpublished data). The substitution S763L was present at 58.9% and 18.6% frequency in the tonsils and serum, respectively, and E2 sequences of wt Koslov, in the CSF database, also contain this motif.

In the previous study (Fahnøe U, Pedersen AG, Höper D, Beer M, Rasmussen TB., unpublished), 159 SNPs scattered across the genome were detected (>1% frequency), while 10 SNPs present at 40% frequency, were observed in the inoculum derived from blood of pigs infected with the Koslov strain of CSFV [31] used to challenge pigs. The Koslov strain, being a wt 'field isolate', likely consists of a much more diverse quasispecies with a typical distribution, in which a few haplotypes are dominant and many others are present at a very low frequency, than the viruses rescued from cDNA clones, as reported previously [32].

Over 77-87%, 47-68%, and 67-86% of the SNPs detected in the inoculums and the different tissues of pig 1, pig 8, and pig 12 infected with vKos_SP, vKos_LP and vKos, respectively, were also present in the respective sera. This is expected since the virus in serum is likely a collection of all the viruses present in the different tissues. The virus spreads through the peripheral blood from its primary site of replication in the tonsils to the regional lymph nodes, then to the bone-marrow, visceral lymph nodes, and lymphoid structures associated with the small intestine and spleen [26]. Over 57% and 79% of the SNPs detected in the tonsils and spleen, respectively, were also present in the bone-marrow.

Interestingly, S763L was detected in the serum of pig 11 inoculated with vKos, and has previously been suggested, together with P968H, to contribute to the difference in virulence between vKos and the attenuated vKos_3aa [11]. The L764P substitution was observed in the serum of most pigs infected with vKos from animal experiment I, and also in several tissues of pig 12 infected with vKos from animal experiment II. In our previous study with vKos, L764P was detected at 2% frequency in inoculated pigs, and fixed in one contact pig. Several studies indicate that residue 764 is under positive selection [33, 34]. Residues 763 and 764 are located in the antigenic motif ^{753}RYLASLHKKALPT^{765}, in particular L763 and P764, together with K761, are critical for reactivity with certain monoclonal antibodies (mAbs) [35].

Pigs infected with vKos_LP exhibited earlier signs of disease as judged by nearly all parameters, and therefore may be considered more virulent than vKos but each of the variants resulted in severe disease. The LP motif likely does not play a role in humoral immune evasion, as the infected pigs succumb to disease before an immune response has been activated. However, the faster appearance of clinical disease could be due to the LP motif having an effect on a variety of different aspects of the infection cycle within the natural host (e.g. stability, entry, replication, egress etc.). This effect may be occurring in conjunction with

the aa A569T substitution, as E1 has been implicated [15], together with E^{rns} and E2, in virus adsorption to host cells [12], and E1 also seems to play a role in virulence [36]. This warrants further study.

The cDNA clones obtained from serum of pig 1 and pig 7 infected with vKos_SP and vKos_LP, respectively, reflected the major haplotypes present in the viral population. The majority of the cDNA clones contained unique SNPs, and the majority of the SNPs were observed in the serum of the infected pigs or in published full-length CDS and full E2 glycoprotein sequences of CSFV. The remaining unique SNPs are likely very low frequency SNPs in the viral population. As the virus inoculum in our study originally stems from a BAC clone, errors could have been introduced into the virus inoculum by the T7 RNA polymerase. However, it is unlikely that the SNPs observed in the cDNA clones are errors introduced by the T7 RNA polymerase or the reverse transcriptase, as they were randomly distributed across the genome, which would not be expected if this was caused by the reverse transcriptase due to the skewed nature of its the error distribution. It is however possible that some of the very low frequency SNPs observed in the SNP analyses are due to NGS errors. As RNA viruses replicate to immense population sizes, this results in many genomic variants existing at very low frequencies within the viral population [37], which makes them difficult to distinguish from NGS errors, although NGS does allow for the generation of data of sufficient depth for characterization of the overall virus population [38]. As the viral RNA samples also have to undergo processing, such as reverse transcription and PCR amplification, before sequencing, errors in the form of artefactual mutations might be introduced into the viral genomes [39].

In summary, we have analyzed the virulence of mutant E2 viruses within infected pigs and characterized the virus population dynamics during infection. The vKos_LP exhibited earlier signs of CSFV infection compared to the other viruses, indicating that modification of residues 763 and 764 play a role in the properties of the highly virulent CSFV strain Koslov. The full-length cDNA clones derived from infected serum reflected the major haplotypes present in the viral populations and thus represents a useful means for identifying individual haplotypes present in infected animals.

Methods

Primers. Oligonucleotide primers used are listed in Supplementary Table S1.

Cells. PK15 cells (obtained from the Cell Culture Collection at the Friedrich-Loeffler-Institut, Germany) were propagated in Dulbecco's Modified Eagles Medium (DMEM) containing 5% FCS.

Generation of BACs containing non-synonymous mutations. The BACs Kos_LL, Kos_SP, and Kos_LP were obtained by site-directed mutagenesis using a megaprimer approach [40]. Briefly, the BAC consensus clone Kos [11] was used as template for the megaprimer PCR with forward primers Kos-ELL-F, CSFV-Kos-ESP-F, and CSFV-Kos-ELP-F and reverse primer Kos-2720R, respectively, Supplementary Table S1. The megaprimer,

after gel purification with a GeneJET Gel extraction kit (Thermo Scientific), was used for the site-directed mutagenesis with Kos as vector backbone and downstream cloning in *E. coli* DH10B (Invitrogen, Carlsbad, USA). BAC DNAs were purified from 4 ml overnight cultures using the Zymo BAC DNA Miniprep kit (Zymo Research). Full length amplicons were obtained by long PCR, as previously described [11, 41], using primers CSF-Kos_Not1-T7-1-59 and CSF-Kos_12313aR, Supplementary Table S1. PCR products were purified using GeneJET PCR purification kit (Thermo Scientific) and *in vitro* transcribed using Megascript T7 kit (Invitrogen).

Rescue of viruses. Virus was rescued from RNA transcripts following electroporation of PK15 cells, as described previously [42], and passaged once in PK15 cells. Titrations were performed, in triplicate, using polyclonal porcine antiserum for staining of infected cells.

Animal infection experiment I. In total, 10 crossbred pigs, 14 weeks of age, obtained from the high health status swine herd at DTU were used for the animal experiment. For both viruses, three pigs were inoculated with vKos or vKos_LL via the intranasal route with a defined virus dose (10^6 $TCID_{50}$) and two in-contact pigs, in each group, were mock inoculated with cell culture medium. Rectal body temperature and clinical signs were monitored on a daily basis. At predefined days (PID 0, 1, 2, 3, 4, 5, 7, 10 and 14), EDTA-blood and serum samples were collected for virological examination. Furthermore, nasal swabs were obtained on the same sampling days and the viral RNA from these and from EDTA-blood was purified using a MagNA Pure LC total nucleic acid isolation kit (Roche). RT-qPCR was used to determine the level of viral RNA, as described previously [43]. Finally, all pigs were subjected to necropsy and gross-pathological examination after euthanasia with intravascular injection of pentobarbital.

Animal infection experiment II. In total, 12 weaner pigs, 6 weeks of age, obtained from a conventional Danish swine herd with specific pathogen free status were used for the animal experiment. For each virus, four pigs were inoculated with vKos, vKos_SP or vKos_LP, respectively, via the intranasal route with a defined virus dose (10^6 $TCID_{50}$). Rectal body temperature and clinical signs were monitored on a daily basis. At predefined days (PID 0, 2, 3, 4, 7 and 10), EDTA-blood and serum samples were collected for virological examination as above. Nasal swabs were obtained on the same days, and tissue samples from tonsils, lymph nodes, spleen, bone-marrow, cerebellum and cerebrum were collected during post mortem examination after euthanasia with intravascular injection of pentobarbital. The viral RNA from collected samples was purified and the level of viral RNA was determined using RT-qPCR as described previously [43]. Pigs 4, 6 and 10 (one from each group) were not included in the NGS dataset, due to them being euthanized together with the second last pig in their group, for animal welfare reasons. All experimental procedures, animal care and maintenance were conducted in accordance with Danish and EU legislation (Consolidation Act 474 15/05/2014 and EU Directive 2010/63/EU) and with the approval from the Danish Animal Experimentation Inspectorate (license number 2012-15-2934-00182).

Preparation of cDNA from viral RNA. Viral RNA was extracted, using a combined Trizol/RNeasy protocol [44], from tonsils, bone-marrow, serum, lymph nodes, spleen, cerebellum, and cerebrum of pigs on the day of euthanasia (*Supplementary*, Table S2 and Table S3). This extracted RNA was used to generate full-length or two overlapping half-length cDNA amplicons, using a modified version of the long RT-PCR method described previously [11, 41]. Briefly, the total RNA was reverse transcribed using the Maxima H Minus Reverse Transcriptase (Thermo Scientific) and the specific cDNA primers, CSF-cDNA-1 and CSF-Kos-6240-RT (Supplementary Table S1). The cDNA was then amplified by long PCR using AccuPrime High Fidelity DNA polymerase (Thermo Scientific) with primers CSF-Kos_NotI-T7-1-59 and CSF-Kos_12313aR for full-length amplicons, and CSF-Kos_NotI-T7-1-59 and CSF-Kos-6176R for the 5' end and CSF-Kos-5981-F and CSF-Kos_12313aR for 3' end of the half-length cDNA amplicons, respectively.

Cloning in pCR XL-2-TOPO vector. Full-length cDNA amplicons, representing vKos_SP, and vKos LP (*Supplementary*, Table S3), were obtained from extracted RNA from serum of infected animals, and cloned using the TOPO XL-2 kit (Thermo Scientific), as previously described [27]. Briefly, the cDNA was generated as above and full-length amplified by long PCR, using the Q5 high-fidelity DNA polymerase kit (New England BioLabs) and primers CSF-Kos_1-59 and CSF-Kos_12313aR. The products were gel purified with a GeneJet Gel extraction kit (Thermo Scientific) and quantified using a Qubit Fluorometric quantitation system (Thermo Scientific), cloned into the pCR-XL-2-TOPO vector and transformed into *E. coli*.

Next generation sequencing (NGS). Full- and half-length amplified cDNA amplicons and cDNA clones were sequenced by NGS at the DTU Multi-Assay Core (DMAC, Kgs. Lyngby, Denmark) using a MiSeq Nextera XT system (Illumina, San Diego, USA). Consensus sequences were obtained by mapping the reads to the vKos reference sequence (KF977607.1) using CLC Genomics Workbench v.9.5.2 (CLC bio, Aarhus, Denmark). Consensus sequences were aligned using MAFFT in Geneious (Biomatters, Auckland, New Zealand). Low frequency SNPs (>0.1%) were identified for cDNA amplicons using a combination of BWA, Samtools, Lo-Freq-snp-caller, and SnpEff, as described previously [11, 45].

Acknowledgements

We thank laboratory technicians and animal caretakers at Lindholm for their invaluable work during the animal experiments. We thank Dr. Jens Nielsen for management of animal experiment I. We are grateful for excellent assistance from Marlene D. Dalgaard (DMAC, DTU). This study was funded by internal resources from the National Veterinary Institute within the Technical University of Denmark.

References

1. Lindenbach BD, Thiel HJ, Rice CM, Murray CL, Thiel HJ, Rice CM. Flaviviridae: The viruses and their replication. In: Fields Virology. 6th edition. New York: Lippincott Williams & Wilkins; 2013. p. 712–46.
2. Collett MS, Anderson DK, Retzel E. Comparisons of the pestivirus bovine viral diarrhoea virus with members of the Flaviviridae. J Gen Virol. 1988;69:2637–43.
3. Meyers G, Rümenapf T, Thiel HJ. Molecular cloning and nucleotide sequence of the genome of hog cholera virus. Virology. 1989;171:555–67.
4. Lauring AS, Andino R. Quasispecies theory and the behavior of RNA viruses. PLoS Pathog. 2010;6:e1001005.
5. Domingo E, Sheldon J, Perales C. Viral quasispecies evolution. Microbiol Mol Biol Rev. 2012;76:159–216.
6. Vignuzzi M, Stone JK, Arnold JJ, Cameron CE, Andino R. Quasispecies diversity determines pathogenesis through cooperative interactions in a viral population. Nature. 2006;439:344–8.
7. Bordería A V., Isakov O, Moratorio G, Henningsson R, Agüera-González S, Organtini L, et al. Group selection and contribution of minority variants during virus adaptation determines virus fitness and phenotype. PLoS Pathog. 2015;11:e1004838.
8. Peck KM, Lauring AS. The complexities of viral mutation rates. J Virol. 2018; May:JVI.01031-17.
9. Floegel-Niesmann G, Blome S, Gerß-Dülmer H, Bunzenthal C, Moennig V. Virulence of classical swine fever virus isolates from Europe and other areas during 1996 until 2007. Vet Microbiol. 2009;139:165–9.
10. Mittelholzer C, Moser C, Tratschin JD, Hofmann MA. Analysis of classical swine fever virus replication kinetics allows differentiation of highly virulent from avirulent strains. Vet Microbiol. 2000;74:293–308.
11. Fahnøe U, Pedersen AG, Risager PC, Nielsen J, Belsham GJ, Höper D, et al. Rescue of the highly virulent classical swine fever virus strain “Koslov” from cloned cDNA and first insights into genome variations relevant for virulence. Virology. 2014;468–470:379–87.
12. Hulst MM, Moormann RJM. Inhibition of pestivirus infection in cell culture by envelope proteins Erns and E2 of classical swine fever virus: Erns and E2 interact with different receptors. J Gen Virol. 1997;78:2779–87.
13. van Gennip HGP, van Rijn PA, Widjojoatmodjo MN, de Smit AJ, Moormann RJM. Chimeric classical swine fever viruses containing envelope protein Erns or E2 of bovine viral diarrhoea virus protect pigs against challenge with CSFV and induce a distinguishable antibody response. Vaccine. 2000;19:447–59.

14. Liang D, Fernandez-Sainz I, Ansari IH, Gil LHVG, Vassilev V, Donis RO. The envelope glycoprotein E2 is a determinant of cell culture tropism in ruminant pestiviruses. J Gen Virol. 2003;84:1269–74.
15. Wang Z, Nie Y, Wang P, Ding M, Deng H. Characterization of classical swine fever virus entry by using pseudotyped viruses: E1 and E2 are sufficient to mediate viral entry. Virology. 2004;330:332–41.
16. Leifer I, Blome S, Blohm U, König P, Küster H, Lange B, et al. Characterization of C-strain Riems TAV-epitope escape variants obtained through selective antibody pressure in cell culture. Vet Res. 2012;43:1–11.
17. Risatti GR, Borca M V., Kutish GF, Lu Z, Holinka LG, French RA, et al. The E2 glycoprotein of classical swine fever virus is a virulence determinant in swine. J Virol. 2005;79:3787–96.
18. Risatti GR, Holinka LG, Carrillo C, Kutish GF, Lu Z, Tulman ER, et al. Identification of a novel virulence determinant within the E2 structural glycoprotein of classical swine fever virus. Virology. 2006;355:94–101.
19. Risatti GR, Holinka LG, Fernandez-Sainz I, Carrillo C, Kutish GF, Lu Z, et al. Mutations in the carboxyl terminal region of E2 glycoprotein of classical swine fever virus are responsible for viral attenuation in swine. Virology. 2007;364:371–82.
20. Risatti GR, Holinka LG, Fernandez Sainz I, Carrillo C, Lu Z, Borca M V. N-linked glycosylation status of classical swine fever virus strain Brescia E2 glycoprotein influences virulence in swine. J Virol. 2007;81:924–33.
21. van Gennip HGP, Vlot AC, Hulst MM, De Smit AJ, Moormann RJM. Determinants of virulence of classical swine fever virus strain Brescia. J Virol. 2004;78:8812–23.
22. Tamura T, Sakoda Y, Yoshino F, Nomura T, Yamamoto N, Sato Y, et al. Selection of classical swine fever virus with enhanced pathogenicity reveals synergistic virulence determinants in E2 and NS4B. J Virol. 2012;86:8602–13.
23. Clark K, Karsch-Mizrachi I, Lipman DJ, Ostell J, Sayers EW. GenBank. http://www.ncbi.nlm.nih.gov/genbank/. Accessed 27 Oct 2017.
24. Greiser-Wilke I, Zimmermann B. The CSF database of the European Community Reference Laboratory. http://viro60.tiho-hannover.de/eg/csf/. Accessed 27 Oct 2017.
25. Postel A, Schmeiser S, Zimmermann B, Becher P. The European Classical Swine Fever Virus Database: Blueprint for a pathogen-specific sequence database with integrated sequence analysis tools. Viruses. 2016;8:302.
26. Mmerman JJ, Karriker LA, Ramirez A, Schwartz KJ, Stevenson GWZ. Diseases of swine. 10th edition. Oxford: John Wiley & Sons; 2012.
27. Johnston CM, Fahnøe U, Belsham GJ, Rasmussen TB. Strategy for efficient generation of numerous

full-length cDNA clones of classical swine fever virus for haplotyping. BMC Genomics. 2018;19:600.

28. El Omari K, Iourin O, Harlos K, Grimes JM, Stuart DI. Structure of a pestivirus envelope glycoprotein E2 clarifies its role in cell entry. Cell Rep. 2013;3:30–5.
29. Drummer HE, Boo I, Poumbourios P. Mutagenesis of a conserved fusion peptide-like motif and membrane-proximal heptad-repeat region of hepatitis C virus glycoprotein E1. J Gen Virol. 2007;88 Pt 4:1144–8.
30. Li H-F, Huang C-H, Ai L-S, Chuang C-K, Chen SSL. Mutagenesis of the fusion peptide-like domain of hepatitis C virus E1 glycoprotein: Involvement in cell fusion and virus entry. J Biomed Sci. 2009;16:89.
31. Blome S, Gabriel C, Schmeiser S, Meyer D, Meindl-Böhmer A, Koenen F, et al. Efficacy of marker vaccine candidate CP7-E2alf against challenge with classical swine fever virus isolates of different genotypes. Vet Microbiol. 2014;169:8–17.
32. Jenckel M, Blome S, Beer M, Höper D. Quasispecies composition and diversity do not reveal any predictors for chronic classical swine fever virus infection. Arch Virol. 2017;162:775–86.
33. Tang F, Pan Z, Zhang C. The selection pressure analysis of classical swine fever virus envelope protein genes Erns and E2. Virus Res. 2008;131:132–5.
34. Wu Z, Wang Q, Feng Q, Liu Y, Teng J, Yu AC, et al. Correlation of the virulence of CSFV with evolutionary patterns of E2 glycoprotein. Front Biosci (Elite Ed). 2010;2:204–20.
35. Chang CY, Huang CC, Deng MC, Huang YL, Lin YJ, Liu HM, et al. Antigenic mimicking with cysteine-based cyclized peptides reveals a previously unknown antigenic determinant on E2 glycoprotein of classical swine fever virus. Virus Res. 2012;163:190–6.
36. Risatti GR, Holinka LG, Lu Z, Kutish GF, Tulman ER, French R a, et al. Mutation of E1 glycoprotein of classical swine fever virus affects viral virulence in swine. Virology. 2005;343:116–27.
37. Whitfield ZJ, Andino R. Characterization of viral populations by using circular sequencing. J Virol. 2016;90:8950–3.
38. Acevedo A, Brodsky L, Andino R. Mutational and fitness landscapes of an RNA virus revealed through population sequencing. Nature. 2014;505:686–90.
39. Orton RJ, Wright CF, Morelli MJ, King DJ, Paton DJ, King DP, et al. Distinguishing low frequency mutations from RT-PCR and sequence errors in viral deep sequencing data. BMC Genomics. 2015;16:1–15.
40. Risager PC, Fahnøe U, Gullberg M, Rasmussen TB, Belsham GJ, Fahnoe U, et al. Analysis of classical swine fever virus RNA replication determinants using replicons. J Gen Virol. 2013;94 Pt_8:1739–48.
41. Rasmussen TB, Reimann I, Uttenthal Å, Leifer I, Depner K, Schirrmeier H, et al. Generation of recombinant pestiviruses using a full-genome amplification strategy. Vet Microbiol. 2010;142:13–7.

42. Friis MB, Rasmussen TB, Belsham GJ. Modulation of translation initiation efficiency in classical swine fever virus. J Virol. 2012;86:8681–92.
43. Hoffmann B, Depner K, Schirrmeier H, Beer M. A universal heterologous internal control system for duplex real-time RT-PCR assays used in a detection system for pestiviruses. J Virol Methods. 2006;136:200–9.
44. Rasmussen TB, Reimann I, Hoffmann B, Depner K, Uttenthal Å, Beer M. Direct recovery of infectious pestivirus from a full-length RT-PCR amplicon. J Virol Methods. 2008;149:330–3.
45. Fahnøe U, Pedersen AG, Dräger C, Orton RJ, Blome S, Höper D, et al. Creation of functional viruses from non-functional cDNA clones obtained from an RNA virus population by the use of ancestral reconstruction. PLoS One. 2015;10:e0140912.
46. Leifer I, Hoffmann B, Hoper D, Rasmussen TB, Blome S, Strebelow G, et al. Molecular epidemiology of current classical swine fever virus isolates of wild boar in Germany. J Gen Virol. 2010;91:2687–97.

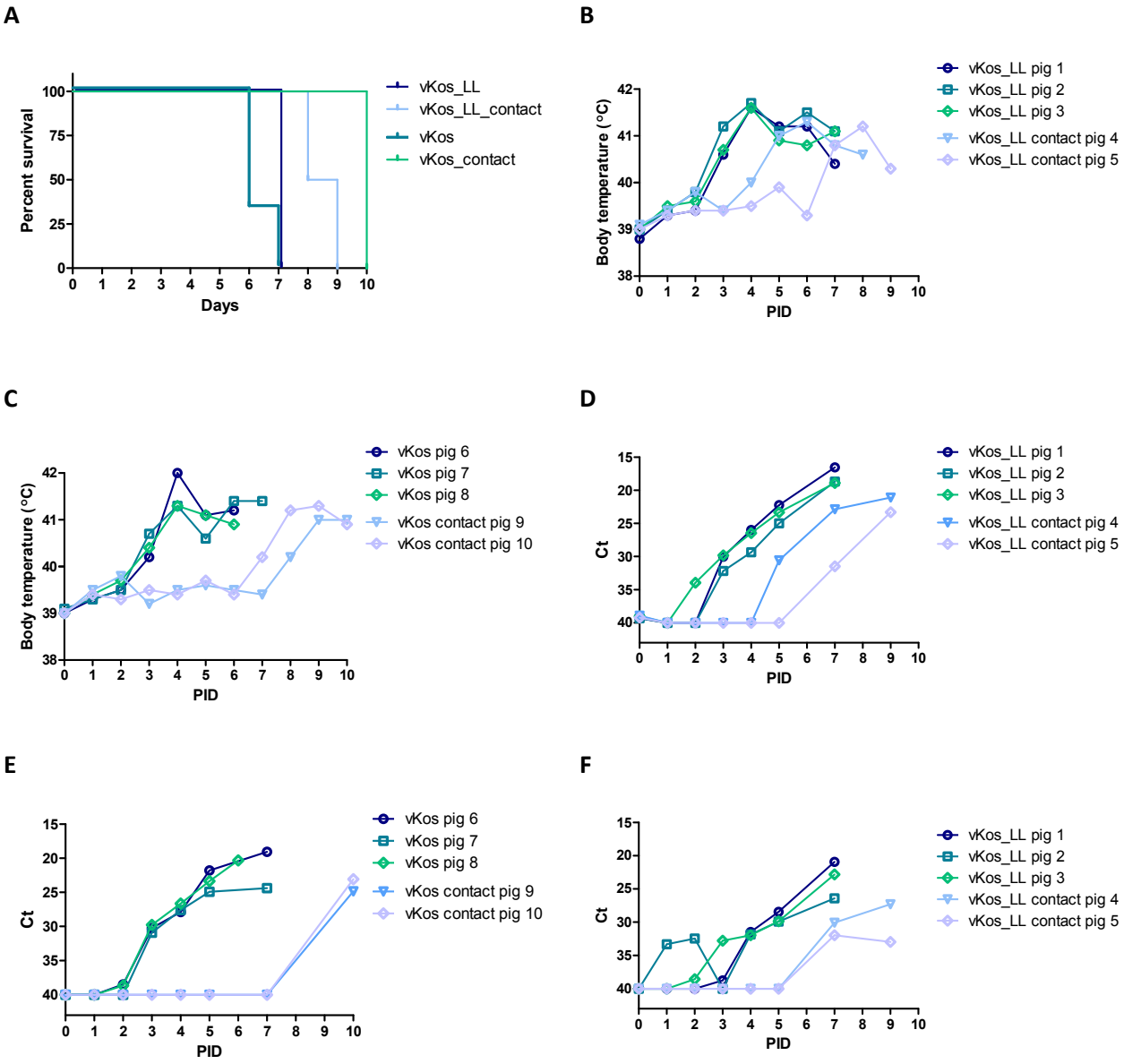
A
Percent survival
Days
vKos_LL
vKos_LL_contact
vKos
vKos_contact
B
Body temperature (°C)
PID
vKos_LL pig 1
vKos_LL pig 2
vKos_LL pig 3
vKos_LL contact pig 4
vKos_LL contact pig 5
C
Body temperature (°C)
PID
vKos pig 6
vKos pig 7
vKos pig 8
vKos contact pig 9
vKos contact pig 10
D
Ct
PID
vKos_LL pig 1
vKos_LL pig 2
vKos_LL pig 3
vKos_LL contact pig 4
vKos_LL contact pig 5
E
Ct
PID
vKos pig 6
vKos pig 7
vKos pig 8
vKos contact pig 9
vKos contact pig 10
F
Ct
PID
vKos_LL pig 1
vKos_LL pig 2
vKos_LL pig 3
vKos_LL contact pig 4
vKos_LL contact pig 5

Figure 1 A-F

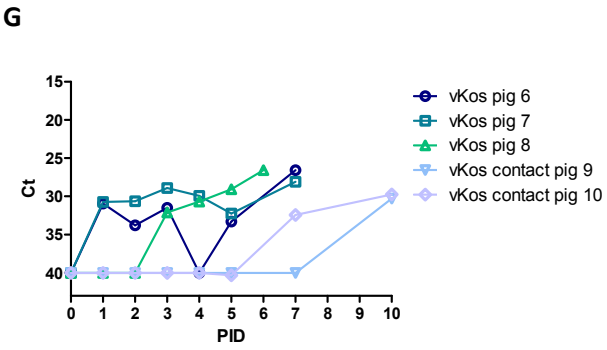

Figure 1

Infection of pigs in animal experiment I with vKos and vKos_LL. A) Survival of pigs. B) Body temperatures of pigs inoculated with vKos_LL during the infection. C) Body temperatures of pigs inoculated with vKos during the infection. D) Level of CSFV RNA in the blood of pigs inoculated with vKos_LL measured by RT-qPCR. E) Level of CSFV RNA in the blood of pigs inoculated with vKos measured by RT-qPCR. F) Level of viral RNA in nasal swabs of pigs inoculated with vKos_LL measured by RT-qPCR. G) Level of viral RNA in nasal swabs of pigs inoculated with vKos measured by RT-qPCR.

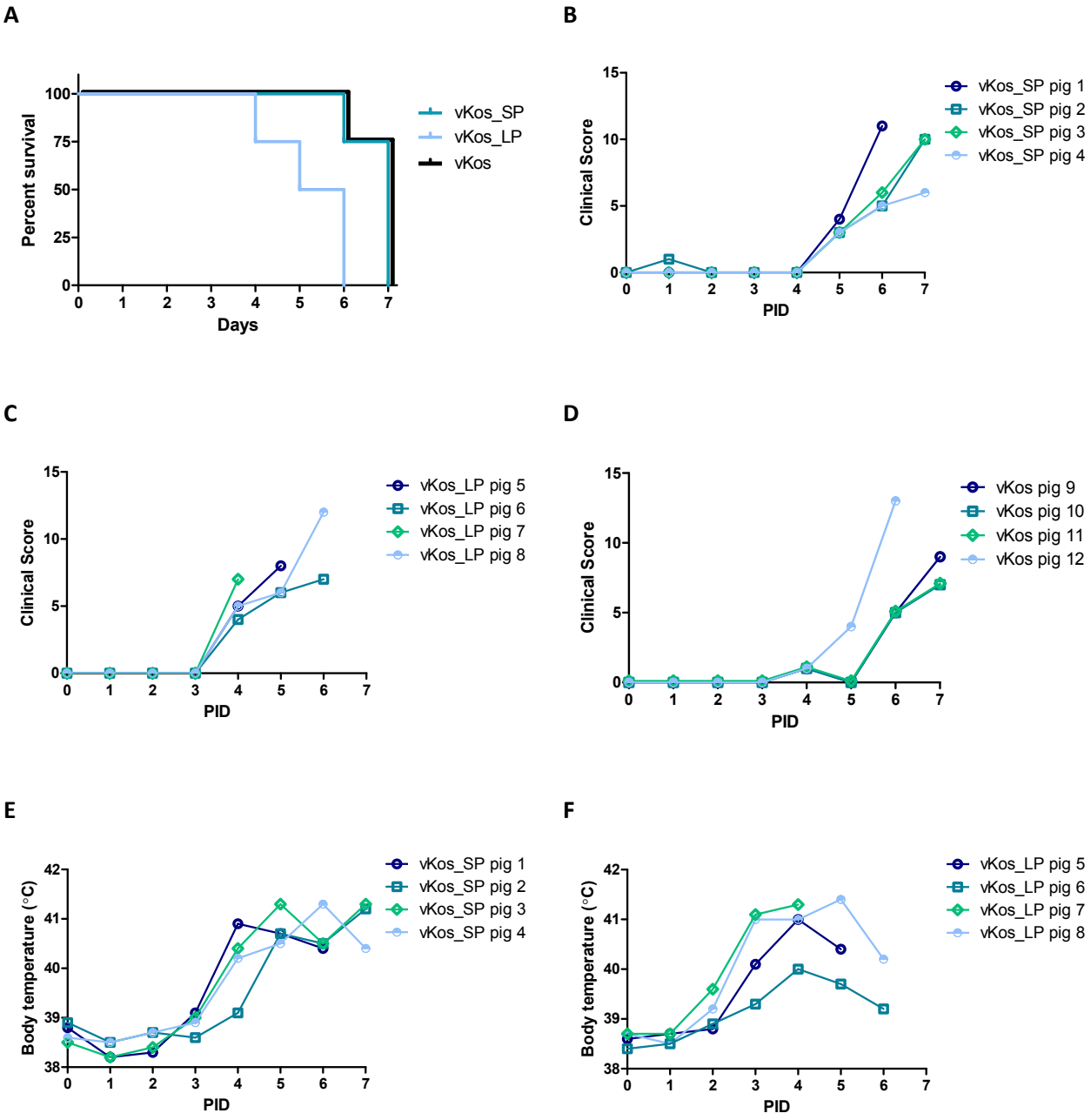
A
Percent survival
100
75
50
25
0
0 1 2 3 4 5 6 7
Days
vKos_SP
vKos_LP
vKos
B
Clinical Score
15
10
5
0
0 1 2 3 4 5 6 7
PID
vKos_SP pig 1
vKos_SP pig 2
vKos_SP pig 3
vKos_SP pig 4
C
Clinical Score
15
10
5
0
0 1 2 3 4 5 6 7
PID
vKos_LP pig 5
vKos_LP pig 6
vKos_LP pig 7
vKos_LP pig 8
D
Clinical Score
15
10
5
0
0 1 2 3 4 5 6 7
PID
vKos pig 9
vKos pig 10
vKos pig 11
vKos pig 12
E
Body temperature (°C)
42
41
40
39
38
0 1 2 3 4 5 6 7
PID
vKos_SP pig 1
vKos_SP pig 2
vKos_SP pig 3
vKos_SP pig 4
F
Body temperature (°C)
42
41
40
39
38
0 1 2 3 4 5 6 7
PID
vKos_LP pig 5
vKos_LP pig 6
vKos_LP pig 7
vKos_LP pig 8

Figure 2 A-F

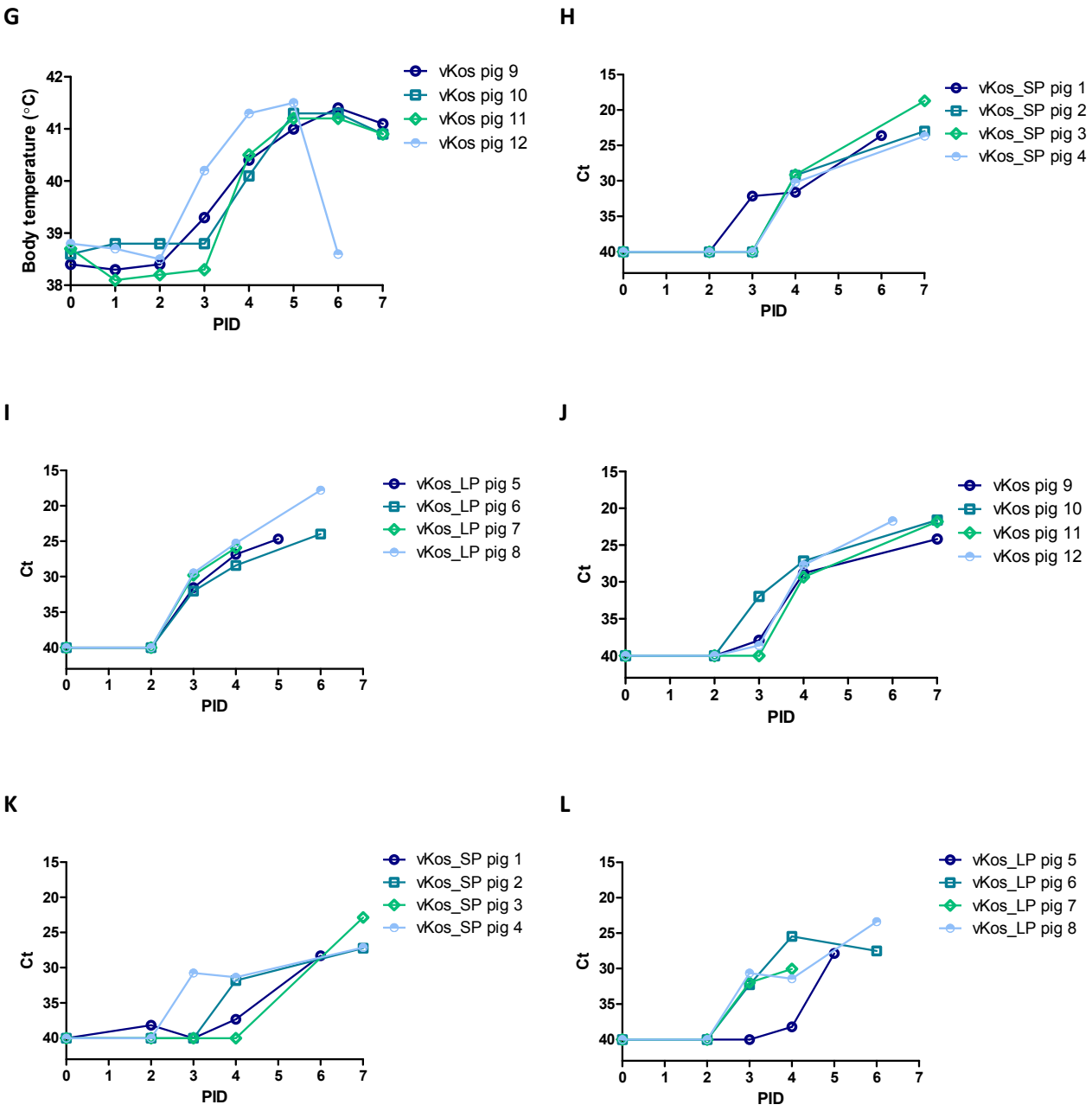
G
Body temperature (°C)
PID
vKos pig 9
vKos pig 10
vKos pig 11
vKos pig 12
H
Ct
PID
vKos_SP pig 1
vKos_SP pig 2
vKos_SP pig 3
vKos_SP pig 4
I
Ct
PID
vKos_LP pig 5
vKos_LP pig 6
vKos_LP pig 7
vKos_LP pig 8
J
Ct
PID
vKos pig 9
vKos pig 10
vKos pig 11
vKos pig 12
K
Ct
PID
vKos_SP pig 1
vKos_SP pig 2
vKos_SP pig 3
vKos_SP pig 4
L
Ct
PID
vKos_LP pig 5
vKos_LP pig 6
vKos_LP pig 7
vKos_LP pig 8

Figure 2 G-L

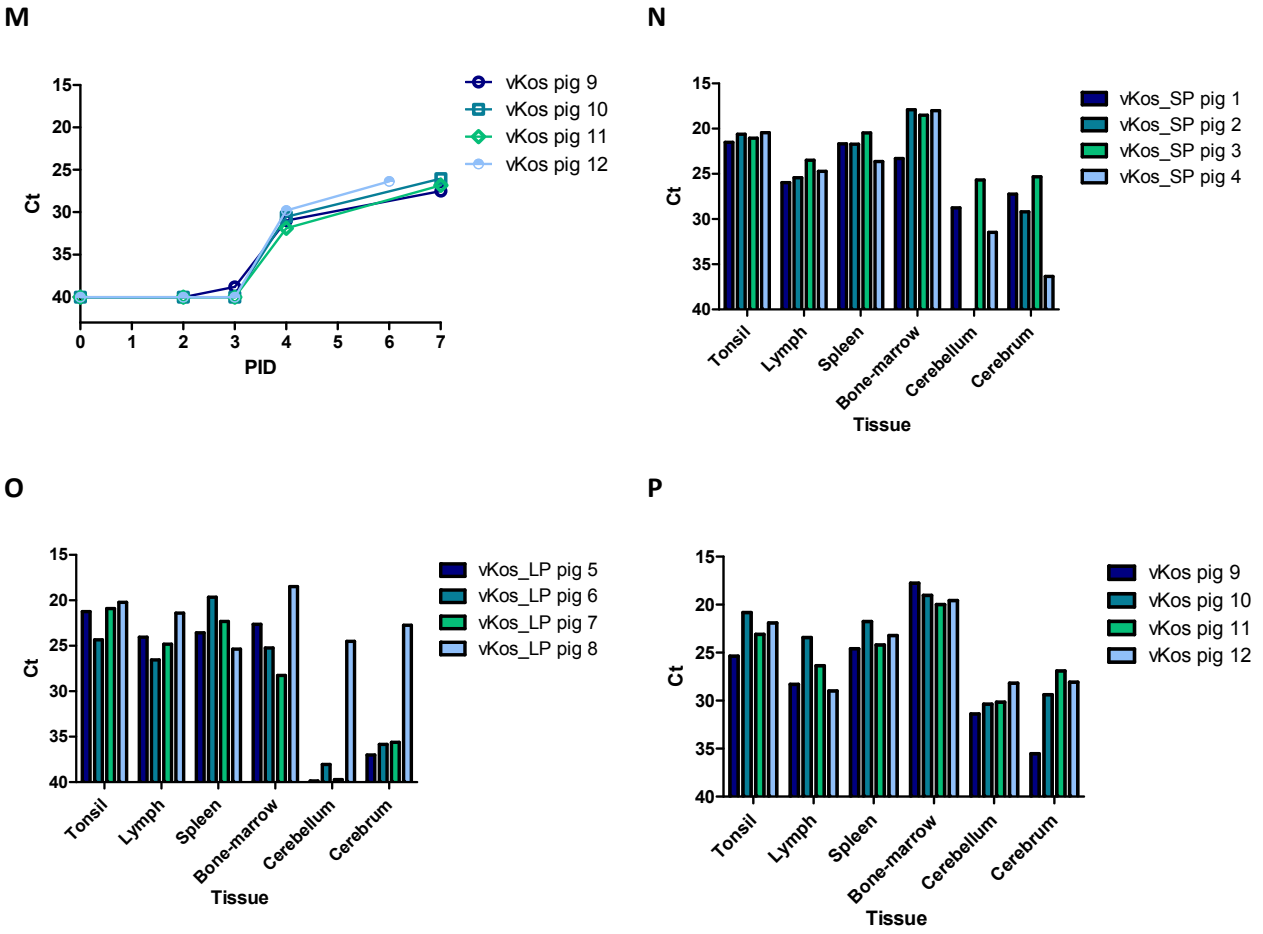

Figure 2

Infection of pigs in animal experiment II with vKos, vKos_LP, and vKos_SP. A) Survival of pigs. B) Clinical scores of pigs inoculated with vKos_SP during the infection. C) Clinical scores of pigs inoculated with vKos_LP during the infection. D) Clinical scores of pigs inoculated with vKos during the infection. E) Body temperatures of pigs inoculated with vKos_SP during the infection. F) Body temperatures of pigs inoculated with vKos_LP during the infection. G) Body temperatures of pigs inoculated with vKos during the infection. H) Level of RNA in the blood of pigs inoculated with vKos_SP measured by RT-qPCR. I) Level of RNA in the blood of pigs inoculated with vKos_LP measured by RT-qPCR. J) Level of RNA in the blood of pigs inoculated with vKos measured by RT-qPCR. K) Level of viral RNA in nasal swabs of pigs inoculated with vKos_SP measured by RT-qPCR. L) Level of viral RNA in nasal swabs of pigs inoculated with vKos_LP measured by RT-qPCR. M) Level of viral RNA in nasal swabs of pigs inoculated with vKos measured by RT-qPCR. N) Level of viral RNA in tissues of pigs inoculated with vKos_SP measured by RT-qPCR. O) Level of viral RNA in tissues of pigs inoculated with vKos_LP measured by RT-qPCR. P) Level of viral RNA in tissues of pigs inoculated with vKos measured by RT-qPCR.

A

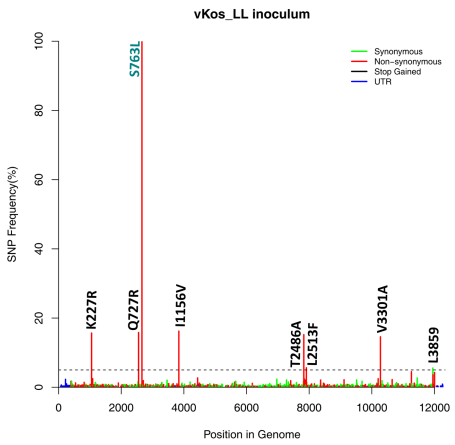

B

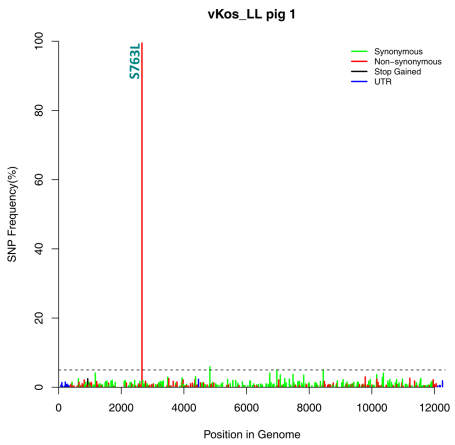

C

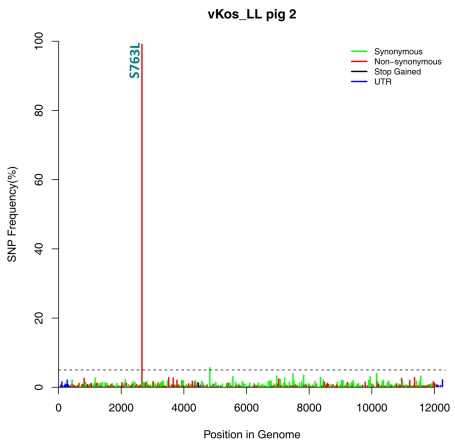

D

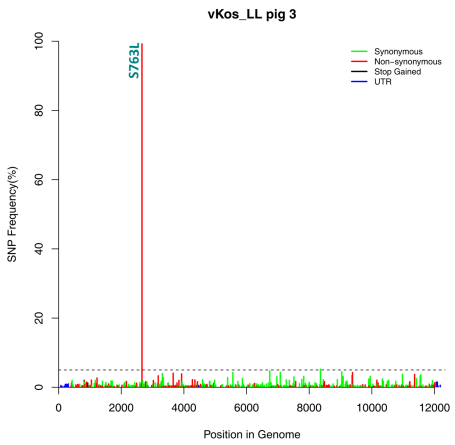

E

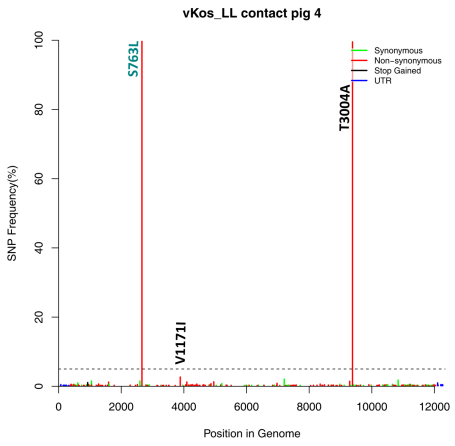

F

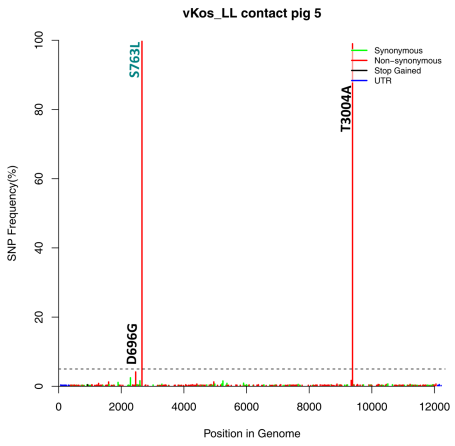

Figure 3 A-F

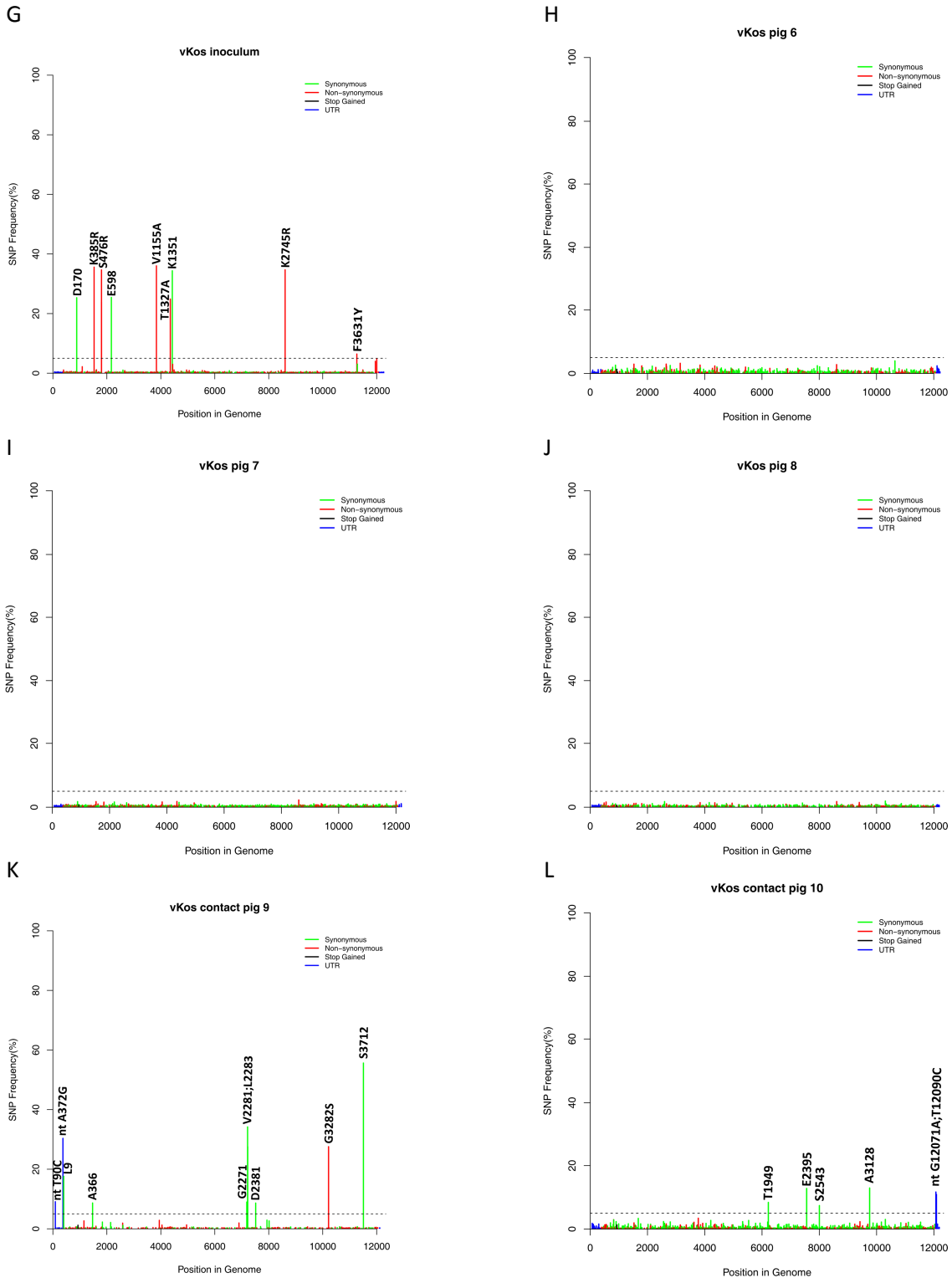

Figure 3

SNP frequency plot of samples from animal experiment I. A) vKos_LL inoculum. B) vKos_LL pig 1. C) vKos_LL pig 2. D) vKos_LL pig 3. E) vKos_LL pig 4. F) vKos_LL pig 5. G) vKos inoculum. H) vKos pig 6. I) vKos pig 7. J) vKos pig 8. K) vKos pig 9. L) vKos pig 10.

A

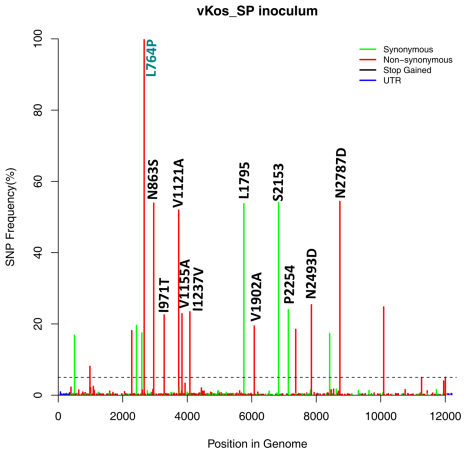

B

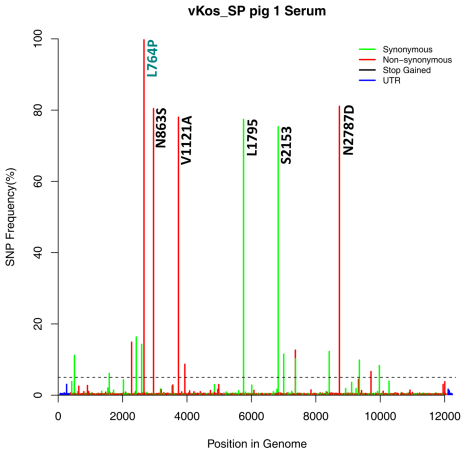

C

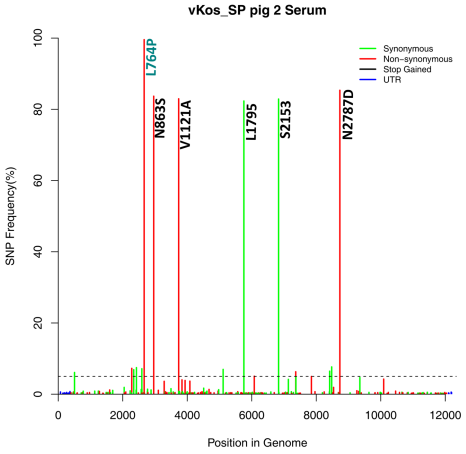

D

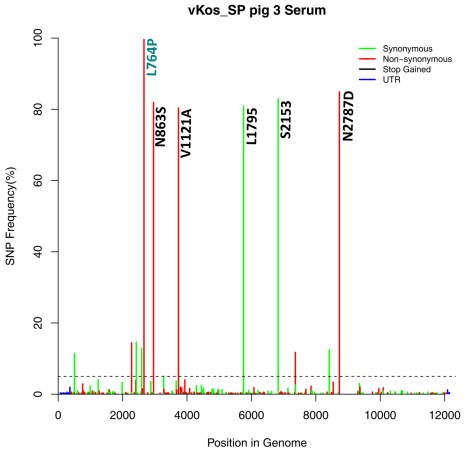

E

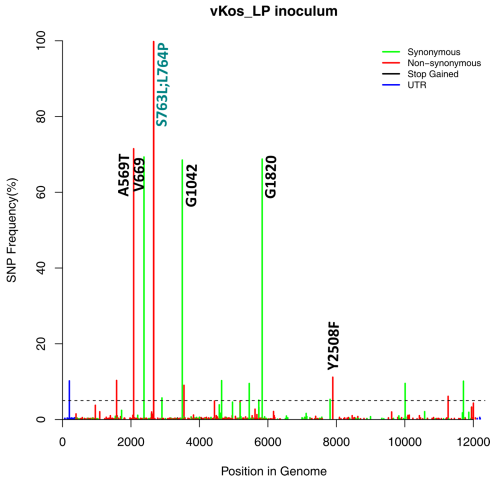

F

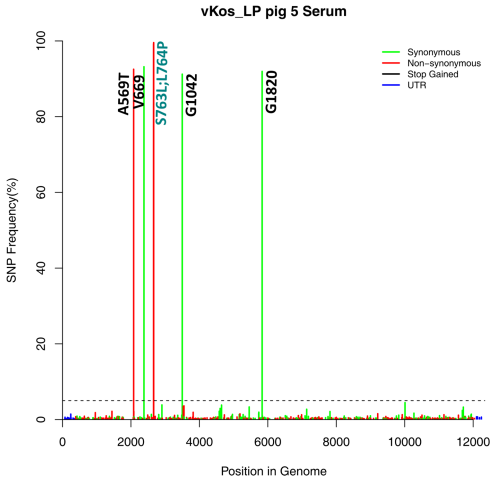

Figure 4 A-F

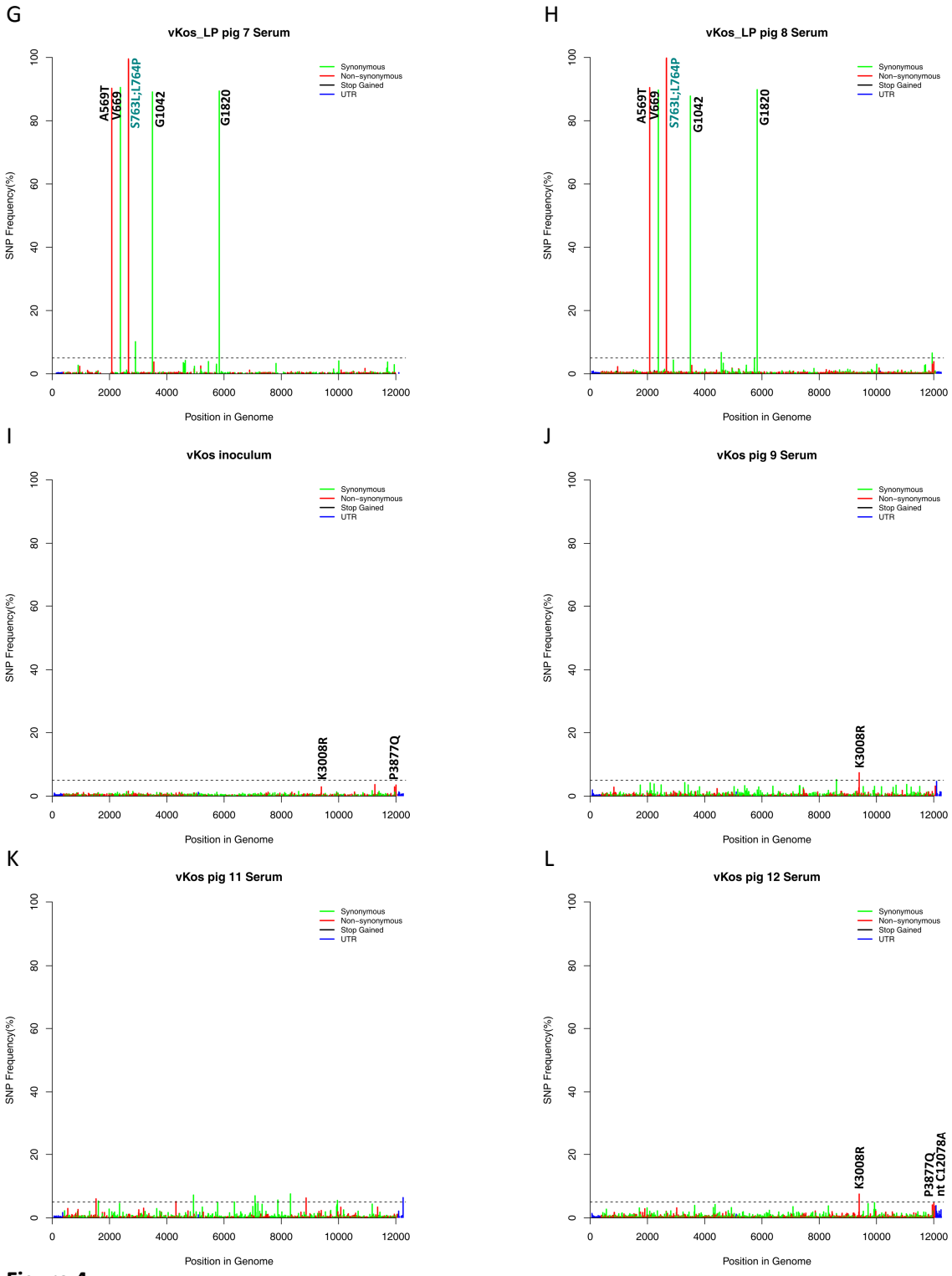

Figure 4

SNP frequencies plots of inoculum and serum samples from animal experiment II. A) vKos_SP inoculum. B) vKos_SP pig 1 serum. C) vKos_SP pig 2 serum. D) vKos_SP pig 3 serum. E) vKos_LP inoculum. F) vKos_LP pig 5 serum. G) vKos_LP pig 7 serum. H) vKos_LP pig 8 serum. I) vKos inoculum. J) vKos pig 9 serum. K) vKos pig 11 serum. L) vKos pig 12 serum.

Table 1

A

Clone	T2664C L764P	A2961G N863S	T3735C V1121A	T5756C L1795	T6832C S2153	A8732G N2787D
ESP 11.1	+	-	-	-	-	-
ESP 12.1	+	+	+	+	+	+
ESP 15.1	+	-	-	-	-	-
ESP 17.1	+	+	+	+	+	+
ESP 1.2	+	+	+	+	+	-
ESP10.2	+	+	+	+	+	+
ESP 12.2	+	+	+	+	+	+
ESP 18.2	+	+	+	+	+	+
ESP 22.2	+	-	-	-	-	-
ESP 24.2	+	+	+	+	+	+
vKos_SP pig 1 serum	+ (100%)	+ (80%)	+ (78%)	+(77%)	+(75%)	+(81%)

Each (-) indicates that the variant was not detected in the clone and (+) indicates that the variant was detected.

B

Clone	C2661T S763L	T2664C L764P	G2078A A569T	A2380G V669	G3499A G1042	A5833G G1820
ELP 12.1	+	+	+	+	+	+
ELP 1.2	+	+	+	+	+	+
ELP 5.2	+	+	+	+	+	+
ELP 6.2	+	+	+	+	+	+
ELP 8.2	+	+	+	+	+	+
vKos_LP pig 7 serum	+ (100%)	+ (99%)	+(90%)	+(90%)	+(89%)	+(89%)

Each (-) indicates that the variant was not detected in the clone and (+) indicates that the variant was detected.

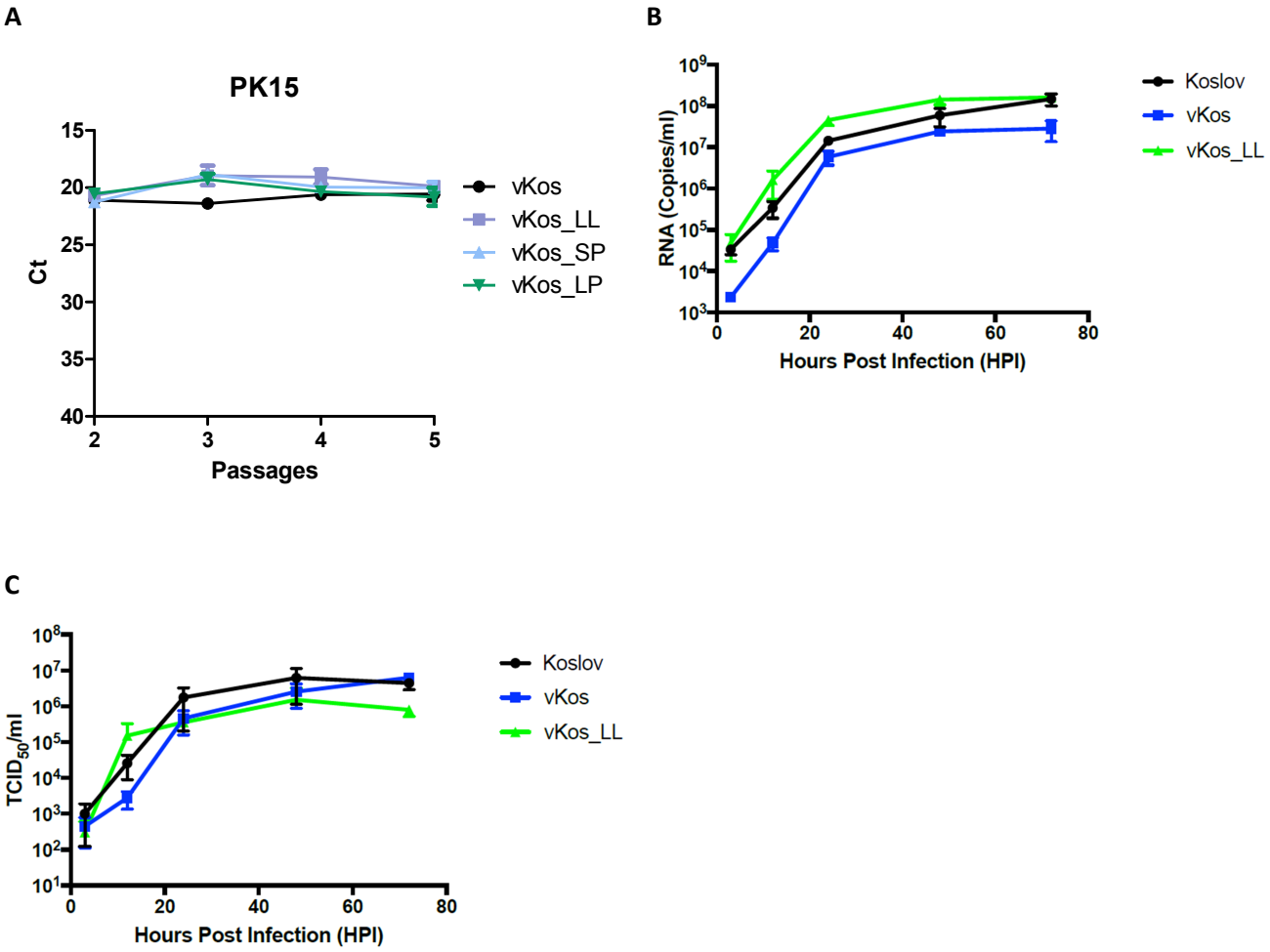

Figure S1

Virus yield during serial passaging and growth kinetics of vKos constructs. A) RT-qPCR of rescued vKos and its variants serial passaged in PK15 cells. B) Growth kinetics of wt Koslov (vKoslov), consensus BAC clone-derived vKos, and vKos_LL in PK15 cells measured by RT-qPCR assays (viral RNA copies/ml) at 3, 12, 24, 48, and 72 hours after infection. C) Growth kinetics of wt Koslov (vKoslov), consensus BAC clone vKos, and vKos_LL in PK15 cells measured by titration ($TCID_{50}$/ml) at 3, 12, 24, 48, and 72 hours after infection.

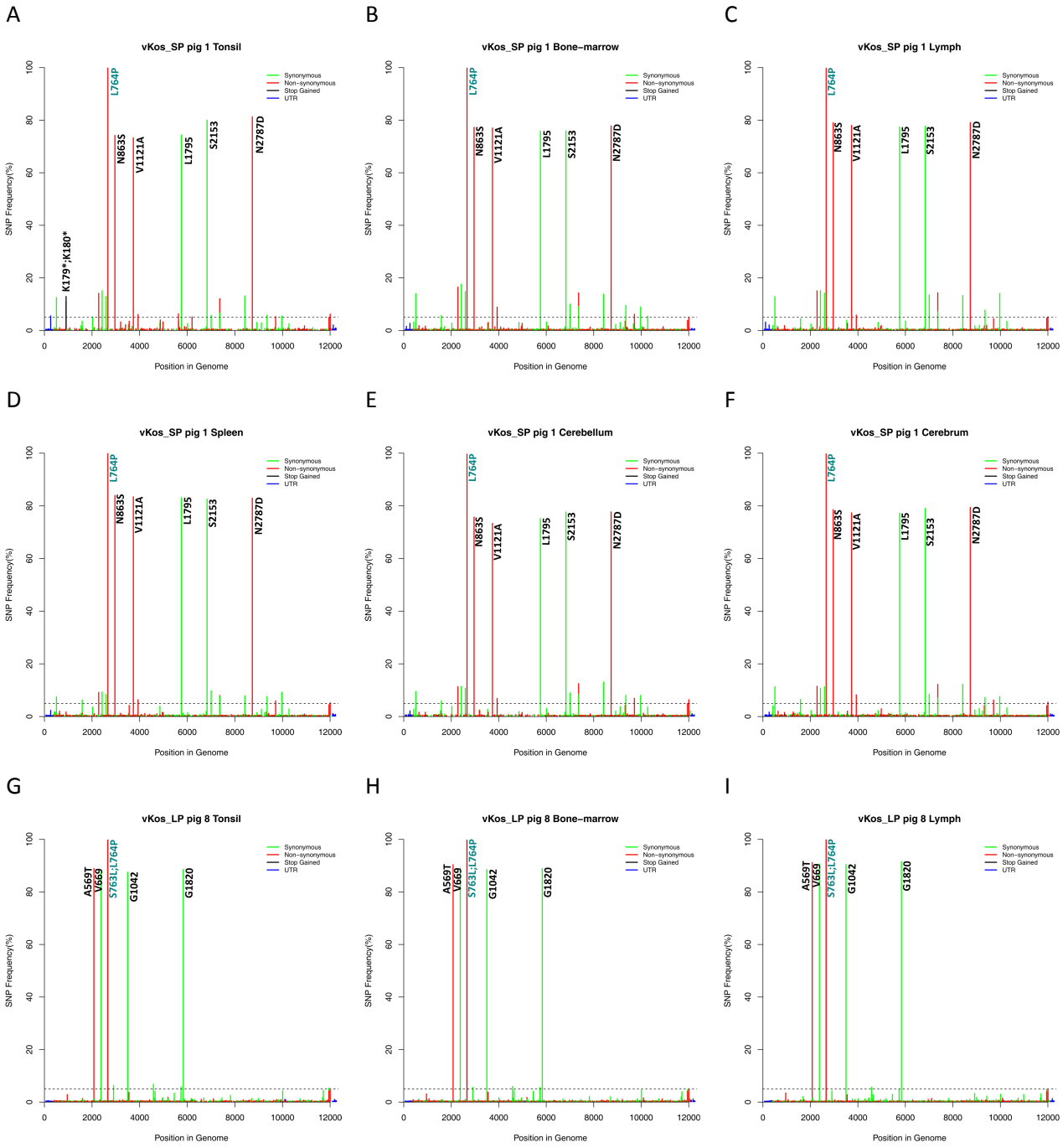
A
vKos_SP pig 1 Tonsil
B
vKos_SP pig 1 Bone−marrow
C
vKos_SP pig 1 Lymph
D
vKos_SP pig 1 Spleen
E
vKos_SP pig 1 Cerebellum
F
vKos_SP pig 1 Cerebrum
G
vKos_LP pig 8 Tonsil
H
vKos_LP pig 8 Bone−marrow
I
vKos_LP pig 8 Lymph
Synonymous
Non−synonymous
Stop Gained
UTR
SNP Frequency(%)
Position in Genome
K179*,K180*
L764P
N863S
V1121A
L1795
S2153
N2787D
A569T
V669
S763L,L764P
G1042
G1820

Figure S2 A-I

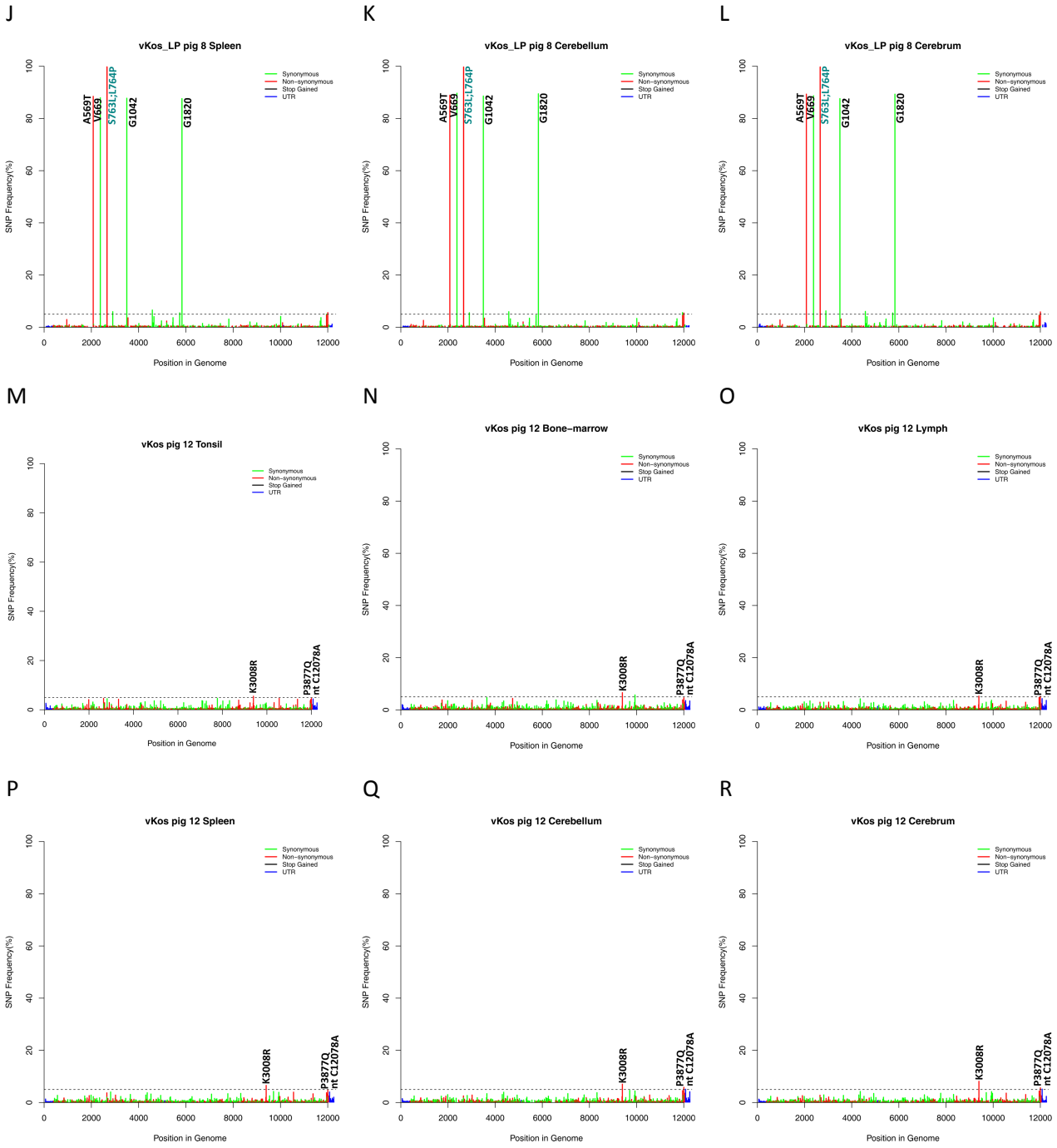

Figure S2

SNP frequency plots of all tissues samples from animal experiment II. A) vKos_SP tonsil. B) vKos_SP bone-marrow. C) vKos_SP lymph node. D) vKos_SP spleen. E) vKos_SP cerebellum. F) vKos_SP cerebrum. G) vKos_LP tonsil. H) vKos_LP bone-marrow. I) vKos_LP lymph node. J) vKos_LP spleen. K) vKos_LP cerebellum. L) vKos_LP cerebrum. M) vKos tonsil. N) vKos bone-marrow. O) vKos lymph node. P) vKos spleen. Q) vKos cerebellum. R) vKos cerebrum.

Table S1

Primer	Sequence (5'→3')	Reference
CSF-cDNA-1	GGG CCG TTA GGA AAT TAC CTT AG	Johnston et al. 2018
CSF-Kos_NotI-T7-1-59	TCT ATA TGC GGC CGC TAA TAC GAC TCA CTA TAG TAT ACG AGG TTA GTT CAT TCT CGT ATG CAT GAT TGG ACA AAT CAA AAT TTC AAT TTG G	Leifer et al., 2010
CSF-Kos_1-59	GTA TAC GAG GTT AGT TCA TTC TCG TAT GCA TGA TTG GAC AAA TCA AAA TTT CAA TTT GG	Modified from Leifer et al., 2010
CSF-Kos_12313aR	GGG CCG TTA GGA AAT TAC CTT AGT CCA ACT GT	Leifer et al., 2010
CSF-Kos-6240-RT	TCT ATA GGG TGT TTC TGC CC	This study
CSF-Kos-6176-R	CTG GTG TTG CGG TCA TGG CTA CTA C	Fahnøe et al. unpublished
CSF-Kos-5981-F	GGG GAG ATG AAA GAA GGG GAC ATG	Fahnøe et al. unpublished
CSFV-Kos-ELL-F	GGC ATC ACT GCA TAA GGA GGC TT**T** ACT CAC TTC CGT GAC	This study
CSFV-Kos-ESP-F	GGC ATC ACT GCA TAA GGA GGC TTC AC**C** CAC TTC CGT GAC	This study
CSFV-Kos-ELP-F	GGC ATC ACT GCA TAA GGA GGC TT**T** AC**C** CAC TTC CGT GAC	This study
Kos-2720R	CCG AAC CCG AAG TCA TCT CCC AT	This study

Table S2

Overview of samples and sample preparation obtained from animal experiment I. Serum samples were obtained from pigs infected with vKos_LL or vKos at day of euthanasia. Total RNA was extracted and full-length RT-PCR was performed.

	PCR	**Sample type**	**Euthanasia**
vKos_LL			
Pig 1	Full-length	Serum	PID 7
Pig 2	Full-length	Serum	PID 7
Pig 3	Full-length	Serum	PID 7
Contact			
Pig 4	Full-length	Serum	PID 8
Pig 5	Full-length	Serum	PID 9
vKos			
Pig 6	Full-length	Serum	PID 6
Pig 7	Full-length	Serum	PID 7
Pig 8	Full-length	Serum	PID 6
Contact			
Pig 9	Full-length	Serum	PID 10
Pig 10	Full-length	Serum	PID 10

Table S3

Overview of samples and sample preparation obtained from animal experiment II. Various serum and tissue samples were obtained from pigs infected with vKos_SP, vKos_LP or vKos at day of euthanasia. Total RNA was extracted and full- or overlapping half-length RT-PCR was performed. Pigs 4, 6 and 10 (one from each group) were not included in the NGS dataset, due to them being euthanized together with the second last pig in their group, for animal welfare reasons.

	Day	Tonsil	Bone-marrow	Serum	Lymph	Spleen	Cerebellum	Cerebrum
vKos_SP								
Pig 1	PID 6	+[a]	+[b]	+[b]*	+[b]	+[b]	+[a]	+[a]
Pig 2	PID 7	n.d.	n.d.	+[a]	n.d.	n.d.	n.d.	n.d.
Pig 3	PID 7	n.d.	n.d.	+[a]	n.d.	n.d.	n.d.	n.d.
vKos_LP								
Pig 5	PID 5	n.d.	n.d.	+[b]	n.d.	n.d.	n.d.	n.d.
Pig 7	PID 4	n.d.	n.d.	+[b]*	n.d.	n.d.	n.d.	n.d.
Pig 8	PID 6	+[a]	+[b]	+[b]	+[a]	+[b]	+[b]	+[b]
vKos								
Pig 9	PID 7	n.d.	n.d.	+[b]	n.d.	n.d.	n.d.	n.d.
Pig 11	PID 7	n.d.	n.d.	+[b]	n.d.	n.d.	n.d.	n.d.
Pig 12	PID 7	+[a]	+[b]	+[b]	+[a]	+[b]	+[a]	+[a]

[a] Overlapping half-length RT-PCR

[b] Full-length RT-PCR

*Full-length cloned using TOPO XL-2.

n.d. not done

Manuscript III

Analysis of a specific E2 motif within classical swine fever virus as determinant of cell specificity

In preparation

Analysis of a specific E2 motif within classical swine fever virus as determinant of cell specificity

Camille Melissa Johnston[1], Ulrik Fahnøe[2], Yoshihiro Sakoda[3], Graham J. Belsham[1], Thomas Bruun Rasmussen[1*]

[1]DTU National Veterinary Institute, Technical University of Denmark, Lindholm, DK-4771 Kalvehave, Denmark.

[2]Copenhagen Hepatitis C Program (CO-HEP), Department of Infectious Diseases, Hvidovre Hospital and Department of Immunology and Microbiology, Faculty of Health and Medical Sciences, University of Copenhagen, Denmark

[3]Laboratory of Microbiology, Department of Disease Control, Graduate School of Veterinary Medicine, Hokkaido University, Sapporo 060-0818, Japan

[*]Corresponding author

Abstract

The E2 glycoprotein, the major surface component of classical swine fever virus (CSFV) contains a specific motif in the N-terminal B/C- domain that differs between CSFV strains of different virulence. This motif comprises residues 761, 763 and 764 in the polyprotein (72, 74 and 75 in E2), and has been termed the 'SL'-motif. The combination E761/S763/L764 is only seen in highly virulent strains, including the CSFV strains Koslov and ALD, whereas moderately virulent strains largely have R761/L763/P763 and many low virulent or vaccine strains contain a K761/L763/P764 motif. In this study, mutations were introduced into the consensus cDNA clones of the highly virulent CSFV strains Koslov (Kos) and the moderately virulent ALD/A76 (ALD/A76); the latter is derived from the highly virulent ALD by serial passages in swine testicle cells and contains the motif L763/L764 in combination, with K761. Growth experiments were performed using rescued vKos and vALD/A76 mutants in SK6 cells. The growth experiments revealed no significant differences in the growth of vKos (wt and variants), and also there were no apparent differences in the growth rates between vKos and the vALD/A76 variants. To compare the cell type specificity of these viruses *in vitro*, serial passaging of engineered variants of vKos were performed in PK15 cells and in three types of primary porcine cells: plexus choroideus (plex), swine kidney and spleen cells. The serial passaging revealed no significant differences in the growth of vKos (wt and variants). Consensus sequencing of partial E2 revealed no changes to the modified motifs except for an adaptation in vKos_KSL from K761 to R761 in the 9^{th} passage in plex cells. To further investigate this event, the plex 6^{th}-10^{th} passage of vKos and vKos_KSL were deep sequenced by NGS. vKos displayed similar SNP profiles from 6^{th}-10^{th} passage, whereas the SNP

profile for vKos_KSL radically changed from the 9th passage with the emergence of R671 (>99% frequency) and three additional consensus changes: P3006L in NS5A and C3268R/I3319M in NS5B. vKos passages 6-10 and vKos_KSL passages 6-8 all contained the commonly cell-culture adaptation S476R in E^{rns}. This indicates that R761, alone or in combination with the changes in NS5A/B, has a profound effect on the virus replication in plex cells.

Introduction

Classical swine fever (CSF) is an economically important and highly contagious disease of pigs caused by CSF virus (CSFV). CSFV is a pestivirus within the *Flaviviridae* family (Lindenbach et al., 2013); it is a small, enveloped virus, containing a linear positive stranded RNA genome of approximately 12.3 kb. This genome contains a single long open reading frame (ORF) encoding a large polyprotein, and is flanked by 5' and 3' untranslated regions (UTRs) (Lindenbach et al., 2013). Cellular and viral proteases co- and post-translationally process the polyprotein to yield 12 mature cleavage products: 4 structural (C, E^{rns}, E1 and E2) and 8 non-structural (N^{pro}, p7, NS2, NS3, NS4A, NS4B, NS5A, and NS5B) (Lindenbach et al., 2013). Positive-strand RNA viruses have high evolutionary rates, partly due to their high error rate, due to a lack of proof-reading activity of the RNA-dependent RNA polymerase (RdRp). Additional factors such as cell tropism and within-host dynamics (e.g. virus growth rate, virus clearance rate, cell infection rate, cell death rate, etc.) also affect the evolutionary rate. This high evolutionary rate causes the virus population to exist as a quasispecies of different, but closely related variants (Peck & Lauring, 2018).

The pestivirus glycoprotein E2 is the major surface component of the virion; it is the main immunogen and essential for virus replication (Hulst & Moormann, 1997). Together with E^{rns} and E1, the E2 has been implicated in viral adsorption to host cells (Hulst & Moormann, 1997; van Gennip et al., 2000; Liang et al., 2003; Wang et al., 2004) and for determining tropism in cell cultures (van Gennip et al., 2000; Liang et al., 2003). Porcine complement regulatory protein CD46 seems to play an important role as a cellular receptor for CSFV. However, it is not the only component involved (Dräger et al., 2015a). Heparan sulfate (HS) and the laminin receptor are also indicated as attachment receptors for CSFV (Hulst et al., 2000; Chen et al., 2015; Dräger et al., 2015a). E2 shows high variability among different CSFV isolates (Leifer et al., 2012). Modifications introduced into this glycoprotein appear to have an important effect on CSFV virulence (van Gennip et al., 2004; Risatti et al., 2005, Risatti et al., 2006, Risatti et al., 2007a, Risatti et al., 2007b). Our previous study have shown that modifications in a specific motif within the E2, at residues 763 and 764, influence CSFV virulence of the highly virulent strain Koslov (Johnston C, Fahnøe U, Lohse L, Belsham GJ, Rasmussen TB, manuscript II). In Koslov this motif comprises residues S763 and L764 in the polyprotein (S74 and L75 in E2). We have termed this motif, in conjunction with residue 761, the 'SL'-motif. The S763/L764

combination, along with E761, is only seen in highly virulent strains, including the CSFV strain ALD. This virus also exist as ALD/A76 derived from ALD by serial passages in swine testicle cells (Komaniwa et al., 1981). vALD/A76 exhibits moderately virulence in pigs (Tamura et al., 2012), and contains the L763/L764 motif in combination with K761. Residues R761, L763 and P764 are the most common variants in CSFV strains of moderate virulence; low virulent or vaccine strains contain a K761/L763/P764 motif based on sequence and virulence status data (Leifer et al., 2011; Postel et al., 2016).

K761/L763/P764 is predominately seen in attenuated viruses (Wu et al., 2010), and residue 761 has been linked to a decrease in virulence of field strains and could be associated with viral evasion of the host immune response (Pérez et al., 2012; Hu et al., 2016), as it is responsible for the differences in antigenicity between vaccine and field strains (Chang et al., 2010). K761, together with L763 and P764 are critical for the reactivity with monoclonal antibodies (mAbs) and are located in the antigenic motif ^{753}RYLASLHKKALPT^{765} (Chang et al., 2012a). Previous studies have indicated that residue 761 is under positive selection (Tang et al., 2008; Wu et al., 2010; Pérez et al., 2012; Hu et al., 2016; Rios et al., 2017), as well as residue 763 (Rios et al., 2017). Furthermore, a change from L763 to S763 has been shown to give a HS binding phenotype (Dräger et al., 2015b).

In this study, mutations in E2 were introduced into the consensus cDNA clones of the highly virulent CSFV strains Koslov (vKos) and the moderately virulent ALD/A76 (vALD/A76). Growth rate studies and serial passaging were performed using vKos, vALD/A76 and mutants with amino acid substitutions at residues 761 (E or K), 763 (S or L), and 764 (L or P) in order to elucidate their role in the cell type specificity and growth rate in vitro.

Results

Time Course Analyses

To elucidate whether modifications in residues 761, 763, and 764 influenced the growth rate of vKos and vALD/A76, a time course experiment was performed in SK6 cells. SK6 cells infected with vKos constructs displayed similar growth rates (**Figure 1 A**). SK6 cells infected with vALD/A76 constructs also displayed similar growth rates, except for vALD/A76_ESL, vALD/A76_KLP, and vALD/A76_RSL, which all exhibited slower growth rates (**Figure 1 B)**. vALD/A76_ESL and vALD/A76_RSL also displayed lower levels of viral RNA present in the samples at 48 hrs. As the virus inoculums were derived from a 1st passage electroporated *in vitro* transcribed BAC clones, residual DNA might have been present in the samples, and the presence of this DNA might have skewed the results. However, it seems likely that the modifications in residues 761, 763, and 764 did not affect the growth rate of vKos in the cell types tested, and neither did they play an

important role in the growth rate of vALD/A76, even though vALD/A76_KLP did exhibit slightly lower growth rate compared to the majority of the other constructs.

Serial passages of vKos constructs

To elucidate the role of the 'SL'-motif (residues 761, 763, and 764) in cell type specificity, rescued virus vKos constructs were serially passaged in PK15, primary swine kidney (SN), spleen and plex cells. RT-qPCR was performed on virus harvests from passages 2-10 for all cell types (**Figure 2**). The vKos (wildtype (wt) and mutants) generated high levels of viral RNA in SN, PK15, and plex cells (**Figure 2 A, B,** and **D**, respectively), and this pattern remained relatively stable from passage 2-10. No discernable differences in growth was observed for these viruses, except for vKos_SP in SN cells, where it exhibited lower viral RNA production. However, this could also be due to a lower initial titer as it reached the same viral load as other constructs by passage 10. Much lower levels of viral RNA were observed in infected spleen cells, and the growth was much less consistent (see **Figure 2 C**).

Adaptive changes to a conserved motif in E2 during serial passaging

Wt and mutant forms of vKos harvested after the 10^{th} passage in plex cells were sequenced (at a consensus level), as were selected constructs passaged in SN and PK15 cells, to elucidate whether adaptive changes had taken place in the motif. Only the vKos_KSL in plex cells exhibited substitutions in the motif (K761R), as all other viruses remained stable (incl. vKos_KSL in SN and PK15 cells). Consensus sequencing of vKos_KSL plex cell passages 5-9 revealed that the adaptation took place during passage 9, as the vKos_KSL remained stable in passages 5-8. To see if the K761R adaptation would repeat itself, vKos_KSL plex passage 8 was passaged again until 10^{th} passage (vKos_KSL plex passage 9.2 and 10.2). However, in this process no adaptations occurred and the motif remained vKos_KSL.

SNP Analyses

vKos and vKos_KSL plex passages 6-10, as well as vKos_KSL 9.2, and 10.2 were deep sequenced by NGS to reveal insights into the different haplotypes that constitute the viral subpopulations in the serial passaging of these two constructs. vKos displayed 6 single nucleotide polymorphism (SNPs) (C1801A (aa S476R), A1812G (aa K480R), G2060A (aa A563T), T3061C (aa C896), G6529A (aa L2052), and G12091A in the 3'UTR) at the consensus level (>99% frequency) in plex passage 6-8, with 1 additional SNP in passage 9-10 (C9829T (aa I3152)) of ca. 52% frequency (**Figure 3 A-E**). S476R, K480R, C896 and L2052 is observed in published CSFV coding sequences (CDS), with A563 being highly conserved (retrieved from GenBank (Clark et al.)). However, the SNP C1801A (aa S476R) located in E^{rns} was only seen in 19% of the published CSFV CDSs, with

C1801T (aa S476) being the most common at 43%. I3152 observed in vKos plex passage 9 and 10 was detected in 33% of published CSFV CDSs. SNPs A1812G (aa K480R), T3061C (aa C896), G6529A (aa L2052), and G12091A were all observed in the vKos inoculum at <0.7% frequency (Johnston C, Fahnøe U, Lohse L, Belsham GJ, Rasmussen TB, manuscript II). vKos plex passages 6, 7, and 8 had 445, 438 and 256 SNPs scattered across the genome (>0.1% frequency), respectively (**Figure 3 A-C**). vKos passages 6-8 contained 4 SNPs (A108T, C7805A (aa L2478M), A9184G (aa K2937), and T9670A (aa P3099)) between 6-25% frequency (see **Table 1).** A108T was relatively stable at 9% in passages 6-8, as was the SNP encoding P3099 and these SNPs were not detected in passages 9 and 10 (**Figure 3 D-E**). An increase in frequency was seen for L2478M and K2937 respectively, from passage 6 to 8. However, they were not detected in passages 9 and 10. The vKos passages 9 and 10 displayed 281 and 430 SNPs in total scattered across the genome (>0.1 % frequency; **Figure 3 D-E**), respectively, with 18 SNPs present between 4% and 31%, which were not detected in passages 6-8 (**Table 1**). These 18 SNPs remained relatively stable in frequency from passage 9 to 10.

vKos_KSL displayed 5 SNPs (A88G, C408A (aa T12K), C1801A (aa S476R), A6267G (aa K1965R), and A10453 (aa Q3360)) in plex cell passages 6 to 8 at the consensus level (>73% frequency) (**Figure 4 A-C, Table 2**). These SNPs all steadily increased to >90% by passage 8. In total, vKos_KSL passages 6-8 displayed 234, 283, and 427 SNPs scattered across the genome (>0.1% frequency), respectively. Of these, 9 SNPs were observed with frequencies between 5-8% (**Figure 4 A-C**).

vKos_KSL plex passage 9 and 10 displayed 9 SNPs (A2284C (aa G637), A2655G (aa K761R), T4255C (aa I1294), C5134C (aa V1587), C9390T (aa P3006L), T10175C (aa C3268R), A10330G (aa I3319M), C10720A (aa V3449), and C11659T (aaY3762)) at the consensus level (>74% frequency) (**Figure 4 D-E**). The 9 SNPs remained stable from passage 9 to 10. G637, K761R, I1294, V1587, C3268R, and Y3762 were observed in published CSFV CDSs. However, the SNP A2284C encoding G637 was only observed in one CSFV strain, 0406/CH/01/TWN (GenBank acc. AY568569.1), belonging to genotype 2.1. The SNP C10720A was not seen in any of the published CSFV CDSs, however, C10720T, also encoding V3449 was observed in 24.8% of the published CSFV CDSs. The SNP T10175C was seen in conjunction with T10177C in one CSFV strain, HeN1505 (GenBank acc. KU556758.1), belonging to subgenotype 2.1d. In total, vKos_KSL passage 9 and 10 displayed 368 and 234 SNPs scattered across the genome (>0.1% frequency), respectively, with 3 SNPs (C589T (aa G72), T7057C (aa D2228), and T10406C (aa F3345L)) at 5-20% frequency. C589T and T7057C remained stable from passage 9 to 10, whereas T10406C (aa F3345L) decreased from 20% to 17% from passage 9 to 10. C589T, T7057C, and T10406C were not detected in vKos_KSL passage 6, 7, 8. Interestingly, K761R was not detected in vKos_KSL passages 6, 7, 8 and the SNPs encoding T10175C (aa C3268R), A10330G (aa I3319M), T10406C (aa F3345L), C10720A (aa V3449), and C11659T (aaY3762) were all located in the RdRp,

NS5B. C3268R and I3319M were located specifically in the N-terminal domain and in the finger domain of NS5B, respectively. The SNP encoding P3006L was located in the NS5A.

vKos_KSL plex passages 9.2 and 10.2 (re-passaged from passage 8) displayed SNP profiles similarly to those observed in vKos_KSL plex passages 6-8, with 5 SNPs (A88G, C408A (aa T12K), C1801A (aa S476R), A6267G (aa K1965R), and A10453 (aa Q3360)) at the consensus level (>93% frequency) (**Figure 4 F-G, Table 2**). These 5 SNPs seemed to have become fixed in the population. vKos_KSL passages 9.2 and 10.2 displayed 299 and 428 SNPs scattered across the genome (>0.1% frequency), respectively. Nine SNPs were observed at 3-9% frequency, similarly to what was seen in vKos_KSL passages 6-8.

To compare how many SNPs vKos_KSL passage 8 relatively had in common with vKos_KSL passage 9 and 9.2, 100 SNPs from each dataset were randomly selected. vKos_KSL passage 8 had 31 and 36 SNPs in common with vKos_KSL passage 9 and 9.2, respectively, indicating that although the high frequency SNPs differed, the low frequency viral subpopulations remained relatively similar.

Discussion

To elucidate the role of the 'SL'-motif (residues 761, 763, and 764) in the cell specificity and growth rate of the virulent strains Koslov and ALD/A76, mutations were introduced into the consensus cDNA clone Kos and ALD/A76 by site-directed mutagenesis. A time course experiment was performed to elucidate the role the 'SL'-motif on growth rate of vKos and vALD/A76. No discernable difference in growth rate was observed for any of the vKos constructs in SK6 and SK6-CD46KO cells, which was also the case for vALD/A76 constructs, although vALD/A76_KLP did exhibited slightly lower growth rate compared to the other constructs. However, there seemed to be a correlation between the amount of residual DNA present in the samples and lowered growth rate. The nature of this correlation will need further study.

Rescued vKos (wt and variants) were serially passaged in PK15, SN, spleen and plex cells, and no adaptive mutations took place in the motif, except for vKos_KSL plex passage 9 and 10, which changed to K761R. However, repeating the serial passage from passage 8 to 10 did not result in the reappearance of K761R.

Deep sequencing of vKos and vKos_KSL plex passage 6-10, 9.2, and 10.2 revealed several SNPs at the consensus level in both vKos and vKos_KSL. Notably in the vKos plex passages is the SNP encoding for S476R, which is a known cell culture adaptation within the E^{rns} protein, enabling HS binding (Hulst et al., 2000). However, cell culture adapted phenotypes of CSFV do not necessarily require S476R adaptation, as S763 has also been implicated to play a role in binding to HS in the presence of DSTP27, an HS blocking compound (Dräger et al., 2015b), although, S476R together with S763 did not seem to have an effect on growth in this study. The S476R adaptation was also present in the vKos_KSL passages, except for passage 9 and 10. No adaptation of L763S was observed at the consensus level in the constructs containing L763. It

would be interesting to investigate whether the L763 variants also contain an S476R adaptation, as it seems that this is the preferred cell culture adaptation for HS binding. vKos passages also contained a non-synonymous SNP encoding A563T located in the E1. A563 seems to be highly conserved in CSFV, and was not observed in the vKos inoculum. Pestivirus E1 is suggested to be responsible for fusion (El Omari et al., 2013), and a stretch of hydrophobic residues (aa 551-579) are similar to a fusion peptide-like motif located in the middle of the hepatitis C virus E1 sequence, another member of the *Flaviviridae* (Drummer et al., 2007; Li et al., 2009). The switch from a small hydrophobic aa to an uncharged polar aa, could have an impact on this putative motif, and warrants further study. vKos passages contained a synonymous SNP encoding C896, which is conserved among pestiviruses, as it is critical for the structural integrity of the conformational epitopes on the C-terminal region of E2 (Chang et al., 2012b). Several of the consensus SNPs were observed in the vKos inoculum (Johnston C, Fahnøe U, Lohse L, Belsham GJ, Rasmussen TB., manuscript II). SNP analyses of vKos_KSL plex passage 9 and 10 revealed distinct virus populations from vKos_KSL passage 6-8, 9.2 and 10.2, with respect to high frequency SNPs. Several non-synonymous SNPs were located in the NS5A/B in vKos_KSL passages 9 and 10. Interestingly, the SNP encoding K761R was not detected in vKos_KSL passage 8, indicating that this variant likely arose in passage 9. It is presumably the adaptations seen in the RdRp NS5B, which enabled this variant to out-replicate all others in the virus population, and establish itself as the major haplotype, which is known as a selective sweep. Selective sweeps are characterized by the fixation of a new mutant haplotype and the extinction of the former haplotype. Neutral mutations which occur in the sweeping haplotype, are amplified along with it, and this process is referred to as genetic hitchhiking (Domingo & Schuster, 2016). It is likely that K761R hitchhiked along with the mutations in NS5B. The non-synonymous mutations C3268R and I3319M were located in the N-terminal domain and in the finger domain of NS5B, respectively. Mutagenesis studies on NS5B indicate the importance of the N-terminal domain in the catalytic activity of the RdRp, and the finger domain has been shown to determine the preference of RNA templates (Li et al., 2018). These residues may play a role in the replication of CSFV, and need further study.

In summary, we report that modifications in the 'SL'-motif did not seem to affect the growth rate of the highly virulent CSFV strain Koslov and the moderately virulent strain ALD/A76. Neither did this motif appear to play a major role in the cell specificity of CSFV strain Koslov *in vitro*, but this warrants further investigation. The known cell culture adaptation S476R was observed in the majority of the deep sequenced passages. Residue R761, alone or in combination with the changes in NS5A/B, seemed to have a profound effect on the virus replication in plex cells, which needs to be investigated further.

Methods

Primers

Oligonucleotide primers used are listed in Supplementary, Table S1.

Cells

PK15 cells (obtained from the Cell Culture Collection at the Friedrich-Loeffler-Institut, Germany) and primary porcine swine kidney (SN) cells were propagated in Dulbecco's Modified Eagles Medium (DMEM) containing 5% FCS. Primary porcine plexus choroideus (plex) and primary porcine spleen cells were propagated in Roswell Park Memorial Institute (RPMI) 1640 medium with Glutamax-I containing 10% FCS. SK6 cells were propagated in DMEM containing 7% horse serum. The primary plex cells were passaged 14-15 times.

Generation of BACs containing non-synonymous mutations

The BACs Kos_LL, Kos_LP and Kos_SP were obtained from a previous study (Johnston C, Fahnøe U, Lohse L, Belsham GJ, Rasmussen TB, manuscript II). The BACs Kos_KSL, Kos_KLL, Kos_KLP, Kos_KSP, and Kos_RLP were obtained by site-directed mutagenesis using a megaprimer approach (Risager et al., 2013). Briefly, the BAC consensus clone Kos (Fahnøe et al., 2014) was used as template for the megaprimer PCR with forward primers containing the desired mutations (CSFV-Kos-KSL-F, CSFV-Kos-KLL-F, CSFV-Kos-KLP-F, CSFV-Kos-KSP-F, and Kos-RLP-2633F) and reverse primer Kos-2720R, *Supplementary* Table S1. The megaprimer, after gel purification with a GeneJET Gel extraction kit (Thermo Scientific), was used for the site-directed mutagenesis with Kos as vector backbone and downstream cloning in *E. coli* DH10B (Invitrogen, Carlsbad, USA). A similar approach was used to create mutants in the ALD/A76 clone in a pACNR1180 plasmid backbone (Tamura et al., 2012) using the Kos mutants above as template and primers Kos-2589F and Kos-2720R.

Rescue of viruses

BAC DNAs and plasmids were purified from 4 ml overnight cultures using GeneJET Miniprep kit (Thermo Scientific) or FastGene Plasmid Mini Kit (Nippon Genetics). Full length amplicons were obtained by long PCR, as previously described (Rasmussen et al., 2010; Fahnøe et al., 2014), using forward primers CSF-Kos_Not1-T7-1-59 and CSF-ALD_NotI-T7-1-59, respectively, and reverse primer CSF-Kos_12313aR, Supplementary Table S1. PCR products were purified using GeneJET PCR purification kit (Thermo Scientific) or FastGene Gel/PCR extraction kit (Nippon Genetics) and *in vitro* transcribed using Megascript T7 kit (Invitrogen). Virus was rescued from RNA transcripts by electroporation of PK15 or SK6 cells, as described previously (Friis et

al., 2012), and passaged once in PK15 or SK6 cells. Titration was performed in triplicate using NS3-specific murine antibodies (mAb 46/1 (Kameyama et al., 2006)) or polyclonal porcine antiserum for staining of infected cells.

Cell culture passaging and growth curves

Rescued vKos (except vKos_RLP) were passaged in PK15, SN, and plex cells with an initial MOI of 0.05. Ten passages were performed in total by transferring 100 µl supernatant from the previous passage to the next. Viral RNA was extracted using a MagNA Pure LC total nucleic acid isolation kit (Roche). RT-qPCR was used to determine the level of viral RNA, as described previously (Hoffmann et al., 2006), for passage 2-10 for all cell types. E2 fragments were amplified using QIAGEN OneStep RT-PCR Kit (Qiagen) with primers CSF2250f and CSF3710r, and subsequently sequenced to elucidate changes in the SL-motif. Growth curves were performed using SK6 cells infected with vKos and vALD/A76 constructs with an MOI of 0.01 and 0.5, respectively. Supernatant was collected at 3, 12, 24, and 48 hrs. The level of viral RNA was determined as above. RT-qPCR was performed ± the reverse transcriptase for the 3 hour samples to determine the amount of DNA remaining in the samples, which should remain the same across all time points, as this may skew the results.

Preparation of cDNA from viral RNA

Viral RNA was extracted, using a combined Trizol/RNeasy protocol (Rasmussen et al., 2008) from vKos and vKos_KSL plex passages 6-10. This extracted RNA was used to generate two overlapping half-length cDNA amplicons, using a modified version of the long RT-PCR method described previously (Rasmussen et al., 2010; Fahnøe et al., 2014). Briefly, the total RNA was reverse transcribed using the Maxima H Minus Reverse Transcriptase (Thermo Scientific) and the specific cDNA primers, CSF-cDNA-1 and CSF-Kos-6240-RT (Supplementary, Table S1). The cDNA was then amplified by a modified long PCR using the primers CSF-Kos_NotI-T7-1-59 and CSF-Kos-6176R for the 5’ end and CSF-Kos-5981-F and CSF-Kos_12313aR for 3’ end of the half-length cDNA amplicons, respectively.

NGS and SNP analysis

cDNA amplicons were sequenced by NGS at the DTU Multi-Assay Core (DMAC, Kgs. Lyngby, Denmark) using a MiSeq Nextera XT system (Illumina, San Diego, USA). Consensus sequences were obtained by mapping the reads to the vKos reference sequence (KF977607.1) using CLC Genomics Workbench v.9.5.2 (CLC bio, Aarhus, Denmark). Consensus sequences were aligned using MAFFT in Geneious (Biomatters, Auckland, New Zealand). Low frequency SNPs (>0.5%) were identified for cDNA amplicons using a combination of

BWA, Samtools, Lo-Freq-snp-caller, and SnpEff, as described previously (Fahnøe et al., 2014, Fahnøe et al., 2015).

Acknowledgements

We thank laboratory and cell culture technicians for their work, especially lab-technician students Marco Hansen and Marie Hornstrup Christensen. We are also grateful for the assistance from Louise Lohse (DTU Lindholm), master student Noriko Fukushi (Hokkaido University), and the staff at Hokkaido University. The research stay at Hokkaido University was partially funded by the Augustinus foundation, the Otto Mønsteds foundation, the Sasakawa foundation, the Torben & Alice Frimodts foundation, and the Norma & Frode S. Jacobsens foundation.

References

Chang C.Y., Huang C.C., Lin Y.J., Deng M.C., Tsai C.H., Chang W.M., Wang F.I. 2010. Identification of antigen-specific residues on E2 glycoprotein of classical swine fever virus. Virus Res. 152, 65–72.

Chang C.Y., Huang C.C., Deng M.C., Huang Y.L., Lin Y.J., Liu H.M., Lin Y.L., Wang F.I. 2012a. Antigenic mimicking with cysteine-based cyclized peptides reveals a previously unknown antigenic determinant on E2 glycoprotein of classical swine fever virus. Virus Res. 163, 190–6.

Chang C.Y., Huang C.-C., Deng M.-C., Huang Y.-L., Lin Y.-J., Liu H.-M., Lin Y.-L., Wang F.-I. 2012b. Identification of conformational epitopes and antigen-specific residues at the D/A domains and the extramembrane C-terminal region of E2 glycoprotein of classical swine fever virus. Virus Res. 168, 56–63.

Chen J., He W.-R., Shen L., Dong H., Yu J., Wang X., Yu S., Li Y., Li S., Luo Y., Sun Y., Qiu H.-J. 2015. The laminin receptor is a cellular attachment receptor for classical swine fever virus. J Virol. 89, 4894–906.

Clark K., Karsch-Mizrachi I., Lipman D.J., Ostell J., Sayers E.W. GenBank. http://www.ncbi.nlm.nih.gov/genbank/. Accessed 27 Oct 2017.

Domingo E., Schuster P. 2016. Quasispecies: From Theory to Experimental Systems. Cham: Springer International Publishing; 2016.

Dräger C., Beer M., Blome S. 2015a. Porcine complement regulatory protein CD46 and heparan sulfates are the major factors for classical swine fever virus attachment in vitro. Arch Virol. 160, 739–46.

Dräger C., Blome S., Beer M., Reimann I., Rasmussen T.B. 2015b. A cell culture-adapted classical swine fever virus phenotype does not require the 476Arg Erns mutation. In: 9th Annual Meeting of EPIZONE. 2015.

Drummer H.E., Boo I., Poumbourios P. 2007. Mutagenesis of a conserved fusion peptide-like motif and membrane-proximal heptad-repeat region of hepatitis C virus glycoprotein E1. J Gen Virol. 88 Pt 4,

1144–8.

Fahnøe U., Pedersen A.G., Risager P.C., Nielsen J., Belsham G.J., Höper D., Beer M., Rasmussen T.B. 2014. Rescue of the highly virulent classical swine fever virus strain “Koslov” from cloned cDNA and first insights into genome variations relevant for virulence. Virology. 468–470, 379–87.

Fahnøe U., Pedersen A.G., Dräger C., Orton R.J., Blome S., Höper D., Beer M., Rasmussen T.B. 2015. Creation of functional viruses from non-functional cDNA clones obtained from an RNA virus population by the use of ancestral reconstruction. PLoS One. 10, e0140912.

Friis M.B., Rasmussen T.B., Belsham G.J. 2012. Modulation of translation initiation efficiency in classical swine fever virus. J Virol. 86, 8681–92.

van Gennip H.G.P., van Rijn P.A., Widjojoatmodjo M.N., de Smit A.J., Moormann R.J.M. 2000. Chimeric classical swine fever viruses containing envelope protein Erns or E2 of bovine viral diarrhoea virus protect pigs against challenge with CSFV and induce a distinguishable antibody response. Vaccine. 19, 447–59.

van Gennip H.G.P., Vlot A.C., Hulst M.M., De Smit A.J., Moormann R.J.M. 2004. Determinants of virulence of classical swine fever virus strain Brescia. J Virol. 78, 8812–23.

Hoffmann B., Depner K., Schirrmeier H., Beer M. 2006. A universal heterologous internal control system for duplex real-time RT-PCR assays used in a detection system for pestiviruses. J Virol Methods. 136, 200–9.

Hu D., Lv L., Gu J., Chen T., Xiao Y., Liu S. 2016. Genetic diversity and positive selection analysis of classical swine fever virus envelope protein gene E2 in East China under C-strain vaccination. Front Microbiol. 7 FEB, 1–10.

Hulst M.M., Moormann R.J.M. 1997. Inhibition of pestivirus infection in cell culture by envelope proteins Erns and E2 of classical swine fever virus: Erns and E2 interact with different receptors. J Gen Virol. 78, 2779–87.

Hulst M.M., van Gennip H.G.P., Moormann R.J.M. 2000. Passage of classical swine fever virus in cultured swine kidney cells selects virus variants that bind to heparan sulfate due to a single amino acid change in envelope protein Erns. J Virol. 74, 9553–61.

Kameyama K., Sakoda Y., Tamai K., Igarashi H., Tajima M., Mochizuki T., Namba Y., Kida H. 2006. Development of an immunochromatographic test kit for rapid detection of bovine viral diarrhea virus antigen. J Virol Methods. 138, 140–6.

Komaniwa H., Fukusho A., Shimizu Y. 1981. Micro method for performing titration and neutralization test of hog cholera virus using established porcine kidney cell strain. Natl Inst Anim Health Q (Tokyo). 21, 153–8.

Leifer I., Hoffmann B., Hoper D., Rasmussen T.B., Blome S., Strebelow G., Horeth-Bontgen D., Staubach C., Beer M. 2010. Molecular epidemiology of current classical swine fever virus isolates of wild boar in Germany. J Gen Virol. 91, 2687–97.

Leifer I., Hoeper D., Blome S., Beer M., Ruggli N. 2011. Clustering of classical swine fever virus isolates by codon pair bias. BMC Res Notes. 4, 521.

Leifer I., Blome S., Blohm U., König P., Küster H., Lange B., Beer M. 2012. Characterization of C-strain Riems TAV-epitope escape variants obtained through selective antibody pressure in cell culture. Vet Res. 43, 1–11.

Li H.-F., Huang C.-H., Ai L.-S., Chuang C.-K., Chen S.S.L. 2009. Mutagenesis of the fusion peptide-like domain of hepatitis C virus E1 glycoprotein: Involvement in cell fusion and virus entry. J Biomed Sci. 16, 89.

Li W., Wu B., Soc W.A., An L. 2018. Crystal structure of classical swine fever virus NS5B reveals a novel N-terminal domain. J Virol. 92, 1–13.

Liang D., Fernandez-Sainz I., Ansari I.H., Gil L.H.V.G., Vassilev V., Donis R.O. 2003. The envelope glycoprotein E2 is a determinant of cell culture tropism in ruminant pestiviruses. J Gen Virol. 84, 1269–74.

Lindenbach B.D., Thiel H.J., Rice C.M., Murray C.L., Thiel H.J., Rice C.M. 2013. Flaviviridae: The viruses and their replication. In: Fields Virology. 6th edition. New York: Lippincott Williams & Wilkins; 2013. p. 712–46.

El Omari K., Iourin O., Harlos K., Grimes J.M., Stuart D.I. 2013. Structure of a pestivirus envelope glycoprotein E2 clarifies its role in cell entry. Cell Rep. 3, 30–5.

Peck K.M., Lauring A.S. 2018. The complexities of viral mutation rates. J Virol. May, JVI.01031-17.

Pérez L.J., Díaz de Arce H., Perera C.L., Rosell R., Frías M.T., Percedo M.I., Tarradas J., Dominguez P., Núñez J.I., Ganges L. 2012. Positive selection pressure on the B/C domains of the E2-gene of classical swine fever virus in endemic areas under C-strain vaccination. Infect Genet Evol. 12, 1405–12.

Postel A., Schmeiser S., Zimmermann B., Becher P. 2016. The European Classical Swine Fever Virus Database: Blueprint for a pathogen-specific sequence database with integrated sequence analysis tools. Viruses. 8, 302.

Rasmussen T.B., Reimann I., Hoffmann B., Depner K., Uttenthal Å., Beer M. 2008. Direct recovery of infectious pestivirus from a full-length RT-PCR amplicon. J Virol Methods. 149, 330–3.

Rasmussen T.B., Reimann I., Uttenthal Å., Leifer I., Depner K., Schirrmeier H., Beer M. 2010. Generation of recombinant pestiviruses using a full-genome amplification strategy. Vet Microbiol. 142, 13–7.

Rios L., Coronado L., Naranjo-Feliciano D., Martínez-Pérez O., Perera C.L., Hernandez-Alvarez L., Díaz de Arce H., Núñez J.I., Ganges L., Pérez L.J. 2017. Deciphering the emergence, genetic diversity and evolution of classical swine fever virus. Sci Rep. 7, 17887.

Risager P.C., Fahnøe U., Gullberg M., Rasmussen T.B., Belsham G.J., Fahnoe U., Gullberg M., Rasmussen T.B., Belsham G.J. 2013. Analysis of classical swine fever virus RNA replication determinants using replicons. J Gen Virol. 94 Pt_8, 1739–48.

Risatti G.R., Borca M. V., Kutish G.F., Lu Z., Holinka L.G., French R.A., Tulman E.R., Rock D.L. 2005. The E2 glycoprotein of classical swine fever virus is a virulence determinant in swine. J Virol. 79, 3787–96.

Risatti G.R., Holinka L.G., Carrillo C., Kutish G.F., Lu Z., Tulman E.R., Sainz I.F., Borca M. V. 2006. Identification of a novel virulence determinant within the E2 structural glycoprotein of classical swine fever virus. Virology. 355, 94–101.

Risatti G.R., Holinka L.G., Fernandez-Sainz I., Carrillo C., Kutish G.F., Lu Z., Zhu J., Rock D.L., Borca M. V. 2007a. Mutations in the carboxyl terminal region of E2 glycoprotein of classical swine fever virus are responsible for viral attenuation in swine. Virology. 364, 371–82.

Risatti G.R., Holinka L.G., Fernandez Sainz I., Carrillo C., Lu Z., Borca M. V. 2007b. N-linked glycosylation status of classical swine fever virus strain Brescia E2 glycoprotein influences virulence in swine. J Virol. 81, 924–33.

Tamura T., Sakoda Y., Yoshino F., Nomura T., Yamamoto N., Sato Y., Okamatsu M., Ruggli N., Kida H. 2012. Selection of classical swine fever virus with enhanced pathogenicity reveals synergistic virulence determinants in E2 and NS4B. J Virol. 86, 8602–13.

Tang F., Pan Z., Zhang C. 2008. The selection pressure analysis of classical swine fever virus envelope protein genes Erns and E2. Virus Res. 131, 132–5.

Wang Z., Nie Y., Wang P., Ding M., Deng H. 2004. Characterization of classical swine fever virus entry by using pseudotyped viruses: E1 and E2 are sufficient to mediate viral entry. Virology. 330, 332–41.

Wu Z., Wang Q., Feng Q., Liu Y., Teng J., Yu A.C., Chen J. 2010. Correlation of the virulence of CSFV with evolutionary patterns of E2 glycoprotein. Front Biosci (Elite Ed). 2, 204–20.

A

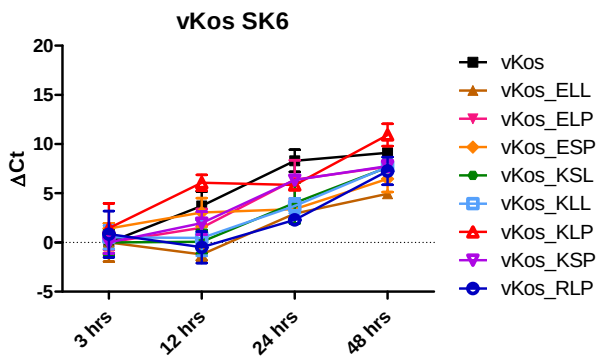

B

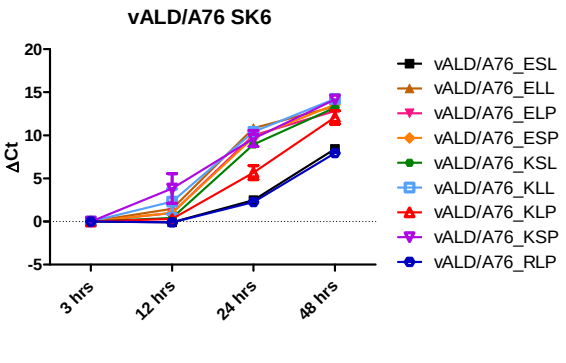

Figure 1

Time courses of viral RNA yields after infection of SK6. Cells were infected with the vKos and vALD/A76 constructs at an MOI of 0.01 and 0.5, respectively, and were harvested after 3, 12, 24 and 48 hours. A) SK6 cells infected with vKos constructs. B) SK6 cells infected with vALD/A76 constructs.

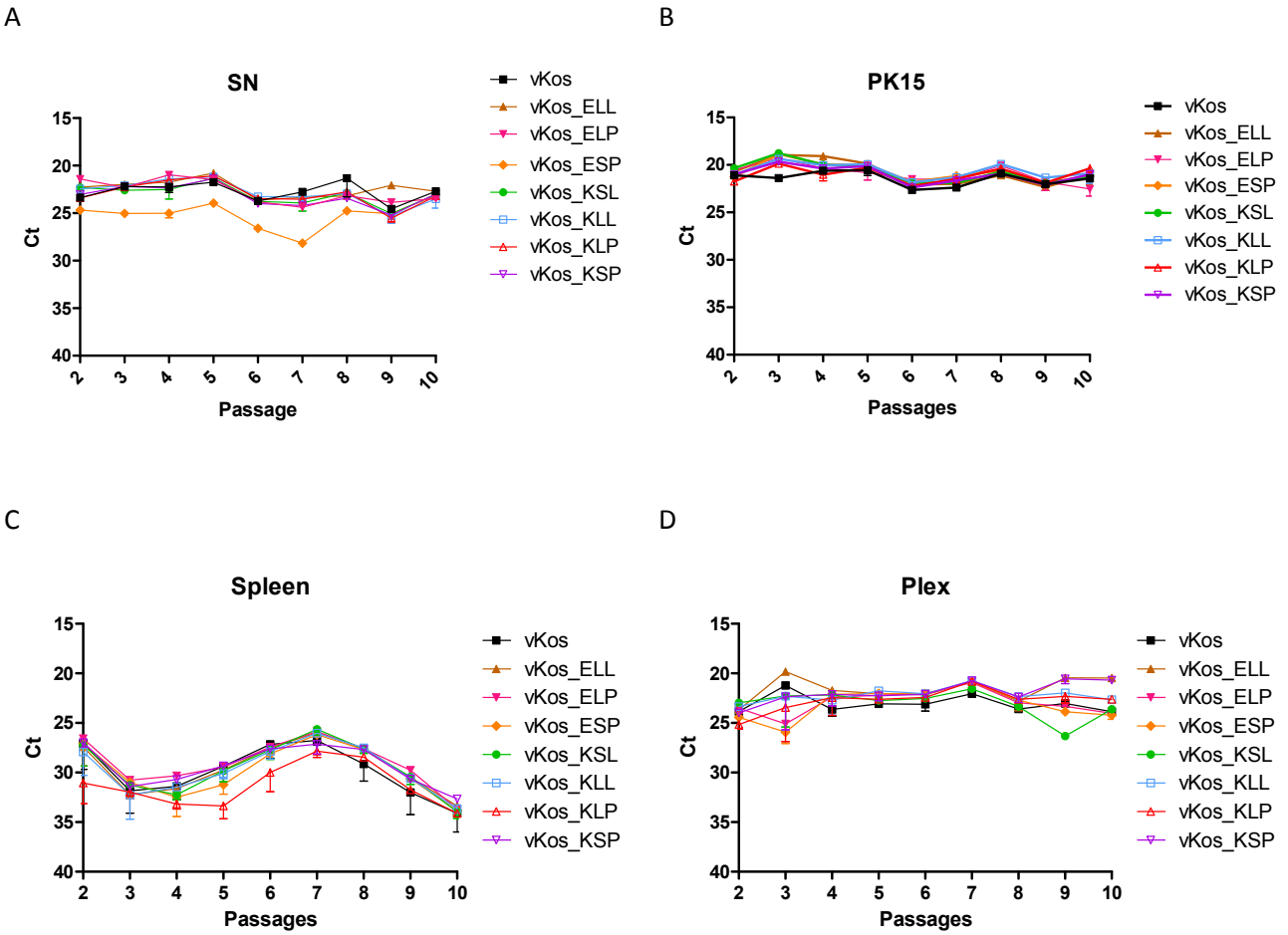

Figure 2

RT-qPCR of vKos constructs passaged in different cell types. A) Swine primary kidney cells. B) PK15 cells. C) Spleen cells. D) Plexus choroidus (plex) cells

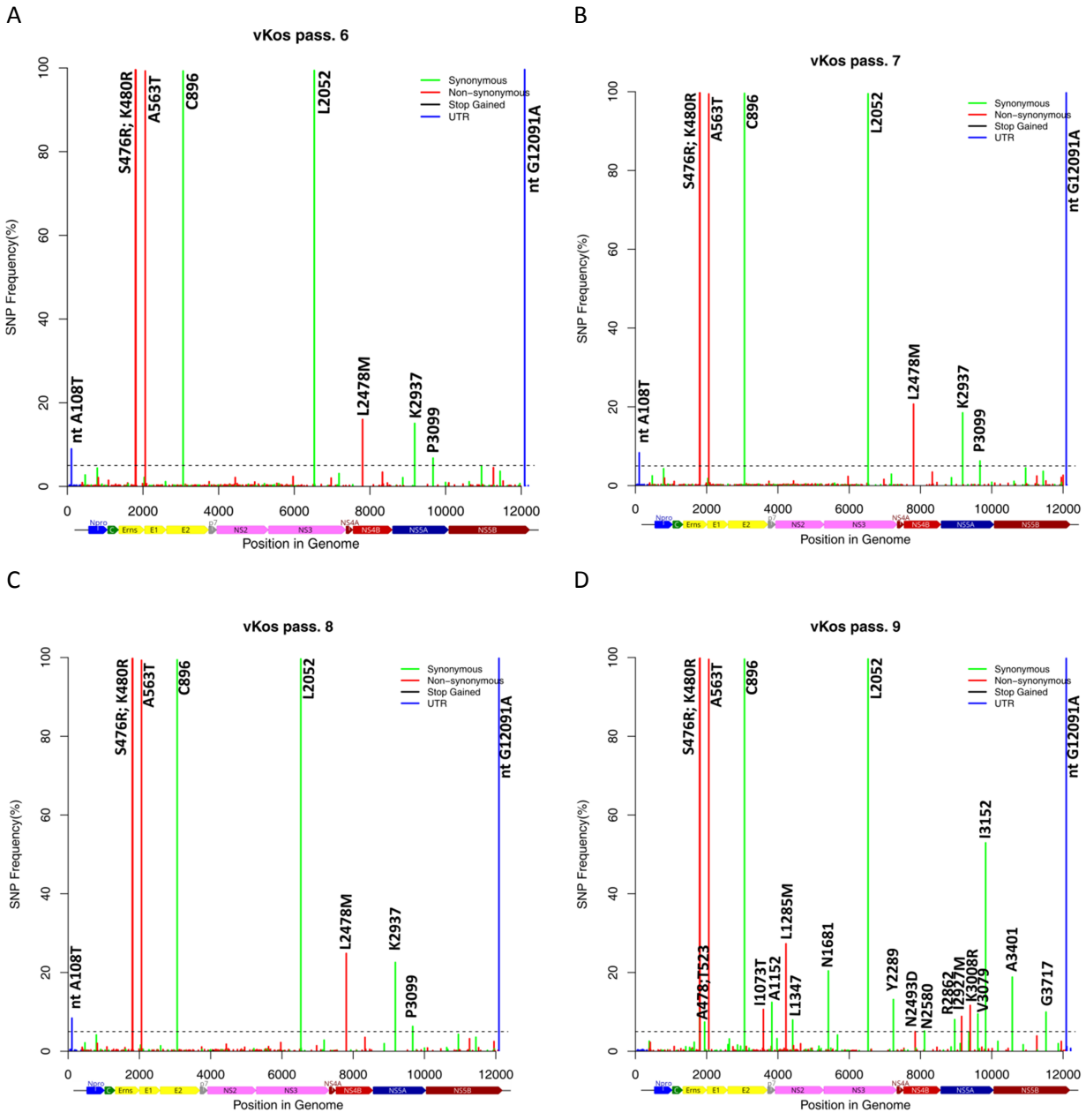
A
vKos pass. 6
B
vKos pass. 7
C
vKos pass. 8
D
vKos pass. 9
SNP Frequency(%)
Position in Genome
Synonymous
Non-synonymous
Stop Gained
UTR
nt A108T
S476R; K480R
A563T
C896
L2052
L2478M
K2937
P3099
nt G12091A
A478;T523
I1073T
A1152
L1347
L1285M
N1681
Y2289
N2493D
N2580
I3152
A3401
G3717
Npro
Erns
E1
E2
p7
NS2
NS3
NS4A
NS4B
NS5A
NS5B

Figure 3 A-D

E

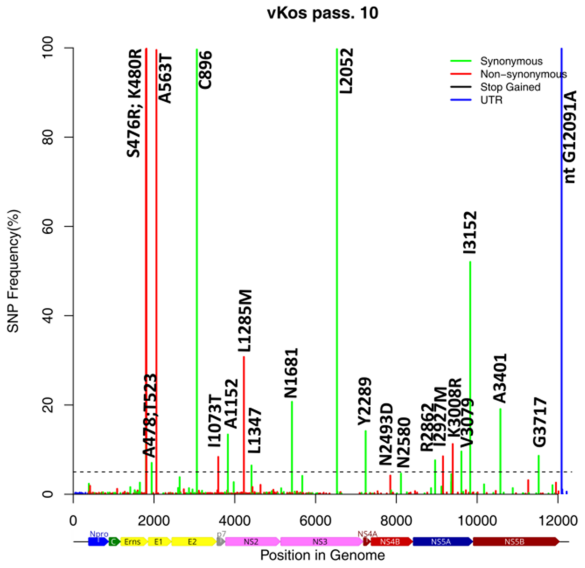

Figure 3

SNP frequency plot of vKos passaged in plex cells. A) vKos passage 6. B) vKos passage 7. C) vKos passage 8. D) vKos passage 9. E) vKos passage 10.

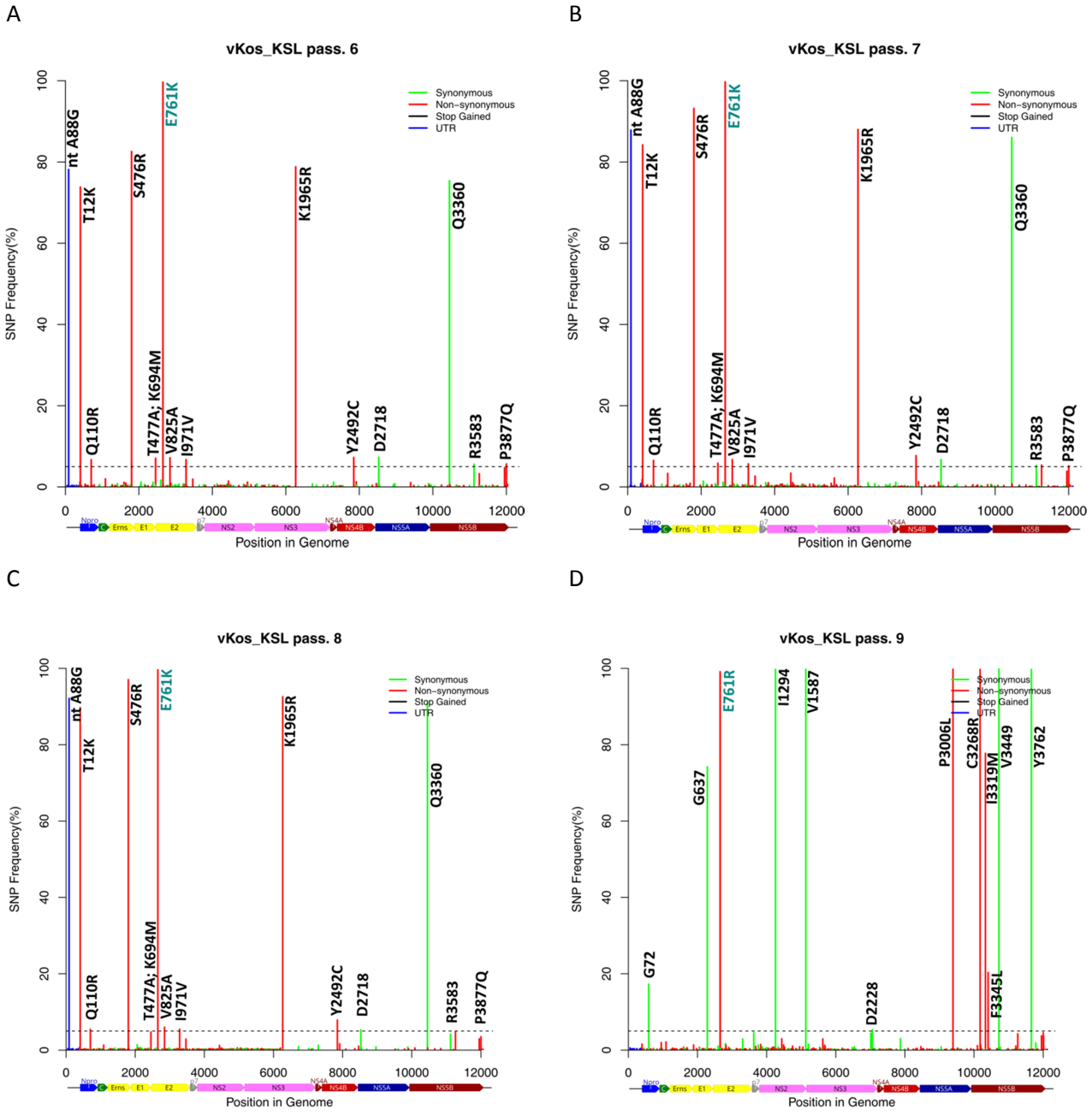
A
vKos_KSL pass. 6
B
vKos_KSL pass. 7
C
vKos_KSL pass. 8
D
vKos_KSL pass. 9
Synonymous
Non−synonymous
Stop Gained
UTR
SNP Frequency(%)
Position in Genome
nt A88G
T12K
Q110R
S476R
T477A; K694M
V825A
I971V
E761K
K1965R
Y2492C
D2718
Q3360
R3583
P3877Q
G72
G637
I1294
V1587
P3006L
C3268R
I3319M
V3449
Y3762
F3345L
D2228

Figure 4 A-D

E

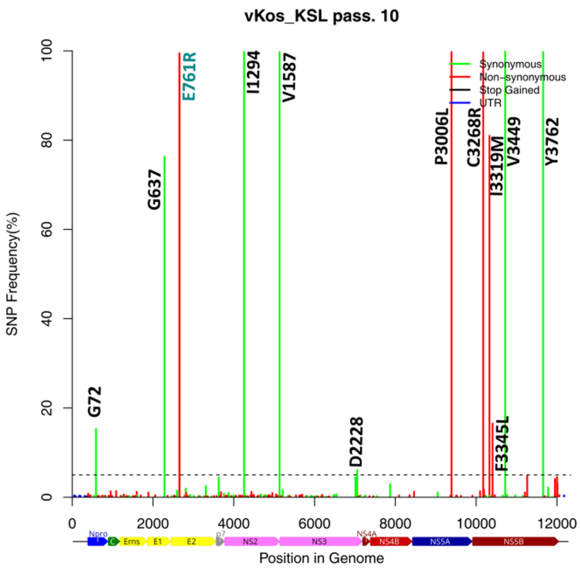

F

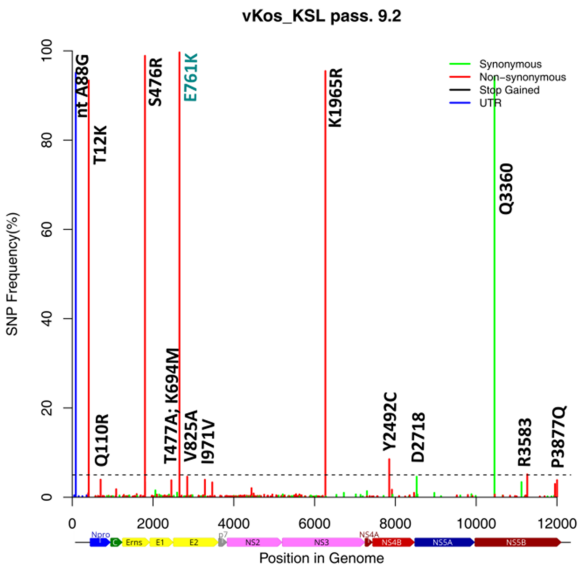

G

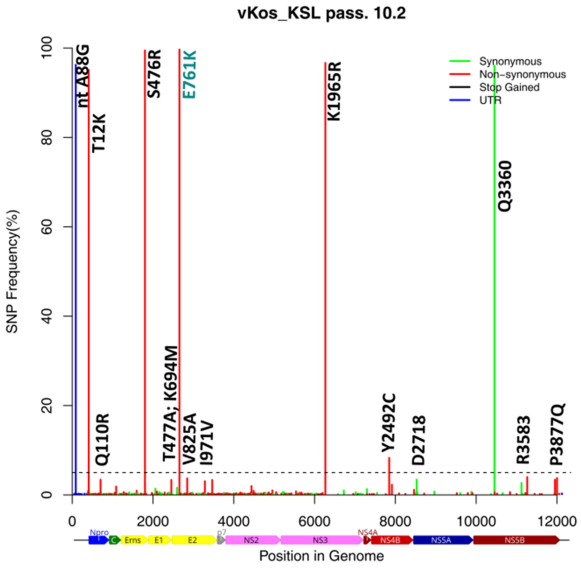

Figure 4

SNP frequency plots of vKos_KSL passaged in plex cells. A) vKos_KSL passage 6. B) vKos_KSL passage 7. C) vKos_KSL passage 8. D) vKos_KSL passage 9. E) vKos_KSL passage 10. F) vKos_KSL passage 9.2. G) vKos_KSL passage 10.2.

Table 1

Table of SNP frequencies detected above 5% in one or more passages of vKos.

					vKos	vKos	vKos	vKos	vKos
ORF	*Pos.*	*Ref.*	*Alt.*	*AA*	**P6**	**P7**	**P8**	**P9**	**P10**
5' UTR	108	A	T	-	9.0%	8.4%	8.4%	-	-
E^{rns}	1801	C	A	S476R	99.6%	99.7%	99.7%	99.8%	99.7%
E^{rns}	1807	C	T	A478	-	-	-	10.7%	11.9%
E^{rns}	1812	A	G	K480R	99.5%	99.7%	99.8%	99.9%	99.8%
E1	1942	A	G	T523	-	-	-	7.4%	7.0%
E1	2060	G	A	A563T	99.3%	99.4%	99.3%	99.5%	99.5%
E2	3061	T	C	C896	99.3%	99.6%	99.4%	99.6%	99.6%
p7	3591	T	C	I1073T	-	-	-	10.6%	8.4%
NS2	3829	G	T	A1152	-	-	-	12.4%	13.4%
NS2	4226	T	A	L1285M	-	-	-	27.3%	30.8%
NS2	4414	T	C	L1347	-	-	-	7.9%	6.4%
NS3	5416	T	C	N1681	-	-	-	20.4%	20.7%
NS3	6529	G	A	L2052	99.4%	99.5%	99.6%	99.6%	99.7%
NS4A	7240	T	C	Y2289	-	-	-	13.1%	14.2%
NS4B	7805	C	A	L2478M	16.0%	20.7%	24.9%	-	-
NS4B	7850	A	G	N2493D	-	-	-	5.0%	4.2%
NS4B	8113	T	C	N2580	-	-	-	5.2%	4.6%
NS5A	8959	G	A	R2862	-	-	-	8.1%	7.6%
NS5A	9154	A	G	I2927M	-	-	-	8.9%	8.5%
NS5A	9184	A	G	K2937	15.1%	18.5%	22.6%	-	-
NS5A	9396	A	G	K3008R	-	-	-	11.7%	11.3%
NS5A	9610	T	C	V3079	-	-	-	9.5%	9.6%
NS5A	9670	T	A	P3099	6.8%	6.3%	6.3%	-	-
NS5A	9829	C	T	I3152	-	-	-	52.9%	52.0%
NS5B	10576	T	A	A3401	-	-	-	18.8%	19.1%
NS5B	11524	T	C	G3717	-	-	-	9.9%	8.6%
NS5B	12091	G	A	-	99.6%	99.7%	99.8%	99.8%	99.8%

Pos.: position Ref: reference nucleotide

Alt.: alternative nucleotide AA: encoding amino acid

Table 2

Table of SNP frequencies detected above 5% in one or more passages of vKos_KSL.

					vKos_KSL	vKos_KSL	vKos_KSL	vKos_KSL	vKos_KSL	vKos_KSL	vKos_KSL
ORF	*Pos.*	*Ref.*	*Alt.*	*AA*	**P6**	**P7**	**P8**	**P9.2**	**P10.2**	**P9**	**P10**
5' UTR	88	A	G	**-**	78.2%	87.8%	92.1%	95.1%	96.3%	-	-
N^{pro}	408	C	A	T12K	73.8%	84.2%	89.7%	93.4%	95.1%	-	-
N^{pro}	589	C	T	G72	-	-	-	-	-	17.3%	15.3%
N^{pro}	702	A	G	Q110R	6.7%	6.5%	5.5%	3.9%	3.4%	-	-
E^{rns}	1801	C	A	S476R	82.6%	93.2%	97.0%	98.9%	99.5%	-	-
E^{rns}	1802	A	G	T477A	6.2%	5.7%	4.7%	3.4%	2.7%	-	-
E1	2284	A	C	G637	-	-	0.3%	0.3%	0.3%	74.2%	76.3%
E2	2454	A	T	K694M	7.1%	5.8%	4.8%	3.8%	3.4%	-	-
E2	2655	A	G	K761R	-	-	-	-	-	98.5%	99.1%
E2	2847	T	C	V825A	7.2%	6.7%	6.0%	4.6%	3.7%	-	-
E2	3284	A	G	I971V	6.7%	5.7%	5.5%	3.9%	3.1%	-	-
NS2	4255	T	C	I1294	-	-	-	0.3%	0.2%	99.7%	99.8%
NS2	5134	C	A	V1587	-	-	-	-	-	99.7%	99.7%
NS3	6267	A	G	K1965R	78.8%	88.0%	92.6%	95.5%	96.7%	-	-
NS3	7057	T	C	D2228	-	-	-	-	-	5.3%	6.0%
NS4B	7848	A	G	Y2492C	7.3%	7.7%	7.9%	8.5%	8.3%	-	-
NS5A	8527	T	C	D2718	7.3%	6.7%	5.3%	4.6%	3.4%	-	-
NS5A	9390	C	T	P3006L	-	-	-	-	-	99.8%	99.7%
NS5B	10175	T	C	C3268R	-	-	-	-	-	99.7%	99.7%
NS5B	10330	A	G	I3319M	-	-	-	-	-	77.7%	81.0%
NS5B	10406	T	C	F3345L	-	-	-	-	-	20.3%	16.5%
NS5B	10453	A	G	Q3360	75.4%	86.0%	91.4%	94.2%	96.1%	-	-
NS5B	10720	C	A	V3449	-	-	-	-	-	99.9%	99.9%
NS5B	11122	A	G	R3583	5.6%	5.3%	4.2%	3.4%	2.7%	-	-
NS5B	11659	C	T	Y3762	0.3%	-	-	-	-	99.7%	99.8%
NS5B	12003	C	A	P3877Q	5.7%	5.2%	3.5%	3.8%	3.8%	4.6%	4.5%

Pos.: position Ref: reference nucleotide

Alt.: alternative nucleotide AA: encoding amino acid

Table S1

Primer	Sequence (5'→3')	Reference
CSF-cDNA-1	GGG CCG TTA GGA AAT TAC CTT AG	Previous study, unpublished
CSF-Kos_NotI-T7-1-59	TCT ATA TGC GGC CGC TAA TAC GAC TCA CTA TAG TAT ACG AGG TTA GTT CAT TCT CGT ATG CAT GAT TGG ACA AAT CAA AAT TTC AAT TTG G	Leifer et al. 2010
CSF-Kos_12313aR	GGG CCG TTA GGA AAT TAC CTT AGT CCA ACT GT	Leifer et al., 2010
CSF-Kos-6240-RT	TCT ATA GGG TGT TTC TGC CC	Manuscript II, unpublished
CSF-Kos-6176-R	CTG GTG TTG CGG TCA TGG CTA CTA C	Fahnøe et al. unpublished
CSF-Kos-5981-F	GGG GAG ATG AAA GAA GGG GAC ATG	Fahnøe et al. unpublished
CSF-ALD_NotI-T7-1-59	TCT ATA TGC GGC CGC TAA TAC GAC TCA CTA TAG TAT ACG AGG TTA GTT CAT TCT CGT ATG CAT GAT TGG ACA AAT TAA AAT TTC AAT TTG G	This study
Kos-2720R	CCG AAC CCG AAG TCA TCT CCC AT	Manuscript II, unpublished
Kos-RLP-2633F	TAT TTG GCA TCA CTG CAT AAG AGG GCT TTA CC	This study
CSFV-Kos-KSL-F	GGCATCACTGCATAAGAAGGCTTCACTCACTTCCGTGAC	This study
CSFV-Kos-KLL-F	GGCATCACTGCATAAGAAGGCTTTACTCACTTCCGTGAC	This study
CSFV-Kos-KLP-F	GGCATCACTGCATAAGAAGGCTTTACCCACTTCCGTGAC	This study
CSFV-Kos-KSP-F	GGCATCACTGCATAAGAAGGCTTCACCCACTTCCGTGAC	This study
Kos-2589F	CAG GTT CCT TTA AAG TCA CAG CAC TTA ATG TGG T	This study

Part III – Conclusions and Future Perspectives

Conclusions and Future Perspectives

RNA viruses replicate to enormous population sizes, and due to the lack of proof-reading activity of their RdRp, this results in many variants existing within the population. With mutation rates ranging from 10^{-6} and 10^{-4} mutations per nt incorporated and short generations times, the resulting high evolutionary rate causes the RNA virus population to exist as a quasispecies of different, but closely related variants. This viral cloud of variants is believed to play a role in determining the virulence of the population and hence pathogenesis. For example, studies of poliovirus have shown that sequence variants present as subpopulations within the infected host also display distinct tissue tropism, i.e. ability to infect CNS or not (Vignuzzi et al., 2006). The diversity and quasispecies composition of CSFV has not been studied in depth. Quasispecies diversity does not *per se* seem to be responsible for virulence of CSFV. As the virulence of CSFV ranges from avirulent to highly virulent with mortality rates for some strains being close to 100% (e.g. Koslov and ALD strains), this raises the question of which characteristics of the virus are responsible for virulence. Several virulence determinants have been identified, among them the E2 glycoprotein seems to play an important role in virulence and also in tropism. With the introduction of NGS, virulence determinants and the role of quasispecies dynamics can be studied in great depth. Deep sequencing can allow for the identification of high frequency and low frequency variants present in the viral population. However, there are challenges as low frequency variants can be difficult to distinguish from errors introduced by the sampling process and sequencing. Several methods have been developed to circumvent these issues, such as Cirseq (Whitfield & Andino, 2016), however, these methods requires copious amounts of pure viral RNA. Furthermore, the short read lengths generated by most NGS methods do not allow for the identification of the distinct haplotypes that constitute the virus population. This can be solved by long-read technologies such as PacBio and the ONT MinIon. These are however limited by lower throughput, higher error rate and cost per base relative to short read sequencing (Pollard et al., 2018), and haplotyping using these methods does not allow for phenotypic characterization. Acquiring full-length cDNA clones represents an approach to identify the individual haplotypes present in the virus population, and the use of reverse genetics to manipulate the viral genomes is a crucial tool for identifying the underlying sequences responsible for virulence, tropism, etc., both *in vivo* and *in vitro*.

This thesis has relied heavily on the CSFV reverse genetics system based on BACs and the SNP analysis method for identification of low frequency SNPs within CSFV, previously developed at Lindholm (Rasmussen et al., 2010, Rasmussen et al., 2013; Risager et al., 2013; Fahnøe et al., 2014, Fahnøe et al., 2015). The reverse genetics approach is most evident in manuscript II and manuscript III, and SNP analysis

was utilized in all three manuscripts. Full-length sequencing has been employed throughout the manuscripts, both in order to identify haplotypes of cDNA clones from a virus population, and to perform SNP analysis, but also to sequence BAC constructs, due to the possibility of secondary mutations being introduced during the mutagenesis, which could affect the end result. Usually, the generated constructs were first screened by Sanger sequencing and then sent for sequencing by Ion Torrent PGM systems or Illumina MiSeq Nextera XT at DMAC, the NGS core facility at DTU. The same consensus sequence was achieved by both systems on identical sample sets, however, MiSeq sequencing resulted in considerably more coverage depth than Ion Torrent. Miseq was therefore employed for manuscript II and III. With regards to the SNP analysis, an important issue is being able to differentiate between errors and true, very low frequency, variants, which can only be mitigated partially by the use of high fidelity polymerases. Errors can also be introduced by the reverse transcriptase, and in the case of virus obtained from a BAC construct, by the RNA polymerase used for making the RNA transcripts from the BAC, and also by the library preparation process used for the sequencing itself.

Manuscript I was mainly focused on creating a high-throughput method for the generation of full-length cDNA clones directly from CSFV infected pigs. We switched from the standard CSFV BAC cloning system (Rasmussen et al. 2010) to the In-Fusion *in vitro* recombination system. We also changed from using AccuPrime High Fidelity DNA polymerase, to the Q5 high-fidelity DNA polymerase in the full-length PCR, as according to the manufacturer, Q5 creates blunt-ended PCR amplicons and has a 30-fold higher fidelity than AccuPrime. A new forward primer, without a NotI site and T7 promoter, had to be designed, in order for Q5 to work optimally in the full-length PCR. A NotI site and T7 promoter is not necessary for the generation of full-length cDNA clones. When the clones have been established, primers containing a T7 promoter can be used together with AccuPrime to make PCR amplicons used for making T7 RNA transcripts. In-Fusion cloning of full-length PCR amplicons obtained from an already established clone resulted in the generation of several colonies, with up to 50% being the correct insert. Switching from PCR purification of the PCR amplicons to gel purification, resulted in a 2-3 fold increase in colonies, and 100% of the screened inserts were correct. We furthermore also used the In-Fusion system to clone BDV Gifhorn from an already established clone with very high efficiency to show that the system also works for other pestiviruses (data not shown). The 'In-Fusion system', therefore, proved to be very efficient when cloning from an already established cDNA clone. However, this was not the case when it came to cloning directly from cDNA amplicons obtained by RT-PCR using serum from an infected pig. After several unsuccessful attempts, we switched from using SuperScript III reverse transcriptase to Maxima H minus Reverse Transcriptase, and also used a newly designed cDNA primer. This modified procedure resulted in the production of a few

colonies, with only 3 clones being of the correct insert size. Subsequent rounds of cloning failed. We then decided to switch to the TOPO XL-2 cloning system. The TOPO XL-2 cloning system uses a high-copy number plasmid, the pCRXL-2-TOPO vector, covalently bound to topoisomerase. Full-length pestivirus genomes are known not to be stable when propagated through several generations in high-copy plasmids; however, since the purpose of this cloning method was to establish clones used directly for sequencing as mentioned above, stability should not be an issue. The established clones could always be transferred to a BAC using the In-Fusion system to obtain a stable clone if needed. The TOPO XL-2 system proved to be efficient in generating clones of the correct size both from an already established clone but also from cDNA amplicons obtained directly from a virus population. For proof of concept, we obtained 15 unique clones from infected pig serum. Phylogenetic analysis of the TOPO XL-2 clones, and In-Fusion clones revealed a low degree of order, due to low diversity of the quasispecies population, as the viral inoculum used for the infection experiment was derived from a cDNA clone. This was also reflected in the SNP analysis of the cDNA amplicons, which displayed low-level sequence variation scattered across the genome as expected for the rescued vKos.

Koslov is a highly virulent strain with mortality rates of 100% in pigs (Blome et al., 2014; Tarradas et al., 2014). vKos, the consensus cDNA clone of Koslov, proved to be just as virulent as wt Koslov in pigs (Fahnøe et al., 2014). Deep sequencing of inoculated pigs revealed a subpopulation of virus containing a L764P substitution, which was present at 100% in serum from one contact pig. S763L in conjunction with P968H seemed to play a role in the virulence of Koslov, as the vKos_3aa variant containing these mutations was significantly less virulent than vKos (Fahnøe et al., 2014). These findings laid the groundwork for manuscript II, where we studied the role of residues 763 and 764 for the virulence of Koslov. E2 mutants containing non-synonymous substitutions at residues 763 and/or 764 were generated using site-directed mutagenesis in the vKos background. The two infection experiments with these variants showed clear differences in virulence with vKos_LP inducing earlier signs of disease than vKos, while the other variants were as virulent as vKos. SNP analysis revealed low-level sequence variation across the whole genome for vKos and vKos_LL, while vKos_LP and vKos_SP contained several consensus changes and several SNPs above 5%. An apparent transmission bottleneck was observed in contact pigs infected with vKos and vKos_LL, with very low frequency sequence variation. Infection studies with wt Koslov revealed higher diversity in regard to high frequency SNPs (Fahnøe U, Pedersen AG, Höper D, Beer M, Rasmussen TB., unpublished data), however, this study did not contain contact pigs, so it is not known whether wt Koslov would also display a loss of high frequency variants in transmission to contact pigs. vKos_LP contained a non-synonymous substitution (A569T) in E1. The E1 has been implicated in virus adsorption to host cells, together with E2 and E^{rns}, and

may also play a role in virulence, so perhaps this influences the vKos_LP phenotype. Further studies should be performed to elucidate the role of A569T in determining virulence. SNP analysis was performed on tissues from one pig from each group infected with vKos_SP, vKos_LP, and vKos. The SNP profiles across the tissues did not reveal any distinct differences, which is in contrast with BVDV PI animals where the viral population was distinct between different body compartments (Dow et al., 2015). However, in the PI host, the virus replicates in the absence of selective pressure from the adaptive immune system (Chase, 2013), and given the nature of PI animals, the virus likely has more time to establish itself and evolve. This is consistent with observations from PI animals with Hobi-like atypical bovine pestivirus that display an increase in variability of the viral quasispecies over time (Weber et al., 2017). As vKos is highly virulent, with infected pigs being euthanized no later than PID 7, the virus population would likely have less time to evolve distinctively in the different tissues. Using moderately virulent strains (or low virulence strains to produce PI piglets) could elucidate whether CSFV displays the same distinct compartmentalization as BVDV. Only one study has been published on this issue, showing that the virus population in pigs chronically infected with CSFV appears to be stable at the quasispecies level (Jenckel et al., 2017), however, this was only based on blood and leukocyte samples.

Full-length cDNA cloning of vKos_LP and vKos_SP proved to be challenging; emphasizing that full-length cDNA cloning is not a trivial process. Ten clones were obtained for vKos_SP and five for vKos_LP. The vKos_SP clones reflected the major viral haplotypes of the serum sample, as the clones either contained the high frequency SNPs (>75% frequency) or reflected Kos_SP at those positions. The vKos_LP clones also reflected the major viral haplotype present in the serum sample (>89% frequency). The sequences of the clones obtained showed that the high frequency SNPs observed within the populations were linked on the same genomes. The LP motif is commonly found together with R761 in gt 2 strains, and together with K761 in vaccine strains. Residue 761 has been implicated to play a role in virulence of CSFV, and perhaps also in immune escape.

Manuscript III set out to study the role of the 'SL'-motif (residues 761, 763, and 764) in the cell specificity of E2 in Koslov. Part of this work took place at Hokkaido University, Japan, under the guidance of Prof. Yoshihiro Sakoda. Mutations were introduced into the moderately virulent vALD/A76 strain and vKos at residues 761, 763, and/or 764. Growth kinetics studies were performed in SK6 cells to see if these variants had any effect on the growth rate. Originally these constructs were also to be tested in SK6 CD46 knock-out (CD46KO) cells, as CD46 is a cellular receptor for CSFV. However, binding assay studies performed by masters student Noriko Fukushi using vALD/A6 and mutant variants did not reveal any significant differences in virus binding to these cells. The binding assay was not performed in the presence of a HS

blocker, which might have influenced the result, and thus it could not be confirmed that the CD46 had truly been knocked-out. We therefore decided to not include this dataset in manuscript III. The growth kinetics performed in SK6 cells revealed no discernable differences in growth rate of the vKos and vALD/A76 variants. vKos variants were then serial passaged in PK15, primary porcine spleen, kidney and plex cells. The plex cells had been passaged 14-15 times, but are still considered as primary cells and not as an adapted or established cell line. These cells were especially of interest as Koslov has been shown to infect these endothelial cells in the brain (Hansen et al., 2011). The serial passaging revealed no discernable difference in growth of the vKos and variants. Sanger sequencing was performed on plex passage 10 to detect any adaptive changes in the motif. vKos_KSL passage 10 revealed a substitution to R761, which was also detected at passage 9. vKos_KSL was passaged anew in plex cells from passage 8, to see if the same adaptation would take place again. However, it did not, and the motif remained with K761. Deep sequencing was performed on vKos plex passage 6-10, and vKos_KSL passage 6-10 and the two repeated passages (9.2 and 10.2). This revealed the common HS binding adaptation S476R in the passaged E^{rns} of vKos and vKos_KSL, except for vKos_KSL plex passage 9 and 10, containing the R761 substitution. This indicated that a selective sweep had taken place, as the SNP profile was significantly different in these populations than those observed in passages 6-8; they contained several non-synonymous mutations in the NS5A/B coding regions. This is likely the cause of the selective sweep, as this variant was able to out-compete all others and become fixed in the population. As we only performed deep sequencing on vKos and vKos_KSL from passage 6, we do not know the composition of the viral subpopulation in the earlier passages or of the other rescued viruses, and whether they also exhibit the S476R adaptation in E^{rns} to bind to HS. As few as 3 passages in SK6 cells has previously been demonstrated to be sufficient for adaptation to enhanced HS-binding (Eymann-Häni et al., 2011). Residue S763 has also been indicated to play a role in binding to HS in the presence of an HS blocking compound (Dräger et al., 2015b). However, viruses containing S763 did not exhibit higher growth in our study. It would be interesting to perform serial passaging of the vKos mutants in the presence of an HS blocking compound, to see if viruses containing S763 grow more efficiently than those containing L763. The vKos mutants replicated well in plex cells, which correlates with detection of virus in the cerebellum and cerebrum of infected pigs (Manuscript II). It would be interesting to investigate how strains of lower virulence, such as vKos_3aa (Fahnøe et al., 2014), would fare in plex cells, as well as avirulent strains such as C-strain, as these are not known to affect the CNS.

This thesis has given some more insights into the quasispecies nature of CSFV strain Koslov, but perhaps also ended up raising more questions than have been answered so far. The results in manuscript II indicate

that residues 763 and 764, perhaps in conjunction with 761, play a role in modulating the virulence of Koslov, but the underlying mechanisms need further study. The limited dataset in manuscript III indicates that modification of the 'SL'-motif does not change the growth rate and cell specificity, *in vitro*. However, it would be interesting to investigate the virulence of vKos_KLP in infection experiments in pigs, as this motif has only been found in vaccine strains previously. Thus, such studies may give more insights into the role of residue 761 in the modulation of CSFV virulence. The role of quasispecies diversity and composition needs to be studied further. Although quasispecies diversity *per se* does not seem to be responsible for virulence of CSFV, it is the interactions between the individual variants, which shape the characteristics of the population as a whole.

Numerous clones have been obtained from CSFV Roesrath propagated in cell-culture using standard BAC cloning (Fahnøe et al., 2015), but obtaining cDNA clones from blood of pigs infected with wt Koslov, required many rounds of standard BAC cloning, and site-directed mutagenesis to obtain a functional clone (Fahnøe et al., 2014). The high-throughput cloning strategy developed here enables us to obtain numerous clones directly from serum of infected pigs, enabling us to elucidate which haplotypes constitute the virus population. The cloning strategy could also be applied to the study of other viruses such as hepatitis C virus (HCV), another member of the Flaviviridae family. HCV is a major cause of acute and chronic liver disease, and 400,000 people die from HCV infection annually (Bartenschlager et al., 2018). HCV circulates as a quasispecies in individual patients, with mutations distributed throughout the viral genomes. The mutations are frequently linked on the individual virus genomes and function in concert, and this linkage may play an important role in adaptation to drug treatment or antiviral immune responses (Bukh, 2016). Recently, near full-length ORF amplicons of HCV have been generated by long RT-PCR (Pedersen et al., 2018), which is the first step in obtaining full-length cDNA clones. Furthermore, the In-Fusion cloning system has been employed to generate full-length ORF clones of HCV to study the mutagenic effect of the antiviral drug ribavirin on HCV evolution in a cell-culture adapted strain (Mejer et al., 2018). Haplotyping of individual HCV genomes from infected patients could be a powerful tool to study the evolution of HCV and elucidate drug resistance phenotypes.

References

Acevedo A., Brodsky L., Andino R. 2014. Mutational and fitness landscapes of an RNA virus revealed through population sequencing. Nature. 505, 686–90.

Agapov E. V, Murray C.L., Frolov I., Qu L., Myers T.M., Rice C.M. 2004. Uncleaved NS2-3 is required for production of infectious bovine viral diarrhea virus. J Virol. 78, 2414–25.

Archer J., Baillie G., Watson S.J., Kellam P., Rambaut A., Robertson D.L. 2012. Analysis of high-depth sequence data for studying viral diversity: a comparison of next generation sequencing platforms using Segminator II. BMC Bioinformatics. 13, 47.

Avalos-Ramirez R., Orlich M., Thiel H.J., Becher P. 2001. Evidence for the presence of two novel pestivirus species. Virology. 286, 456–65.

Bartenschlager R., Baumert T.F., Bukh J., Houghton M., Lemon S.M., Lindenbach B.D., Lohmann V., Moradpour D., Pietschmann T., Rice C.M., Thimme R., Wakita T. 2018. Critical challenges and emerging opportunities in hepatitis C virus research in an era of potent antiviral therapy: Considerations for scientists and funding agencies. Virus Res. 248, 53–62.

Batschelet E., Domingo E., Weissmann C. 1976. The proportion of revertant and mutant phage in a growing population, as a function of mutation and growth rate. Gene. 1, 27–32.

Becher P., Orlich M., Shannon A.D., Horner G., König M., Thiel H.J. 1997. Phylogenetic analysis of pestiviruses from domestic and wild ruminants. J Gen Virol. 78, 1357–66.

Becher P., Schmeiser S., Oguzoglu T.C., Postel A. 2012. Complete genome sequence of a novel pestivirus from sheep. J Virol. 86, 11412.

Beer M., Reimann I., Hoffmann B., Depner K. 2007. Novel marker vaccines against classical swine fever. Vaccine. 25, 5665–70.

Beer M., Goller K. V, Staubach C., Blome S. 2015. Genetic variability and distribution of classical swine fever virus. Anim Heal Res Rev. 16, 33–9.

Behrens S.-E., Grassmann C.W., Thiel H.J., Meyers G., Tautz N. 1998. Characterization of an autonomous subgenomic pestivirus RNA replicon. J Virol. 72, 2364–72.

Biebricher C.K., Eigen M. 2005. The error threshold. Virus Res. 107, 117–27.

Bielefeldt Ohmann H., Bloch B. 1982. Electron microscopic studies of bovine viral diarrhea virus in tissues of diseased calves and in cell cultures. Arch Virol. 71, 57–74.

Bintintan I., Meyers G. 2010. A new type of signal peptidase cleavage site identified in an RNA virus polyprotein. J Biol Chem. 285, 8572–84.

Blacksell S.D., Khounsy S., Aken D. Van, Gleeson L.J., Westbury H.A. 2006. Comparative susceptibility of

indigenous and improved pig breeds to classical swine fever virus infection: Practical and epidemiological implications in a subsistence-based, developing country setting. Trop Anim Health Prod. 38, 467–74.

Bleidorn C. 2016. Third generation sequencing: technology and its potential impact on evolutionary biodiversity research. Syst Biodivers. 14, 1–8.

Blome S., Gabriel C., Staubach C., Leifer I., Strebelow G., Beer M. 2011. Genetic differentiation of infected from vaccinated animals after implementation of an emergency vaccination strategy against classical swine fever in wild boar. Vet Microbiol. 153, 373–6.

Blome S., Gabriel C., Beer M. 2013. Possibilities and limitations in veterinary vaccine development using the example of classical swine fever. Berl Munch Tierarztl Wochenschr. 126, 481–90.

Blome S., Gabriel C., Schmeiser S., Meyer D., Meindl-Böhmer A., Koenen F., Beer M. 2014. Efficacy of marker vaccine candidate CP7-E2alf against challenge with classical swine fever virus isolates of different genotypes. Vet Microbiol. 169, 8–17.

Blome S., Staubach C., Henke J., Carlson J., Beer M. 2017a. Classical swine fever—an updated review. Viruses. 9, 1–24.

Blome S., Wernike K., Reimann I., König P., Moß C., Beer M. 2017b. A decade of research into classical swine fever marker vaccine CP7-E2alf (Suvaxyn®CSF Marker): A review of vaccine properties. Vet Res. 48, 1–10.

Branza-Nichita N., Lazar C., Dwek R.A., Zitzmann N. 2004. Role of N-glycan trimming in the folding and secretion of the pestivirus protein Erns. Biochem Biophys Res Commun. 319, 655–62.

Brogden G., Adamek M., Proepsting M.J., Ulrich R., Naim H.Y., Steinhagen D. 2015. Cholesterol-rich lipid rafts play an important role in the Cyprinid herpesvirus 3 replication cycle. Vet Microbiol. 179, 204–12.

Brown E.A., Zhang H., Ping L.H., Lemon S.M. 1992. Secondary structure of the 5’ nontranslated regions of hepatitis C virus and pestivirus genomic RNAs. Nucleic Acids Res. 20, 5041–5.

Bukh J. 2016. The history of hepatitis C virus (HCV): Basic research reveals unique features in phylogeny, evolution and the viral life cycle with new perspectives for epidemic control. J Hepatol. 65 1 Suppl, S2–21.

Carrasco P., de la Iglesia F., Elena S.F. 2007. Distribution of fitness and virulence effects caused by single-nucleotide substitutions in Tobacco Etch virus. J Virol. 81, 12979–84.

Chang C.Y., Huang C.C., Lin Y.J., Deng M.C., Chen H.C., Tsai C.H., Chang W.M., Wang F.I. 2010a. Antigenic domains analysis of classical swine fever virus E2 glycoprotein by mutagenesis and conformation-dependent monoclonal antibodies. Virus Res. 149, 183–9.

Chang C.Y., Huang C.C., Lin Y.J., Deng M.C., Tsai C.H., Chang W.M., Wang F.I. 2010b. Identification of

antigen-specific residues on E2 glycoprotein of classical swine fever virus. Virus Res. 152, 65–72.

Chang C.Y., Huang C.C., Deng M.C., Huang Y.L., Lin Y.J., Liu H.M., Lin Y.L., Wang F.I. 2012. Antigenic mimicking with cysteine-based cyclized peptides reveals a previously unknown antigenic determinant on E2 glycoprotein of classical swine fever virus. Virus Res. 163, 190–6.

Chase C.C.L. 2013. The impact of BVDV infection on adaptive immunity. Biologicals. 41, 52–60.

Chen J., He W.-R., Shen L., Dong H., Yu J., Wang X., Yu S., Li Y., Li S., Luo Y., Sun Y., Qiu H.-J. 2015. The laminin receptor is a cellular attachment receptor for classical swine fever virus. J Virol. 89, 4894–906.

Chen N., Tong C., Li D., Wan J., Yuan X., Li X., Peng J., Fang W. 2010. Antigenic analysis of classical swine fever virus E2 glycoprotein using pig antibodies identifies residues contributing to antigenic variation of the vaccine C-strain and group 2 strains circulating in China. Virol J. 7, 378.

Chen Y., Xiao J., Xiao J., Sheng C., Wang J., Jia L., Zhi Y., Li G., Chen J., Xiao M. 2012. Classical swine fever virus NS5A regulates viral RNA replication through binding to NS5B and 3'UTR. Virology. 432, 376–88.

Chen Z., Rijnbrand R., Jangra R.K., Devaraj S.G., Qu L., Ma Y., Lemon S.M., Li K. 2007. Ubiquitination and proteasomal degradation of interferon regulatory factor-3 induced by Npro from a cytopathic bovine viral diarrhea virus. Virology. 366, 277–92.

Choi K.H., Gallei A., Becher P., Rossmann M.G. 2006. The structure of bovine viral diarrhea virus RNA-dependent RNA polymerase and its amino-terminal domain. Structure. 14, 1107–13.

Cingolani P., Platts A., Wang L.L., Coon M., Nguyen T., Wang L., Land S.J., Lu X., Ruden D.M. 2012. A program for annotating and predicting the effects of single nucleotide polymorphisms, SnpEff. Fly (Austin). 6, 80–92.

Clark K., Karsch-Mizrachi I., Lipman D.J., Ostell J., Sayers E.W. GenBank. http://www.ncbi.nlm.nih.gov/genbank/. Accessed 27 Oct 2017.

Collett M.S., Anderson D.K., Retzel E. 1988. Comparisons of the pestivirus bovine viral diarrhoea virus with members of the Flaviviridae. J Gen Virol. 69, 2637–43.

Coronado L., Liniger M., Muñoz-González S., Postel A., Pérez L.J., Pérez-Simó M., Perera C.L., Frías-Lepoureau M.T., Rosell R., Grundhoff A., Indenbirken D., Alawi M., Fischer N., Becher P., Ruggli N., Ganges L. 2017. Novel poly-uridine insertion in the 3'UTR and E2 amino acid substitutions in a low virulent classical swine fever virus. Vet Microbiol. 201, 103–12.

Crooks G.E., Hon G., Chandonia J.-M., Brenner S.E. 2004. WebLogo: a sequence logo generator. Genome Res. 14, 1188–90.

Cuevas J.M., Domingo-Calap P., Sanjuán R. 2012. The fitness effects of synonymous mutations in DNA and RNA viruses. Mol Biol Evol. 29, 17–20.

Danner K., Bachmann P.A. 2010. Vermehrung und Ausbreitung von Schweinepest-Virus, Stamm München-1,

in PK 15-Zellkulturen. Zentralblatt für Veterinärmedizin R B. 17, 353–62.

Deng M.-C., Huang C.-C., Huang T.-S., Chang C.Y., Lin Y.-J., Chien M.-S., Jong M.-H. 2005. Phylogenetic analysis of classical swine fever virus isolated from Taiwan. Vet Microbiol. 106, 187–93.

Deng R., Brock K. V. 1993. 5' and 3' untranslated regions of pestivirus genome: Primary and secondary structure analyses. Nucleic Acids Res. 21, 1949–57.

Depner K.R., Müller A., Gruber A., Rodriguez A., Bickhardt K., Liess B. 1995. Classical swine fever in wild boar (Sus scrofa) - experimental infections and viral persistence. Dtsch Tierarztl Wochenschr. 102, 381–4.

Depner K.R., Bouma A., Koenen F., Klinkenberg D., Lange E., De Smit H., Vanderhallen H. 2001. Classical swine fever (CSF) marker vaccine: Trial II. Challenge study in pregnant sows. Vet Microbiol. 83, 107–20.

Domingo-Calap P., Cuevas J.M., Sanjuán R. 2009. The fitness effects of random mutations in single-stranded DNA and RNA bacteriophages. PLoS Genet. 5, e1000742.

Domingo E. 1978. Nucleotide-sequence heterogeneity of an RNA phage population. Cell. 13.

Domingo E., Sheldon J., Perales C. 2012. Viral quasispecies evolution. Microbiol Mol Biol Rev. 76, 159–216.

Dong X.-N., Chen Y.-H. 2007. Marker vaccine strategies and candidate CSFV marker vaccines. Vaccine. 25, 205–30.

Dow N., Chernick A., Orsel K., van Marle G., van der Meer F. 2015. Genetic variability of bovine viral diarrhea virus and evidence for a possible genetic bottleneck during vertical transmission in persistently infected cattle. PLoS One. 10, e0131972.

Dräger C., Beer M., Blome S. 2015a. Porcine complement regulatory protein CD46 and heparan sulfates are the major factors for classical swine fever virus attachment in vitro. Arch Virol. 160, 739–46.

Dräger C., Blome S., Beer M., Reimann I., Rasmussen T.B. 2015b. A cell culture-adapted classical swine fever virus phenotype does not require the 476Arg Erns mutation. In: 9th Annual Meeting of EPIZONE. 2015.

Drake J.W., Charlesworth B., Charlesworth D., Crow J.F. 1998. Rates of spontaneous mutation. Genetics. 148, 1667–86.

Duarte E.A., Novella I.S., Ledesma S., Clarke D.K., Moya A., Elena S.F., Domingo E., Holland J.J. 1994. Subclonal components of consensus fitness in an RNA virus clone. J Virol. 68, 4295–301.

Edwards S., Fukusho A., Lefèvre P.-C.C., Lipowski A., Pejsak Z., Roehe P., Westergaard J. 2000. Classical swine fever: The global situation. Vet Microbiol. 73, 103–19.

Eigen M., Schuster P. 1977. The hypercycle. A principle of natural self-organization. Naturwissenschaften. 64, 541–65.

Eigen M. 2002. Error catastrophe and antiviral strategy. Proc Natl Acad Sci U S A. 99, 13374–6.

Elbers K., Tautz N., Becher P., Stoll D., Rümenapf T., Thiel H.J. 1996. Processing in the pestivirus E2-NS2

region: Identification of proteins p7 and E2p7. J Virol. 70, 4131–5.

Elena S.F., Sanjuán R. 2005. Adaptive value of high mutation rates of RNA viruses: Separating causes from consequences. J Virol. 79, 11555–8.

Everett H., Crooke H., Gurrala R., Dwarka R., Kim J., Botha B., Lubisi A., Pardini A., Gers S., Vosloo W., Drew T. 2011. Experimental infection of common warthogs (Phacochoerus africanus) and bushpigs (Potamochoerus larvatus) with classical swine fever virus. I: Susceptibility and transmission. Transbound Emerg Dis. 58, 128–34.

Eymann-Häni R., Leifer I., McCullough K.C., Summerfield A., Ruggli N. 2011. Propagation of classical swine fever virus in vitro circumventing heparan sulfate-adaptation. J Virol Methods. 176, 85–95.

Fahnøe U., Pedersen A.G., Risager P.C., Nielsen J., Belsham G.J., Höper D., Beer M., Rasmussen T.B. 2014. Rescue of the highly virulent classical swine fever virus strain "Koslov" from cloned cDNA and first insights into genome variations relevant for virulence. Virology. 468–470, 379–87.

Fahnøe U., Pedersen A.G., Dräger C., Orton R.J., Blome S., Höper D., Beer M., Rasmussen T.B. 2015. Creation of functional viruses from non-functional cDNA clones obtained from an RNA virus population by the use of ancestral reconstruction. PLoS One. 10, e0140912.

Fan Z.-C., Bird R.C. 2008. An improved reverse genetics system for generation of bovine viral diarrhea virus as a BAC cDNA. J Virol Methods. 149, 309–15.

Fernández-Sainz I.J., Largo E., Gladue D.P., Fletcher P., O'Donnell V., Holinka L.G., Carey L.B., Lu X., Nieva J.L., Borca M. V. 2014. Effect of specific amino acid substitutions in the putative fusion peptide of structural glycoprotein E2 on Classical Swine Fever Virus replication. Virology. 456–457, 121–30.

Fetzer C., Tews B.A., Meyers G. 2005. The carboxy-terminal sequence of the pestivirus glycoprotein Erns represents an unusual type of membrane anchor. J Virol. 79, 11901–13.

Firth C., Bhat M., Firth M.A., Williams S.H., Frye M.J., Simmonds P., Conte J.M., Ng J., Garcia J., Bhuva N.P., Lee B., Che X., Quan P.-L., Lipkin W.I. 2014. Detection of zoonotic pathogens and characterization of novel viruses carried by commensal Rattus norvegicus in New York City. MBio. 5, e01933-14-e01933-14.

Flaherty P., Natsoulis G., Muralidharan O., Winters M., Buenrostro J., Bell J., Brown S., Holodniy M., Zhang N., Ji H.P. 2012. Ultrasensitive detection of rare mutations using next-generation targeted resequencing. Nucleic Acids Res. 40, e2.

Fletcher S.P., Jackson R.J. 2002. Pestivirus internal ribosome entry site (IRES) structure and function: elements in the 5' untranslated region important for IRES function. J Virol. 76, 5024–33.

Floegel-Niesmann G., Blome S., Gerß-Dülmer H., Bunzenthal C., Moennig V. 2009. Virulence of classical swine fever virus isolates from Europe and other areas during 1996 until 2007. Vet Microbiol. 139,

165–9.

von Freyburg M., Ege A., Saalmüller A., Meyers G. 2004. Comparison of the effects of RNase-negative and wild-type classical swine fever virus on peripheral blood cells of infected pigs. J Gen Virol. 85 Pt 7, 1899–908.

Friis M.B., Rasmussen T.B., Belsham G.J. 2012. Modulation of translation initiation efficiency in classical swine fever virus. J Virol. 86, 8681–92.

Fritzemeier J., Teuffert J., Greiser-Wilke I., Staubach C., Schluter H., Moennig V. 2000. Epidemiology of classical swine fever in Germany in the 1990s. Vet Microbiol. 77, 29–41.

Garry R.F., Dash S. 2003. Proteomics computational analyses suggest that hepatitis C virus E1 and pestivirus E2 envelope glycoproteins are truncated class II fusion proteins. Virology. 307, 255–65.

van Gennip H.G.P., van Rijn P.A., Widjojoatmodjo M.N., de Smit A.J., Moormann R.J.M. 2000. Chimeric classical swine fever viruses containing envelope protein Erns or E2 of bovine viral diarrhoea virus protect pigs against challenge with CSFV and induce a distinguishable antibody response. Vaccine. 19, 447–59.

van Gennip H.G.P., Vlot A.C., Hulst M.M., De Smit A.J., Moormann R.J.M. 2004. Determinants of virulence of classical swine fever virus strain Brescia. J Virol. 78, 8812–23.

Germi R., Crance J.-M., Garin D., Guimet J., Lortat-Jacob H., Ruigrok R.W.H., Zarski J.-P., Drouet E. 2002. Heparan sulfate-mediated binding of infectious dengue virus type 2 and yellow fever virus. Virology. 292, 162–8.

Gil L.H.V.G., Ansari I.H., Vassilev V., Liang D., Lai V.C.H., Zhong W., Hong Z., Dubovi E.J., Donis R.O. 2006. The amino-terminal domain of bovine viral diarrhea virus Npro protein is necessary for alpha/beta interferon antagonism. J Virol. 80, 900–11.

Gladue D.P., Holinka L.G., Fernandez-Sainz I.J., Prarat M.V., O'Donell V., Vepkhvadze N.G., Lu Z., Rogers K., Risatti G.R., Borca M.V. 2010. Effects of the interactions of classical swine fever virus Core protein with proteins of the SUMOylation pathway on virulence in swine. Virology. 407, 129–36.

Gladue D.P., Gavrilov B.K., Holinka L.G., Fernandez-Sainz I.J., Vepkhvadze N.G., Rogers K., O'Donnell V., Risatti G.R., Borca M. V. 2011. Identification of an NTPase motif in classical swine fever virus NS4B protein. Virology. 411, 41–9.

Gladue D.P., Holinka L.G., Largo E., Fernandez Sainz I., Carrillo C., O'Donnell V., Baker-Branstetter R., Lu Z., Ambroggio X., Risatti G.R., Nieva J.L., Borca M. V. 2012. Classical swine fever virus p7 protein is a viroporin involved in virulence in swine. J Virol. 86, 6778–91.

Goller K. V., Gabriel C., Dimna M. Le, Le Potier M.-F., Rossi S., Staubach C., Merboth M., Beer M., Blome S. 2016. Evolution and molecular epidemiology of classical swine fever virus during a multi-annual

outbreak amongst European wild boar. J Gen Virol. 97, 639–45.

Gong Y., Trowbridge R., Macnaughton T.B., Westaway E.G., Shannon A.D., Gowans E.J. 1996. Characterization of RNA synthesis during a one-step growth curve and of the replication mechanism of bovine viral diarrhoea virus. J Gen Virol. 77, 2729–36.

Grassmann C.W., Isken O., Tautz N., Behrens S.-E. 2001. Genetic analysis of the pestivirus nonstructural coding region: Defects in the NS5A unit can be complemented in trans. J Virol. 75, 7791–802.

Gray E.W., Nettleton P.F. 1987. The ultrastructure of cell cultures infected with border disease and bovine virus diarrhoea viruses. J Gen Virol. 68 (Pt 9), 2339–46.

Greiser-Wilke I., Dittmar K.E., Liess B., Moennig V. 1991. Immunofluorescence studies of biotype-specific expression of bovine viral diarrhoea virus epitopes in infected cells. J Gen Virol. 72 (Pt 8), 2015–9.

Greiser-Wilke I., Depner K., Fritzemeier J., Haas L., Moennig V. 1998. Application of a computer program for genetic typing of classical swine fever virus isolates from Germany. J Virol Methods. 75, 141–50.

Greiser-Wilke I., Moennig V. 2004. Vaccination against classical swine fever virus: Limitations and new strategies. Anim Heal Res Rev. 5, 223–6.

Griffin S.D.C., Harvey R., Clarke D.S., Barclay W.S., Harris M., Rowlands D.J. 2004. A conserved basic loop in hepatitis C virus p7 protein is required for amantadine-sensitive ion channel activity in mammalian cells but is dispensable for localization to mitochondria. J Gen Virol. 85 Pt 2, 451–61.

Grummer B., Beer M., Liebler-Tenorio E., Greiser-Wilke I. 2001. Localization of viral proteins in cells infected with bovine viral diarrhoea virus. J Gen Virol. 82 Pt 11, 2597–605.

Hansen M.S., Bille-Hansen V., Uttenthal Å., Lohse L., Nielsen J. 2011. Localization of classical swine fever virus (CSFV) in the brain of pigs infected with strain Kozlov. In: 8th ESVV Pestivirus Symposium. 2011.

Harada T., Tautz N., Thiel H.J. 2000. E2-p7 region of the bovine viral diarrhea virus polyprotein: Processing and functional studies. J Virol. 74, 9498–506.

Hause B.M., Collin E.A., Peddireddi L., Yuan F., Chen Z., Hesse R.A., Gauger P.C., Clement T., Fang Y., Anderson G. 2015. Discovery of a novel putative atypical porcine pestivirus in pigs in the USA. J Gen Virol. 96, 2994–8.

Heimann M., Sosa G.R., Martoglio B., Thiel H.-J., Rümenapf T. 2006. Core protein of pestiviruses is processed at the C terminus by signal peptide peptidase. J Virol. 80, 1915–21.

Holinka L.G., Largo E., Gladue D.P., Risatti G.R., Nieva J.L., Borca M. V. 2016. Alteration of a second putative fusion peptide of structural glycoprotein E2 of classical swine fever virus alters virus replication and virulence in swine. J Virol. 90, 10299–308.

Holland J., Spindler K., Horodyski F., Grabau E., Nichol S., VandePol S. 1982. Rapid evolution of RNA genomes. Science. 215, 1577–85.

Holmes E.C. 2003. Error thresholds and the constraints to RNA virus evolution. Trends Microbiol. 11, 543–6.

Hu D., Lv L., Gu J., Chen T., Xiao Y., Liu S. 2016. Genetic diversity and positive selection analysis of classical swine fever virus envelope protein gene E2 in East China under C-strain vaccination. Front Microbiol. 7 FEB, 1–10.

Hulst M.M., Moormann R.J.M. 1997. Inhibition of pestivirus infection in cell culture by envelope proteins Erns and E2 of classical swine fever virus: Erns and E2 interact with different receptors. J Gen Virol. 78, 2779–87.

Hulst M.M., van Gennip H.G.P., Moormann R.J.M. 2000. Passage of classical swine fever virus in cultured swine kidney cells selects virus variants that bind to heparan sulfate due to a single amino acid change in envelope protein Erns. J Virol. 74, 9553–61.

Jackson T., Ellard F.M., Ghazaleh R.A., Brookes S.M., Blakemore W.E., Corteyn A.H., Stuart D.I., Newman J.W., King A.M. 1996. Efficient infection of cells in culture by type O foot-and-mouth disease virus requires binding to cell surface heparan sulfate. J Virol. 70, 5282–7.

Jenckel M., Blome S., Beer M., Höper D. 2017. Quasispecies composition and diversity do not reveal any predictors for chronic classical swine fever virus infection. Arch Virol. 162, 775–86.

Ji W., Niu D.-D., Si H.-L., Ding N., He C. 2014. Vaccination influences the evolution of classical swine fever virus. Infect Genet Evol. 25, 69–77.

Ji W., Guo Z., Ding N.Z., He C.Q. 2015. Studying classical swine fever virus: Making the best of a bad virus. Virus Res. 197, 35–47.

Jiang D.-L., Gong W.-J., Li R.-C., Liu G.-H., Hu Y.-F., Ge M., Wang S.-Q., Yu X.-L., Tu C. 2013. Phylogenetic analysis using E2 gene of classical swine fever virus reveals a new subgenotype in China. Infect Genet Evol. 17, 231–8.

Kaden V., Lange E., Fischer U., Strebelow G. 2000. Oral immunisation of wild boar against classical swine fever: evaluation of the first field study in Germany. Vet Microbiol. 73, 239–52.

Kaden V., Heyne H., Kiupel H., Letz W., Kern B., Lemmer U., Gossger K., Rothe A., Bohme H., Tyrpe P. 2002. Oral immunisation of wild boar against classical swine fever: Concluding analysis of the recent field trials in Germany. Berl Munch Tierarztl Wochenschr. 115, 179–85.

Kaden V., Lange E., Küster H., Müller T., Lange B. 2010. An update on safety studies on the attenuated “RIEMSER® Schweinepestoralvakzine” for vaccination of wild boar against classical swine fever. Vet Microbiol. 143, 133–8.

Keightley P.D., Eyre-Walker A. 2010. What can we learn about the distribution of fitness effects of new mutations from DNA sequence data? Philos Trans R Soc Lond B Biol Sci. 365, 1187–93.

King A.M.Q., Lefkowitz E.J., Mushegian A.R., Adams M.J., Dutilh B.E., Gorbalenya A.E., Harrach B., Harrison

R.L., Junglen S., Knowles N.J., Kropinski A.M., Krupovic M., Kuhn J.H., Nibert M.L., Rubino L., Sabanadzovic S., Sanfaçon H., Siddell S.G., Simmonds P., Varsani A., Zerbini F.M., Davison A.J. 2018. Changes to taxonomy and the International Code of Virus Classification and Nomenclature ratified by the International Committee on Taxonomy of Viruses (2018). Arch Virol.

Kirkland P.D., Frost M.J., Finlaison D.S., King K.R., Ridpath J.F., Gu X. 2007. Identification of a novel virus in pigs-Bungowannah virus: A possible new species of pestivirus. Virus Res. 129, 26–34.

Komaniwa H., Fukusho A., Shimizu Y. 1981. Micro method for performing titration and neutralization test of hog cholera virus using established porcine kidney cell strain. Natl Inst Anim Health Q (Tokyo). 21, 153–8.

König M., Lengsfeld T., Pauly T., Stark R., Thiel H.J. 1995. Classical swine fever virus: Independent induction of protective immunity by two structural glycoproteins. J Virol. 69, 6479–86.

Kortekaas J., Vloet R.P.M., Weerdmeester K., Ketelaar J., van Eijk M., Loeffen W.L. 2010. Rational design of a classical swine fever C-strain vaccine virus that enables the differentiation between infected and vaccinated animals. J Virol Methods. 163, 175–85.

Krey T., Himmelreich A., Heimann M., Menge C., Thiel H.J., Maurer K., Rümenapf T. 2006. Function of bovine CD46 as a cellular receptor for bovine viral diarrhea virus is determined by complement control protein. J Virol. 80, 3912–22.

Kumar R., Barman N.N., Khatoon E., Rajbongshi G., Deka N., Morla S., Kumar S. 2015. Molecular characterization of E2 glycoprotein of classical swine fever virus: Adaptation and propagation in porcine kidney cells. Vitr Cell Dev Biol - Anim. 51, 441–6.

Lackner T., Müller A., Pankraz A., Becher P., Thiel H.J., Gorbalenya A.E., Tautz N. 2004. Temporal modulation of an autoprotease is crucial for replication and pathogenicity of an RNA virus. J Virol. 78, 10765–75.

Lackner T., Müller A., König M., Thiel H.J., Tautz N., Mu A. 2005. Persistence of bovine viral diarrhea virus is determined by a cellular cofactor of a viral autoprotease. J Virol. 79, 9746–55.

Lackner T., Thiel H.-J., Tautz N. 2006. Dissection of a viral autoprotease elucidates a function of a cellular chaperone in proteolysis. Proc Natl Acad Sci. 103, 1510–5.

Lamp B., Riedel C., Wentz E., Tortorici M.-A., Rümenapf T. 2013. Autocatalytic cleavage within classical swine fever virus NS3 leads to a functional separation of protease and helicase. J Virol. 87, 11872–83.

Langedijk J.P.M., van Veelen P.A., Schaaper W.M.M., de Ru A.H., Meloen R.H., Hulst M.M. 2002. A structural model of pestivirus Erns based on disulfide bond connectivity and homology modeling reveals an extremely rare vicinal disulfide. J Virol. 76, 10383–92.

Lauring A.S., Andino R. 2010. Quasispecies theory and the behavior of RNA viruses. PLoS Pathog. 6,

e1001005.

Lazar C., Zitzmann N., Dwek R.A., Branza-Nichita N. 2003. The pestivirus Erns glycoprotein interacts with E2 in both infected cells and mature virions. Virology. 314, 696–705.

Lecot S., Belouzard S., Dubuisson J., Rouillé Y. 2005. Bovine viral diarrhea virus entry is dependent on clathrin-mediated endocytosis. J Virol. 79, 10826–9.

Leifer I., Hoffmann B., Hoper D., Rasmussen T.B., Blome S., Strebelow G., Horeth-Bontgen D., Staubach C., Beer M. 2010. Molecular epidemiology of current classical swine fever virus isolates of wild boar in Germany. J Gen Virol. 91, 2687–97.

Leifer I., Hoeper D., Blome S., Beer M., Ruggli N. 2011. Clustering of classical swine fever virus isolates by codon pair bias. BMC Res Notes. 4, 521.

Leifer I., Blome S., Blohm U., König P., Küster H., Lange B., Beer M. 2012. Characterization of C-strain Riems TAV-epitope escape variants obtained through selective antibody pressure in cell culture. Vet Res. 43, 1–11.

Li C., Huang J., Li Y., He F., Li D., Sun Y., Han W., Li S., Qiu H.-J. 2013. Efficient and stable rescue of classical swine fever virus from cloned cDNA using an RNA polymerase II system. Arch Virol. 158, 901–7.

Li H., Handsaker B., Wysoker A., Fennell T., Ruan J., Homer N., Marth G., Abecasis G., Durbin R. 2009. The Sequence Alignment/Map format and SAMtools. Bioinformatics. 25, 2078–9.

Li H. 2013. Aligning sequence reads, clone sequences and assembly contigs with BWA-MEM.

Li N., Qiu H.-J., Zhao J.-J., Li Y., Wang M.-J., Lu B.-W., Han C.-G., Hou Q., Wang Z.-H., Gao H., Peng W.-P., Li G.-X., Zhu Q.-H., Tong G.-Z. 2007. A Semliki Forest virus replicon vectored DNA vaccine expressing the E2 glycoprotein of classical swine fever virus protects pigs from lethal challenge. Vaccine. 25, 2907–12.

Li S., Wang J., Yang Q., Anwar M.N., Yu S., Qiu H.J. 2017. Complex virus–host interactions involved in the regulation of classical swine fever virus replication: A minireview. Viruses. 9, 1–15.

Li X., Xu Z., He Y., Yao Q., Zhang K., Jin M., Chen H., Qian P. 2006. Genome comparison of a novel classical swine fever virus isolated in China in 2004 with other CSFV strains. Virus Genes. 33, 133–42.

Li Y., Wang J., Kanai R., Modis Y. 2013. Crystal structure of glycoprotein E2 from bovine viral diarrhea virus. Proc Natl Acad Sci U S A. 110, 6805–10.

Liang D., Fernandez-Sainz I., Ansari I.H., Gil L.H.V.G., Vassilev V., Donis R.O. 2003. The envelope glycoprotein E2 is a determinant of cell culture tropism in ruminant pestiviruses. J Gen Virol. 84, 1269–74.

Liang D., Chen L., Ansari I.H., Gil L.H.V.G., Topliff C.L., Kelling C.L., Donis R.O. 2009. A replicon trans-packaging system reveals the requirement of nonstructural proteins for the assembly of bovine viral diarrhea virus (BVDV) virion. Virology. 387, 331–40.

Lin M., Lin F., Mallory M., Clavijo a. 2000. Deletions of structural glycoprotein E2 of classical swine fever

virus strain alfort/187 resolve a linear epitope of monoclonal antibody WH303 and the minimal N-terminal domain essential for binding immunoglobulin G antibodies of a pig hyperimmune serum. J Virol. 74, 11619–25.

Lin Z., Liang W., Kang K., Li H., Cao Z., Zhang Y. 2014. Classical swine fever virus and p7 protein induce secretion of IL-1β in macrophages. J Gen Virol. 95 Pt_12, 2693–9.

Lindenbach B.D., Thiel H.J., Rice C.M., Murray C.L., Thiel H.J., Rice C.M. 2013. Flaviviridae: The viruses and their replication. In: Fields Virology. 6th edition. New York: Lippincott Williams & Wilkins; 2013. p. 712–46.

Liu J.-J., Wong M.-L., Chang T.-J. 1998. The recombinant nucleocapsid protein of classical swine fever virus can act as a transcriptional regulator. Virus Res. 53, 75–80.

Lowings P., Ibata G., Needham J., Paton D. 1996. Classical swine fever virus diversity and evolution. J Gen Virol. 77, 1311–21.

Luo T.R., Liao S., Wu X., Feng L., Yuan Z.-X., Li H., Liang J.-J., Meng X.-M., Zhang H.-Y. 2011. Phylogenetic analysis of the E2 gene of classical swine fever virus from the Guangxi Province of southern China. Virus Genes. 42, 347–54.

Luo Y., Li S., Sun Y., Qiu H.-J. 2014. Classical swine fever in China: A minireview. Vet Microbiol. 172, 1–6.

Luo Y., Ji S., Liu Y., Lei J.L., Xia S.L., Wang Y., Du M.L., Shao L., Meng X.Y., Zhou M., Sun Y., Qiu H.J. 2016. Isolation and characterization of a moderately virulent classical swine fever virus emerging in China. Transbound Emerg Dis.

Luo Y., Ji S., Lei J.L., Xiang G.T., Liu Y., Gao Y., Meng X.Y., Zheng G., Zhang E.Y., Wang Y., Du M.L., Li Y., Li S., He X.J., Sun Y., Qiu H.J. 2017. Efficacy evaluation of the C-strain-based vaccines against the subgenotype 2.1d classical swine fever virus emerging in China. Vet Microbiol. 201, 154–61.

Luscombe C.A., Huang Z., Murray M.G., Miller M., Wilkinson J., Ewart G.D. 2010. A novel Hepatitis C virus p7 ion channel inhibitor, BIT225, inhibits bovine viral diarrhea virus in vitro and shows synergism with recombinant interferon-alpha-2b and nucleoside analogues. Antiviral Res. 86, 144–53.

Macalalad A.R., Zody M.C., Charlebois P., Lennon N.J., Newman R.M., Malboeuf C.M., Ryan E.M., Boutwell C.L., Power K.A., Brackney D.E., Pesko K.N., Levin J.Z., Ebel G.D., Allen T.M., Birren B.W., Henn M.R. 2012. Highly sensitive and specific detection of rare variants in mixed viral populations from massively parallel sequence data. PLoS Comput Biol. 8, e1002417.

MacLachlan N.J., Dubovi E.J. (Eds.). 2010. Fenner's Veterinary Virology. 4th edition. London, UK: Academic Press Inc.; 2010.

Madu I.G., Chu V.C., Lee H., Regan A.D., Bauman B.E., Whittaker G.R. 2007. Heparan sulfate is a selective attachment factor for the avian coronavirus infectious bronchitis virus Beaudette. Avian Dis. 51, 45–51.

Maurer K., Krey T., Moennig V., Thiel H.-J., Rümenapf T. 2004. CD46 is a cellular receptor for bovine viral diarrhea virus. J Virol. 78, 1792–9.

Mayer D., Thayer T.M., Hofmann M.A., Tratschin J.D. 2003. Establishment and characterisation of two cDNA-derived strains of classical swine fever virus, one highly virulent and one avirulent. Virus Res. 98, 105–16.

Mayer D., Hofmann M.A., Tratschin J.D. 2004. Attenuation of classical swine fever virus by deletion of the viral Npro gene. Vaccine. 22, 317–28.

Mejer N., Fahnøe U., Galli A., Ramirez S., Benfield T., Bukh J. 2018. Ribavirin-induced mutagenesis across the complete open reading frame of hepatitis C virus genotypes 1a and 3a. J Gen Virol. 99, 1066–77.

Mendez E., Ruggli N., Collett M.S., Rice C.M. 1998. Infectious bovine viral diarrhea virus (strain NADL) RNA from stable cDNA clones: a cellular insert determines NS3 production and viral cytopathogenicity. J Virol. 72, 4737–45.

Messerle M., Crnkovic I., Hammerschmidt W., Ziegler H., Koszinowski U.H. 1997. Cloning and mutagenesis of a herpesvirus genome as an infectious bacterial artificial chromosome. Proc Natl Acad Sci U S A. 94, 14759–63.

Meuwissen M.P.M., Horst S.H., Huirne R.B.M., Dijkhuizen A.A. 1999. A model to estimate the financial consequences of classical swine fever outbreaks: Principles and outcomes. Prev Vet Med. 42, 249–70.

Meyer C., Von Freyburg M., Elbers K., Meyers G. 2002. Recovery of virulent and RNase-negative attenuated type 2 bovine viral diarrhea viruses from infectious cDNA clones. J Virol. 76, 8494–503.

Meyers G., Rümenapf T., Thiel H.J. 1989. Molecular cloning and nucleotide sequence of the genome of hog cholera virus. Virology. 171, 555–67.

Meyers G., Thiel H.J., Rümenapf T. 1996. Classical swine fever virus: recovery of infectious viruses from cDNA constructs and generation of recombinant cytopathogenic defective interfering particles. J Virol. 70, 1588–95.

Meyers G., Saalmüller A., Büttner M. 1999. Mutations abrogating the RNase activity in glycoprotein Erns of the pestivirus classical swine fever virus lead to virus attenuation. J Virol. 73, 10224–35.

Meyers G., Ege A., Fetzer C., von Freyburg M., Elbers K., Carr V., Prentice H., Charleston B., Schürmann E.-M. 2007. Bovine viral diarrhea virus: prevention of persistent fetal infection by a combination of two mutations affecting Erns RNase and Npro protease. J Virol. 81, 3327–38.

Misinzo G., Delputte P.L., Meerts P., Lefebvre D.J., Nauwynck H.J. 2006. Porcine circovirus 2 uses heparan sulfate and chondroitin sulfate B glycosaminoglycans as receptors for its attachment to host cells. J Virol. 80, 3487–94.

Mittelholzer C., Moser C., Tratschin J.D., Hofmann M.A. 2000. Analysis of classical swine fever virus

replication kinetics allows differentiation of highly virulent from avirulent strains. Vet Microbiol. 74, 293–308.

Moennig V., Floegel-Niesmann G., Greiser-Wilke I. 2003. Clinical signs and epidemiology of classical swine fever: A review of new knowledge. Vet J. 165, 11–20.

Moennig V., Becher P. 2015. Pestivirus control programs: How far have we come and where are we going? Anim Heal Res Rev. 16, 83–7.

Moormann R.J.M., van Gennip H.G.P., Miedema G.K., Hulst M.M., van Rijn P.A. 1996. Infectious RNA transcribed from an engineered full-length cDNA template of the genome of a pestivirus. J Virol. 70, 763–70.

Moser C., Stettler P., Tratschin J.D., Hofmann M.A. 1999. Cytopathogenic and noncytopathogenic RNA replicons of classical swine fever virus. J Virol. 73, 7787–94.

Moulin H.R., Seuberlich T., Bauhofer O., Bennett L.C., Tratschin J.D., Hofmann M. a., Ruggli N. 2007. Nonstructural proteins NS2-3 and NS4A of classical swine fever virus: Essential features for infectious particle formation. Virology. 365, 376–89.

Murray C.L., Jones C.T., Rice C.M. 2008a. Architects of assembly: Roles of Flaviviridae non-structural proteins in virion morphogenesis. Nat Rev Microbiol. 6, 699–708.

Murray C.L., Marcotrigiano J., Rice C.M. 2008b. Bovine viral diarrhea virus core is an intrinsically disordered protein that binds RNA. J Virol. 82, 1294–304.

Neill J.D., Ridpath J.F., Fischer N., Grundhoff A., Postel A., Becher P. 2014. Complete genome sequence of pronghorn virus, a pestivirus. Genome Announc. 2, e00575-14-e00575-14.

OIE. World organisation for animal health. http://www.oie.int/.

van Oirschot J.T. 1999. Classical Swine Fever (Hog Cholera). In: Shaw BE, D'Allaire S, Mengeling WL, Taylor DJ, editors. Diseases of Swine. 8th edition. Iowa: Iowa State University Press; 1999. p. 159–72.

van Oirschot J.T. 2003a. Vaccinology of classical swine fever: From lab to field. Vet Microbiol. 96, 367–84.

van Oirschot J.T. 2003b. Emergency vaccination against classical swine fever. Dev Biol (Basel). 114, 259–67.

Ojosnegros S., Beerenwinkel N., Antal T., Nowak M.A., Escarmis C., Domingo E. 2010. Competition-colonization dynamics in an RNA virus. Proc Natl Acad Sci. 107, 2108–12.

El Omari K., Iourin O., Harlos K., Grimes J.M., Stuart D.I. 2013. Structure of a pestivirus envelope glycoprotein E2 clarifies its role in cell entry. Cell Rep. 3, 30–5.

Orton R.J., Wright C.F., Morelli M.J., King D.J., Paton D.J., King D.P., Haydon D.T. 2015. Distinguishing low frequency mutations from RT-PCR and sequence errors in viral deep sequencing data. BMC Genomics. 16, 1–15.

Paton D.., Greiser-Wilke I. 2003. Classical swine fever – an update. Res Vet Sci. 75, 169–78.

Paton D.J., McGoldrick A., Greiser-Wilke I., Parchariyanon S., Song J.Y., Liou P.P., Stadejek T., Lowings J.P., Björklund H., Belák S. 2000. Genetic typing of classical swine fever virus. Vet Microbiol. 73, 137–57.

Peck K.M., Lauring A.S. 2018. The complexities of viral mutation rates. J Virol. May, JVI.01031-17.

Pedersen M.S., Fahnøe U., Hansen T.A., Pedersen A.G., Jenssen H., Bukh J., Schønning K. 2018. A near full-length open reading frame next generation sequencing assay for genotyping and identification of resistance-associated variants in hepatitis C virus. J Clin Virol. 105, 49–56.

Pei J., Zhao M., Ye Z., Gou H., Wang J., Yi L., Dong X., Liu W., Luo Y., Liao M., Chen J. 2014. Autophagy enhances the replication of classical swine fever virus in vitro. Autophagy. 10, 93–110.

Peng W.-P., Hou Q., Xia Z.-H., Chen D., Li N., Sun Y., Qiu H.-J. 2008. Identification of a conserved linear B-cell epitope at the N-terminus of the E2 glycoprotein of classical swine fever virus by phage-displayed random peptide library. Virus Res. 135, 267–72.

Pérez L.J., Díaz de Arce H., Perera C.L., Rosell R., Frías M.T., Percedo M.I., Tarradas J., Dominguez P., Núñez J.I., Ganges L. 2012. Positive selection pressure on the B/C domains of the E2-gene of classical swine fever virus in endemic areas under C-strain vaccination. Infect Genet Evol. 12, 1405–12.

Pierro D.J. 2006. Infectious clone construction of dengue virus type 2, strain Jamaican 1409, and characterization of a conditional E6 mutation. J Gen Virol. 87, 2263–8.

Pollard M.O., Gurdasani D., Mentzer A.J., Porter T., Sandhu M.S. 2018. Long reads: Their purpose and place. Hum Mol Genet. 27, R234–41.

Postel A., Schmeiser S., Bernau J., Meindl-Boehmer A., Pridotkas G., Dirbakova Z., Mojzis M., Becher P. 2012. Improved strategy for phylogenetic analysis of classical swine fever virus based on full length E2 encoding sequences. Vet Res. 43, 50.

Postel A., Schmeiser S., Perera C.L., Rodríguez L.J.P., Frias-Lepoureau M.T., Becher P. 2013. Classical swine fever virus isolates from Cuba form a new subgenotype 1.4. Vet Microbiol. 161, 334–8.

Postel A., Hansmann F., Baechlein C., Fischer N., Alawi M., Grundhoff A., Derking S., Tenhündfeld J., Pfankuche V.M., Herder V., Baumgärtner W., Wendt M., Becher P. 2016a. Presence of atypical porcine pestivirus (APPV) genomes in newborn piglets correlates with congenital tremor. Sci Rep. 6, 27735.

Postel A., Schmeiser S., Zimmermann B., Becher P. 2016b. The European Classical Swine Fever Virus Database: Blueprint for a pathogen-specific sequence database with integrated sequence analysis tools. Viruses. 8, 302.

Rasmussen T.B., Reimann I., Hoffmann B., Depner K., Uttenthal Å., Beer M. 2008. Direct recovery of infectious pestivirus from a full-length RT-PCR amplicon. J Virol Methods. 149, 330–3.

Rasmussen T.B., Reimann I., Uttenthal Å., Leifer I., Depner K., Schirrmeier H., Beer M. 2010. Generation of recombinant pestiviruses using a full-genome amplification strategy. Vet Microbiol. 142, 13–7.

Rasmussen T.B., Risager P.C., Fahnøe U., Friis M.B., Belsham G.J., Höper D., Reimann I., Beer M. 2013. Efficient generation of recombinant RNA viruses using targeted recombination-mediated mutagenesis of bacterial artificial chromosomes containing full-length cDNA. BMC Genomics. 14, 819.

Reimann I., Depner K., Trapp S., Beer M. 2004. An avirulent chimeric pestivirus with altered cell tropism protects pigs against lethal infection with classical swine fever virus. Virology. 322, 143–57.

Reimann I., Depner K., Utke K., Leifer I., Lange E., Beer M. 2010. Characterization of a new chimeric marker vaccine candidate with a mutated antigenic E2-epitope. Vet Microbiol. 142, 45–50.

Ridpath J.F., Bayles D.O., Neill J.D., Falkenberg S.M., Bauermann F. V., Holler L., Braun L.J., Young D.B., Kane S.E., Chase C.C.L. 2015. Comparison of the breadth and complexity of bovine viral diarrhea (BVDV) populations circulating in 34 persistently infected cattle generated in one outbreak. Virology. 485, 297–304.

Riedel C., Lamp B., Heimann M., König M., Blome S., Moennig V., Schüttler C., Thiel H.-J., Rümenapf T. 2012. The core protein of classical Swine Fever virus is dispensable for virus propagation in vitro. PLoS Pathog. 8, e1002598.

van Rijn P.A., van Gennip H.G.P., de Meijer E.J., Moormann R.J.M. 1993. Epitope mapping of envelope glycoprotein E1 of hog cholera virus strain Brescia. J Gen Virol. 74, 2053–60.

van Rijn P.A., Miedema G.K., Wensvoort G., van Gennip H.G.P., Moormann R.J.M. 1994. Antigenic structure of envelope glycoprotein E1 of hog cholera virus. J Virol. 68.

van Rijn P.A. 2007. A common neutralizing epitope on envelope glycoprotein E2 of different pestiviruses: Implications for improvement of vaccines and diagnostics for classical swine fever (CSF)? Vet Microbiol. 125.

Rijnbrand R., van der Straaten T., van Rijn P.A., Spaan W.J., Bredenbeek P.J. 1997. Internal entry of ribosomes is directed by the 5' noncoding region of classical swine fever virus and is dependent on the presence of an RNA pseudoknot upstream of the initiation codon. J Virol. 71, 451–7.

Rios L., Coronado L., Naranjo-Feliciano D., Martínez-Pérez O., Perera C.L., Hernandez-Alvarez L., Díaz de Arce H., Núñez J.I., Ganges L., Pérez L.J. 2017. Deciphering the emergence, genetic diversity and evolution of classical swine fever virus. Sci Rep. 7, 17887.

Risager P.C., Fahnøe U., Gullberg M., Rasmussen T.B., Belsham G.J., Fahnoe U., Gullberg M., Rasmussen T.B., Belsham G.J. 2013. Analysis of classical swine fever virus RNA replication determinants using replicons. J Gen Virol. 94 Pt_8, 1739–48.

Risatti G.R., Borca M. V., Kutish G.F., Lu Z., Holinka L.G., French R.A., Tulman E.R., Rock D.L. 2005. The E2 glycoprotein of classical swine fever virus is a virulence determinant in swine. J Virol. 79, 3787–96.

Risatti G.R., Holinka L.G., Carrillo C., Kutish G.F., Lu Z., Tulman E.R., Sainz I.F., Borca M. V. 2006.

Identification of a novel virulence determinant within the E2 structural glycoprotein of classical swine fever virus. Virology. 355, 94–101.

Risatti G.R., Holinka L.G., Fernandez-Sainz I., Carrillo C., Kutish G.F., Lu Z., Zhu J., Rock D.L., Borca M. V. 2007a. Mutations in the carboxyl terminal region of E2 glycoprotein of classical swine fever virus are responsible for viral attenuation in swine. Virology. 364, 371–82.

Risatti G.R., Holinka L.G., Fernandez Sainz I., Carrillo C., Lu Z., Borca M. V. 2007b. N-linked glycosylation status of classical swine fever virus strain Brescia E2 glycoprotein influences virulence in swine. J Virol. 81, 924–33.

La Rocca S.A., Herbert R.J., Crooke H., Drew T.W., Wileman T.E., Powell P.P. 2005. Loss of interferon regulatory factor 3 in cells infected with classical swine fever virus involves the N-terminal protease, Npro. J Virol. 79, 7239–47.

Romero-Brey I., Bartenschlager R. 2014. Membranous replication factories induced by plus-strand RNA viruses. 2014.

Rossi S., Pol F., Forot B., Masse-provin N., Rigaux S., Bronner A., Le Potier M.-F. 2010. Preventive vaccination contributes to control classical swine fever in wild boar (Sus scrofa sp.). Vet Microbiol. 142, 99–107.

Rossi S., Staubach C., Blome S., Guberti V., Thulke H.-H., Vos A., Koenen F., Le Potier M.-F. 2015. Controlling of CSFV in European wild boar using oral vaccination: A review. Front Microbiol. 6.

von Rüden S., Staubach C., Kaden V., Hess R.G., Blicke J., Kühne S., Sonnenburg J., Fröhlich A., Teuffert J., Moennig V. 2008. Retrospective analysis of the oral immunisation of wild boar populations against classical swine fever virus (CSFV) in region Eifel of Rhineland-Palatinate. Vet Microbiol. 132, 29–38.

Ruggli N., Tratschin J.D., Mittelholzer C., Hofmann M.A. 1996. Nucleotide sequence of classical swine fever virus strain Alfort/187 and transcription of infectious RNA from stably cloned full-length cDNA. J Virol. 70, 3478–87.

Ruggli N., Rice C.M. 1999. Functional cDNA clones of the Flaviviridae: Strategies and applications. Adv Virus Res. 53, 183–207.

Ruggli N., Tratschin J.D., Schweizer M., Mccullough K.C., Hofmann M.A., Summerfield A. 2003. Classical swine fever virus interferes with cellular antiviral defense: Evidence for a novel function of Npro. J Virol. 77, 7645–54.

Ruggli N., Bird B.H., Liu L., Bauhofer O., Tratschin J.-D., Hofmann M.A. 2005. Npro of classical swine fever virus is an antagonist of double-stranded RNA-mediated apoptosis and IFN-α/β induction. Virology. 340, 265–76.

Ruggli N., Summerfield A., Fiebach A.R., Guzylack-Piriou L., Bauhofer O., Lamm C.G., Waltersperger S.,

Matsuno K., Liu L., Gerber M., Choi K.H., Hofmann M.A., Sakoda Y., Tratschin J.-D.D. 2009. Classical swine fever virus can remain virulent after specific elimination of the interferon regulatory factor 3-degrading function of Npro. J Virol. 83, 817–29.

Rümenapf T., Unger G., Strauss J.H., Thiel H.J. 1993. Processing of the envelope glycoproteins of pestiviruses. J Virol. 67, 3288–94.

Rümenapf T. 1998. N-terminal protease of pestiviruses: Identification of putative catalytic residues by site-directed mutagenesis. J Virol. 72.

Sainz I.F., Holinka L.G., Lu Z., Risatti G.R., Borca M. V. 2008. Removal of a N-linked glycosylation site of classical swine fever virus strain Brescia Erns glycoprotein affects virulence in swine. Virology. 370, 122–9.

Salonen A., Ahola T., Kääriäinen L. 2004. Viral RNA Replication in Association with Cellular Membranes. In: Membrane Trafficking in Viral Replication. Berlin/Heidelberg: Springer-Verlag; 2004. p. 139–73.

Sanjuán R., Moya A., Elena S.F. 2004. The distribution of fitness effects caused by single-nucleotide substitutions in an RNA virus. Proc Natl Acad Sci U S A. 101, 8396–401.

Sanjuán R. 2010. Mutational fitness effects in RNA and single-stranded DNA viruses: Common patterns revealed by site-directed mutagenesis studies. Philos Trans R Soc Lond B Biol Sci. 365, 1975–82.

Sasahara J. 1970. Hog cholera: Diagnosis and prophylaxis. Natl Inst Anim Health Q (Tokyo). 10, 57–81.

Sawitzky D., Hampl H., Habermehl K.O. 1990. Comparison of heparin-sensitive attachment of pseudorabies virus (PRV) and herpes simplex virus type 1 and identification of heparin-binding PRV glycoproteins. J Gen Virol. 71, 1221–5.

van der Schaar H.M., Rust M.J., Chen, Van Der Ende-Metselaar H., Wilschut J., Zhuang X., Smit J.M. 2008. Dissecting the cell entry pathway of dengue virus by single-particle tracking in living cells. PLoS Pathog. 4.

Schelp C., Greiser-Wilke I., Moennig V. 2000. An actin-binding protein is involved in pestivirus entry into bovine cells. Virus Res. 68, 1–5.

Schirrmeier H., Strebelow G., Depner K., Hoffmann B., Beer M. 2004. Genetic and antigenic characterization of an atypical pestivirus isolate, a putative member of a novel pestivirus species. J Gen Virol. 85, 3647–52.

Schmeiser S., Mast J., Thiel H.-J., König M. 2014. Morphogenesis of pestiviruses: New insights from ultrastructural studies of strain Giraffe-1. J Virol. 88, 2717–24.

Shen H., Pei J., Bai J., Zhao M., Ju C., Yi L., Kang Y., Zhang X., Chen L., Li Y., Wang J., Chen J. 2011. Genetic diversity and positive selection analysis of classical swine fever virus isolates in south China. Virus Genes. 43, 234–42.

Sheng C., Xiao M., Geng X., Liu J., Wang Y., Gu F. 2007. Characterization of interaction of classical swine fever virus NS3 helicase with 3' untranslated region. Virus Res. 129, 43–53.

Sheng C., Zhu Z., Yu J., Wan L., Wang Y., Chen J., Gu F., Xiao M. 2010. Characterization of NS3, NS5A and NS5B of classical swine fever virus through mutation and complementation analysis. Vet Microbiol. 140, 72–80.

Sheng C., Chen Y., Xiao J., Xiao J., Wang J., Li G., Chen J., Xiao M. 2012. Classical swine fever virus NS5A protein interacts with 3'-untranslated region and regulates viral RNA synthesis. Virus Res. 163, 636–43.

Shi B.-J., Liu C.-C., Zhou J., Wang S.-Q., Gao Z.-C., Zhang X.-M., Zhou B., Chen P.-Y. 2016. Entry of classical swine fever virus into PK-15 cells via a pH-, dynamin-, and cholesterol-dependent, clathrin-mediated endocytic pathway that requires Rab5 and Rab7. J Virol. 90, 9194–208.

Shimizu Y., Furuuchi S., Kumagai T., Sasahara J. 1970. A mutant of hog cholera virus inducing interference in swine testicle cell cultures. Am J Vet Res. 31, 1787–94.

Sieczkarski S.B., Whittaker G.R. 2002. Dissecting virus entry via endocytosis. J Gen Virol. 83, 1535–45.

Silva M.N.F., Silva D.M.F., Leite A.S., Gomes A.L. V., Freitas A.C., Pinheiro-Junior J.W., Castro R.S., Jesus A.L.S. 2017. Identification and genetic characterization of classical swine fever virus isolates in Brazil: A new subgenotype. Arch Virol. 162, 817–22.

Simmonds P., Tuplin A., Evans D.J. 2004. Detection of genome-scale ordered RNA structure (GORS) in genomes of positive-stranded RNA viruses: Implications for virus evolution and host persistence. RNA. 10, 1337–51.

Simmonds P., Becher P., Bukh J., Gould E.A., Meyers G., Monath T., Muerhoff S., Pletnev A., Rico-Hesse R., Smith D.B., Stapleton J.T. 2017. ICTV Virus Taxonomy Profile: Flaviviridae. J Gen Virol. 98, 2–3.

Smith D.B., Meyers G., Bukh J., Gould E.A., Monath T., Muerhoff A.S., Pletnev A., Rico-Hesse R., Stapleton J.T., Simmonds P., Becher P. 2017. Proposed revision to the taxonomy of the genus Pestivirus, family Flaviviridae. J Gen Virol. 98, 2106–12.

Stegeman A., Elbers A., de Smit H., Moser H., Smak J., Pluimers F.H. 2000. The 1997–1998 epidemic of classical swine fever in the Netherlands. Vet Microbiol. 73, 183–96.

Steinhauer D.A., Holland J.J. 1987. Rapid evolution of RNA viruses. Annu Rev Microbiol. 41, 409–33.

Sun Y., Li H.-Y., Tian D.-Y., Han Q.-Y., Zhang X., Li N., Qiu H.-J. 2011. A novel alphavirus replicon-vectored vaccine delivered by adenovirus induces sterile immunity against classical swine fever. Vaccine. 29, 8364–72.

Tamura T., Sakoda Y., Yoshino F., Nomura T., Yamamoto N., Sato Y., Okamatsu M., Ruggli N., Kida H. 2012. Selection of classical swine fever virus with enhanced pathogenicity reveals synergistic virulence determinants in E2 and NS4B. J Virol. 86, 8602–13.

Tang F., Pan Z., Zhang C. 2008. The selection pressure analysis of classical swine fever virus envelope protein genes Erns and E2. Virus Res. 131, 132–5.

Tao P., Dai L., Luo M., Tang F., Tien P., Pan Z. 2009. Analysis of synonymous codon usage in classical swine fever virus. Virus Genes. 38, 104–12.

Tarradas J., Monsó M., Muñoz M., Rosell R., Fraile L., Frías M.T., Domingo M., Andreu D., Sobrino F., Ganges L. 2011. Partial protection against classical swine fever virus elicited by dendrimeric vaccine-candidate peptides in domestic pigs. Vaccine. 29, 4422–9.

Tarradas J., de la Torre M.E., Rosell R., Pérez L.J., Pujols J., Muñoz M., Muñoz I., Muñoz S., Abad X., Domingo M., Fraile L., Ganges L. 2014. The impact of CSFV on the immune response to control infection. Virus Res. 185, 82–91.

Tautz N., Harada T., Kaiser A., Rinck G., Behrens S., Thiel H.J. 1999. Establishment and characterization of cytopathogenic and noncytopathogenic pestivirus replicons. J Virol. 73, 9422–32.

Tautz N., Kaiser A., Thiel H.-J. 2000. NS3 serine protease of bovine viral diarrhea virus: Characterization of active site residues, NS4A cofactor domain, and protease–cofactor interactions. Virology. 273, 351–63.

Tellinghuisen T.L., Paulson M.S., Rice C.M. 2006. The NS5A protein of bovine viral diarrhea virus contains an essential zinc-binding site similar to that of the hepatitis C virus NS5A protein. J Virol. 80, 7450–8.

Tews B.A., Meyers G. 2007. The pestivirus glycoprotein Erns is anchored in plane in the membrane via an amphipathic helix. J Biol Chem. 282, 32730–41.

Tews B.A., Schürmann E.-M., Meyers G. 2009. Mutation of cysteine 171 of pestivirus Erns RNase prevents homodimer formation and leads to attenuation of classical swine fever virus. J Virol. 83, 4823–34.

Thiel H.J., Stark R., Weiland E., Rümenapf T., Meyers G. 1991. Hog cholera virus: Molecular composition of virions from a pestivirus. J Virol. 65, 4705–12.

Tio P.H., Jong W.W., Cardosa M.J. 2005. Two dimensional VOPBA reveals laminin receptor (LAMR1) interaction with dengue virus serotypes 1, 2 and 3. Virol J. 2, 25.

Töpfer A., Höper D., Blome S., Beer M., Beerenwinkel N., Ruggli N., Leifer I. 2013. Sequencing approach to analyze the role of quasispecies for classical swine fever. Virology. 438, 14–9.

Tratschin J.D., Moser C., Ruggli N., Hofmann M.A. 1998. Classical swine fever virus leader proteinase Npro is not required for viral replication in cell culture. J Virol. 72, 7681–4.

Tyson J.R., O'Neil N.J., Jain M., Olsen H.E., Hieter P., Snutch T.P. 2018. MinION-based long-read sequencing and assembly extends the Caenorhabditis elegans reference genome. Genome Res. 28, 266–74.

Vanderhallen H., Mittelholzer C., Hofmann M.A., Koenen F. 1999. Classical swine fever virus is genetically stable in vitro and in vivo. Arch Virol. 144, 1669–77.

Velazquez-Salinas L., Risatti G.R., Holinka L.G., O'Donnell V., Carlson J., Alfano M., Rodriguez L.L., Carrillo C.,

Gladue D.P., Borca M. V. 2016. Recoding structural glycoprotein E2 in classical swine fever virus (CSFV) produces complete virus attenuation in swine and protects infected animals against disease. Virology. 494, 178–89.

Vignuzzi M., Stone J.K., Arnold J.J., Cameron C.E., Andino R. 2006. Quasispecies diversity determines pathogenesis through cooperative interactions in a viral population. Nature. 439, 344–8.

Vilcek S., Paton D., Lowings P., Björklund H., Nettleton P., Belák S. 1999. Genetic analysis of pestiviruses at the 3' end of the genome. Virus Genes. 18, 107–14.

Vilcek S., Ridpath J.F., Van Campen H., Cavender J.L., Warg J. 2005. Characterization of a novel pestivirus originating from a pronghorn antelope. Virus Res. 108, 187–93.

Visher E., Whitefield S.E., McCrone J.T., Fitzsimmons W., Lauring A.S. 2016. The mutational robustness of influenza A virus. PLoS Pathog. 12, e1005856.

Wang Z., Nie Y., Wang P., Ding M., Deng H. 2004. Characterization of classical swine fever virus entry by using pseudotyped viruses: E1 and E2 are sufficient to mediate viral entry. Virology. 330, 332–41.

Weaver S.C., Denison M., Roossinck M., Vignuzzi M. 2016. Virus Evolution: Current Research and Future Directions. Caister Academic Press; 2016.

Weber M.N., Bauermann F. V., Bayles D.O., Canal C.W., Neill J.D., Ridpath J.F. 2016. Comparison of 'HoBi'-like viral populations among persistent infected calves generated under experimental conditions and to inoculum virus. Virology. 492, 225–31.

Weber M.N., Bauermann F. V., Canal C.W., Bayles D.O., Neill J.D., Ridpath J.F. 2017. Temporal dynamics of 'HoBi'-like pestivirus quasispecies in persistently infected calves generated under experimental conditions. Virus Res. 227, 23–33.

Weiland E., Stark R., Haas B., Rümenapf T., Meyers G., Thiel H.J. 1990. Pestivirus glycoprotein which induces neutralizing antibodies forms part of a disulfide-linked heterodimer. J Virol. 64, 3563–9.

Weiland E., Ahl R., Stark R., Weiland F., Thiel H.J. 1992. A second envelope glycoprotein mediates neutralization of a pestivirus, hog cholera virus. J Virol. 66, 3677–82.

Weiland F., Weiland E., Unger G., Saalmüller A., Thiel H.J. 1999. Localization of pestiviral envelope proteins Erns and E2 at the cell surface and on isolated particles. J Gen Virol. 80 (Pt 5), 1157–65.

Weiskircher E., Aligo J., Ning G., Konan K. V. 2009. Bovine viral diarrhea virus NS4B protein is an integral membrane protein associated with Golgi markers and rearranged host membranes. Virol J. 6, 185.

Wensvoort G. 1989. Topographical and functional mapping of epitopes on hog cholera virus with monoclonal antibodies. J Gen Virol. 70, 2865–76.

Wensvoort G., Boonstra J., Bodzinga B.G. 1990. Immunoaffinity purification and characterization of the envelope protein E1 of hog cholera virus. J Gen Virol. 71, 531–40.

Whitfield Z.J., Andino R. 2016. Characterization of viral populations by using circular sequencing. J Virol. 90, 8950–3.

Wilke C.O. 2005. Quasispecies theory in the context of population genetics. BMC Evol Biol. 5, 44.

Wilm A., Aw P.P.K., Bertrand D., Yeo G.H.T., Ong S.H., Wong C.H., Khor C.C., Petric R., Hibberd M.L., Nagarajan N. 2012. LoFreq: A sequence-quality aware, ultra-sensitive variant caller for uncovering cell-population heterogeneity from high-throughput sequencing datasets. Nucleic Acids Res. 40, 11189–201.

Wiskerchen M., Belzer S.K., Collett M.S. 1991. Pestivirus gene expression: The first protein product of the bovine viral diarrhea virus large open reading frame, p20, possesses proteolytic activity. J Virol. 65, 4508–14.

Wu R., Li L., Zhao Y., Tu J., Pan Z. 2016. Identification of two amino acids within E2 important for the pathogenicity of chimeric classical swine fever virus. Virus Res. 211, 79–85.

Wu Z., Wang Q., Feng Q., Liu Y., Teng J., Yu A.C., Chen J. 2010. Correlation of the virulence of CSFV with evolutionary patterns of E2 glycoprotein. Front Biosci (Elite Ed). 2, 204–20.

Wu Z., Ren X., Yang L., Hu Y., Yang J., He G., Zhang J., Dong J., Sun L., Du J., Liu L., Xue Y., Wang J., Yang F., Zhang S., Jin Q. 2012. Virome analysis for identification of novel mammalian viruses in bat species from Chinese provinces. J Virol. 86, 10999–1012.

Xiao M., Zhang C.Y., Pan Z.S., Wu H.X., Guo J.Q. 2002. Classical swine fever virus NS5B-GFP fusion protein possesses an RNA-dependent RNA polymerase activity. Arch Virol. 147, 1779–87.

Xiao M., Gao J., Wang W., Wang Y., Chen J., Chen J., Li B. 2004. Specific interaction between the classical swine fever virus NS5B protein and the viral genome. Eur J Biochem. 271, 3888–96.

Xiao M., Li H., Wang Y., Wang X., Wang W., Peng J., Chen J., Li B. 2006. Characterization of the N-terminal domain of classical swine fever virus RNA-dependent RNA polymerase. J Gen Virol. 87 Pt 2, 347–56.

Xiao M., Bai Y., Xu H., Geng X., Chen J., Wang Y., Chen J., Li B. 2008. Effect of NS3 and NS5B proteins on classical swine fever virus internal ribosome entry site-mediated translation and its host cellular translation. J Gen Virol. 89 Pt 4, 994–9.

Xiao M., Wang Y., Zhu Z., Yu J., Wan L., Chen J. 2009. Influence of NS5A protein of classical swine fever virus (CSFV) on CSFV internal ribosome entry site-dependent translation. J Gen Virol. 90, 2923–8.

Xu J., Mendez E., Caron P.R., Lin C., Murcko M.A., Collett M.S., Rice C.M. 1997. Bovine viral diarrhea virus NS3 serine proteinase: Polyprotein cleavage sites, cofactor requirements, and molecular model of an enzyme essential for pestivirus replication. J Virol. 71, 5312–22.

Yang X., Charlebois P., Macalalad A., Henn M.R., Zody M.C. 2013. V-Phaser 2: Variant inference for viral populations. BMC Genomics. 14, 674.

Yoo S.J., Kwon T., Kang K., Kim H., Kang S.C., Richt J.A., Lyoo Y.S. 2018. Genetic evolution of classical swine fever virus under immune environments conditioned by genotype 1-based modified live virus vaccine. Transbound Emerg Dis. 65, 735–45.

Yu M., Wang L.-F., Shiell B.J., Morrissy C.J., Westbury H.A. 1996. Fine mapping of a C-terminal linear epitope highly conserved among the major envelope glycoprotein E2 (gp51 to gp54) of different pestiviruses. Virology. 222, 289–92.

Yu X., Tu C., Li H., Hu R., Chen C., Li Z., Zhang M., Yin Z. 2001. DNA-mediated protection against classical swine fever virus. Vaccine. 19, 1520–5.

Yun S., Kim S., Rice C.M., Lee Y. 2003. Development and application of a reverse genetics system for Japanese encephalitis virus. J Virol. 77, 6450–65.

Zhang F., Yu M., Weiland E., Morrissy C., Zhang N., Westbury H., Wang L.-F. 2006. Characterization of epitopes for neutralizing monoclonal antibodies to classical swine fever virus E2 and Erns using phage-displayed random peptide library. Arch Virol. 151, 37–54.

Zhang H., Leng C., Feng L., Zhai H., Chen J., Liu C., Bai Y., Ye C., Peng J., An T., Kan Y., Cai X., Tian Z., Tong G. 2015. A new subgenotype 2.1d isolates of classical swine fever virus in China, 2014. Infect Genet Evol. 34, 94–105.

Zürcher C., Sauter K.-S., Mathys V., Wyss F., Schweizer M. 2014. Prolonged activity of the pestiviral RNase Erns as an interferon antagonist after uptake by clathrin-mediated endocytosis. J Virol. 88, 7235–43.

Abbreviations

aa	Amino acid
BAC	Bacterial artificial chromosome
BDV	Border disease virus
bp	Base pair
BVDV	Bovine viral diarrhea virus
CAM	Chloramphenicol
CDS	Coding sequence
CirSeq	Circular sequencing
CNS	Central nervous system
CSF	Classical swine fever
CSFV	Classical swine fever virus
DIVA	Differentiating infected from vaccinated animals
DMEM	Dulbecco's Modified Eagles Medium
dpi	Days post-inoculation
EMA	European Medicines Agency
ER	Endoplasmic reticulum
FCS	Fetal calf serum
gt	Genotype
GTR	General time reversible
HCV	Hepatitis C virus
HS	Heparan sulfate
IFN	Interferon
IL	Interleukin
IPTG	Isopropyl β-D-1-thiogalactopyranoside
IRES	Internal ribosome entry site
IRF	Interferon regulatory factor
JEV	Japanese encephalitis virus
KAN	Kanamycin
kb	Kilobases
kDa	Kilodalton
Kos	Koslov consensus BAC clone

LamR	Laminin receptor
mAbs	Monoclonal antibodies
MLV	Modified live vaccine
MOI	Multiplicity of infection
NGS	Next generation sequencing
nst	Number of substituion types
nt	Nucleotide
NTPase	Nucleoside triphosphatase
ON	Overnight
ONT	Oxford Nanopore Technology
ORF	Open reading frame
PacBio	Pacific Biosystems
PI	Persistently infected
PID	Post infection day
Plex	Plexus choroideus
RdRp	RNA-dependent RNA polymerase
RNase	Ribonuclease
RPMI	Roswell Park Memorial Institute
SL'-motif	Residues 761, 763 and 764 in the CSFV polyprotein
SMRT	Single molecule real-time
SN	Swine kidney
SNP	Single nucleotide polymorphism
SUMO	small ubiquitin-like modifier
$TCID_{50}$	50% Tissue culture infective dose
UTR	Untranslated region
vKos	Virus rescued from Kos
wt	Wildtype